

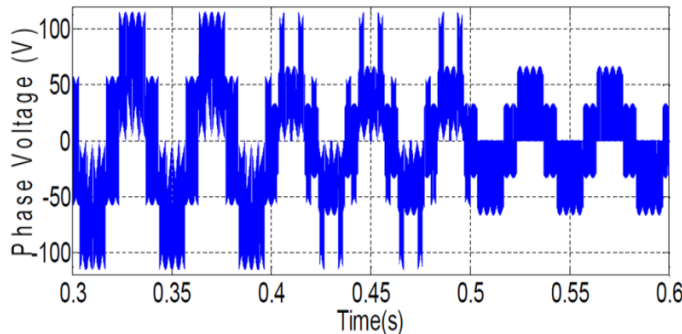
PWM Techniques for Matrix Converters -Investigations & Applications

OPEN VIVA -VOCE

Time: 01:00 PM / Date: 27-08-2013

Supervisor : Dr. Ranganath Muthu
Professor
Department of EEE
SSN College of Engineering
Kalavakkam - 603110

கலாவக்கம் - 603110
SSN COLLEGE OF ENGINEERING
DEPARTMENT OF EEE



Research Scholar : M.Senthil Kumaran
Reg. No: 2007399111/ Ph.D./AR7
Department of EEE
SSN College of Engineering
Kalavakkam - 603110

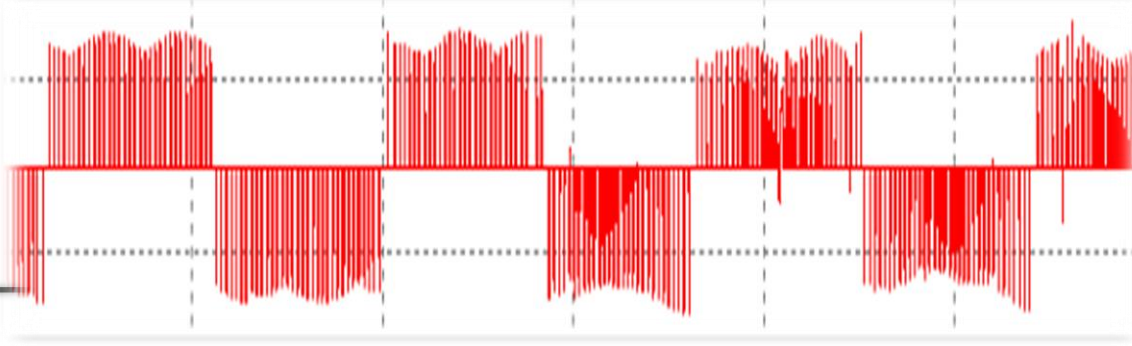
PWM Techniques for Matrix Converters -Investigations & Applications

EXPERT MEMBERS

Indian Examiner
Dr. P. Dananjayan
Professor
Department of ECE
Pondicherry University

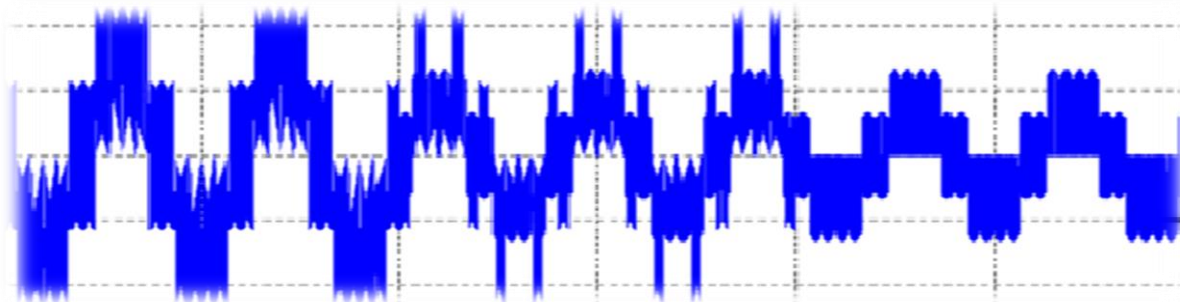
Foreign Examiner Representative
Dr. J. Prakash
Professor & Head
Department of Instrumentation
MIT - Anna University

OPEN VIVA –VOCE
01.00 PM / 27-08-2013



PWM Techniques for Matrix Converters

- Investigations & Applications



Overview of the Research Work - Presentation

- Problem Statement
- Objective
- Introduction to Matrix Converter (MC)
- Decoupled Indirect Duty Cycle (DIDC) PWM Technique of MC
- Rotating Space Vector (RSVM)Technique for MC
- Analysis of MC with Unbalanced and Non-Sinusoidal Inputs
- Direct Three level Matrix converter (DTMC) and its SVPWM
- Direct Torque Control of DTMC
- Conclusion
- Answers to the Queries to the Examiners.
- References
- List of Publication
- Acknowledgement.

Problem Statement

Industrial application of the MC is still limited due to the following practical issues

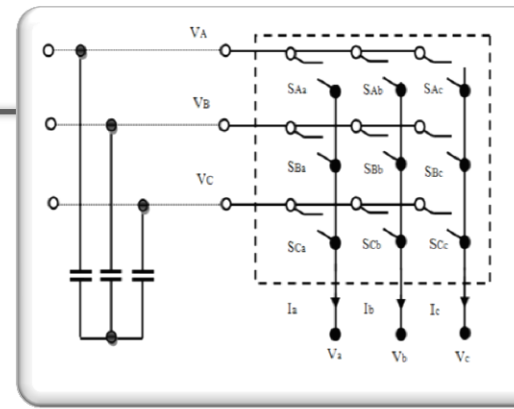
- Difficulty in implementing complex switching methods . ↗
- Common mode voltage effects, . ↗
- High susceptibility to input power disturbances . ↗
- Low voltage ride through capability . ↗
- Commutation issues. . ↗

In order to extend the horizon of matrix converter into several application

The research work proposes several new matrix converter topologies with their control strategies to provide a solution to some of the above issues

Objective

- To propose a relatively simple firing scheme called **DIDC PWM** for MC that strives to reduce the computations.
- To suggest the idea of using a **six phase matrix converter** for a 3-phase induction motor drive system to eliminate the common mode voltage with increased voltage transfer ratio.
- To analyze the performance of MC with **unbalanced and non-sinusoidal** inputs and mitigate the effects of unbalance and harmonics.
- To modify the MC topology termed as **DTMC**, with a focus to reduce the THD. To demonstrate the indirect space vector modulation (ISVM) method for DTMC and develop the **switching loss model**.
- To develop a direct torque control (**DTC**) method for a DTMC fed induction motor drive for the reduction of torque ripple

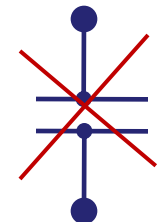


CHAPTER - I

Introduction to Matrix converter and the Developed MESS technique

Introduction -MC

- A Direct AC-AC converter topology with an array of 3×3 bidirectional switches
- It is an alternative to replace traditional AC-DC-AC →



Advantages of MC

- Adjustable Input power factor
- Inherent four quadrant operation
- High quality sinusoidal input/output waveforms
- High power density

Disadvantages of MC

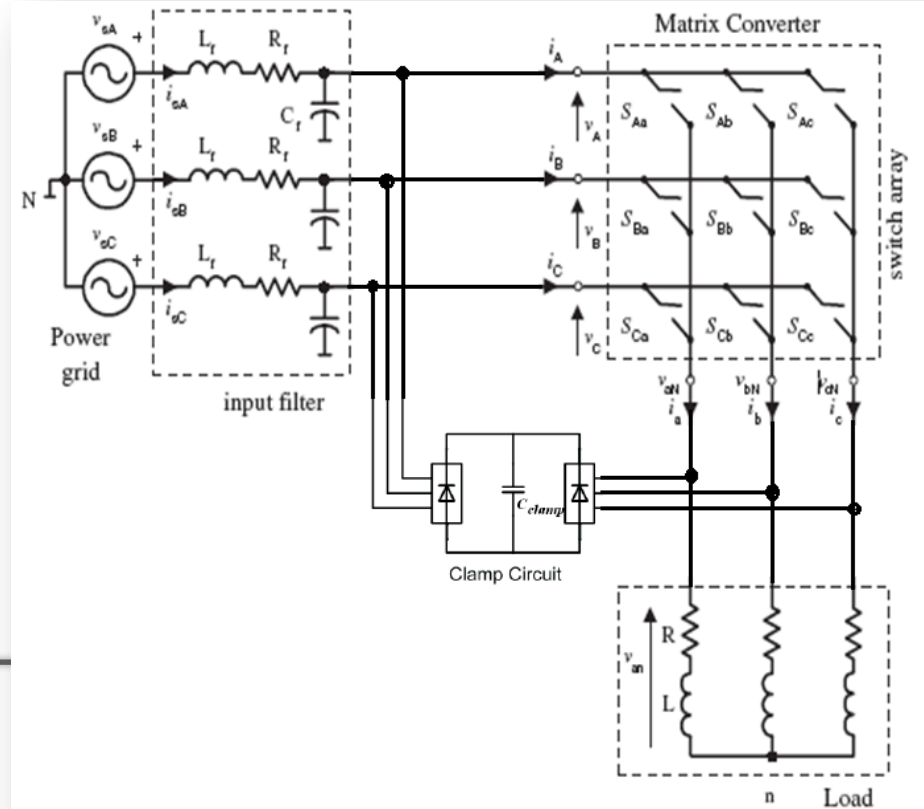
- Difficulty in implementing complex switching methods
- High susceptibility to input power disturbances
- Low voltage ride through capability
- Commutation issues.

Matrix Converter Structure

POWER CIRCUIT (3x3 Bidirectional Switch)
Amplitude / Frequency conversion

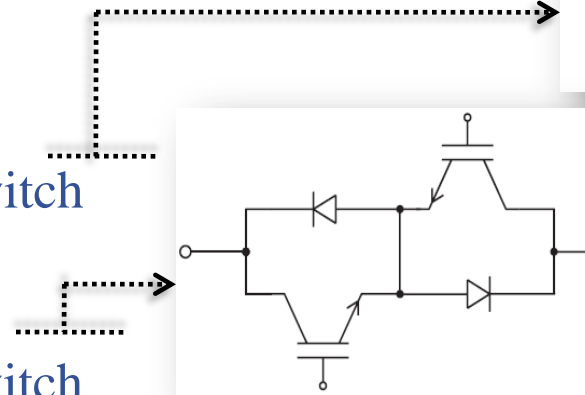
INPUT FILTER (Source Inductance, Line Capacitance, Damping resistor)
Elimination of high order frequency
in input current

CLAMP CIRCUIT (3φ Diode Bridge
Rectifier , clamp capacitor)
Protection against overvoltage

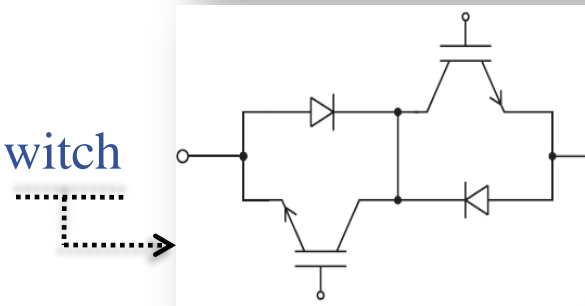


Bidirectional Switch Structure

- Diode Embedded Bi-Directional Switch



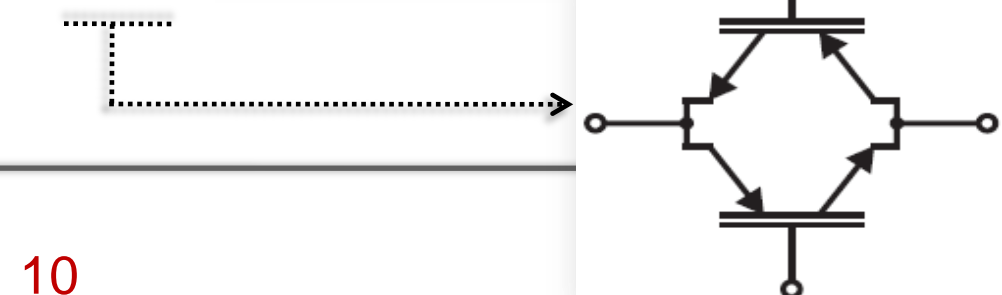
- Common Emitter Bi-Directional Switch



- Common Collector Bi-Directional Switch



- Reverse Blocking IGBTs Bi-Directional Switch



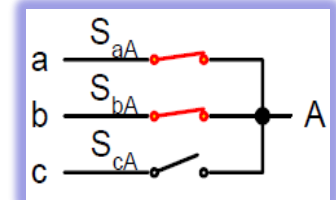
Commutation of the Bidirectional Switch

absence of inherent free wheeling in Matrix Converter

Basic rules for safe operation of the Matrix Converter $\{ S_{aj} + S_{bj} + S_{cj} = 1, \quad j \in \{A, B, C\} \}$

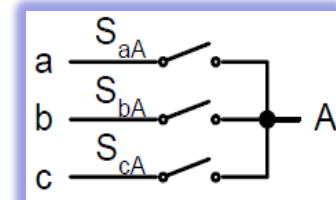
- 1) No two switch of the same output phase should be ON

$$S_{aj} + S_{bj} + S_{cj} > 1, \quad j \in \{A, B, C\}$$



- 2) Not all the switch of an Output phase should be open

$$S_{aj} + S_{bj} + S_{cj} < 1, \quad j \in \{A, B, C\}$$

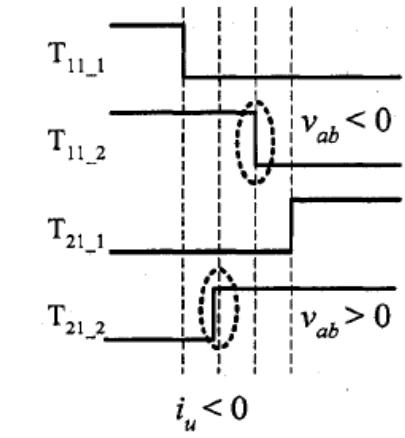
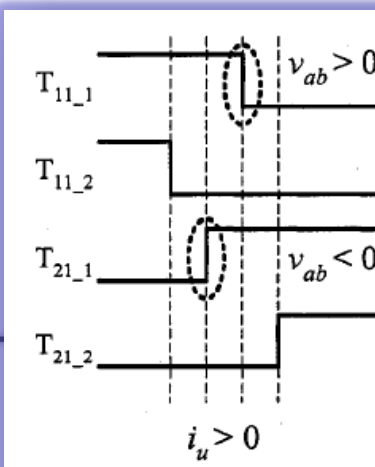
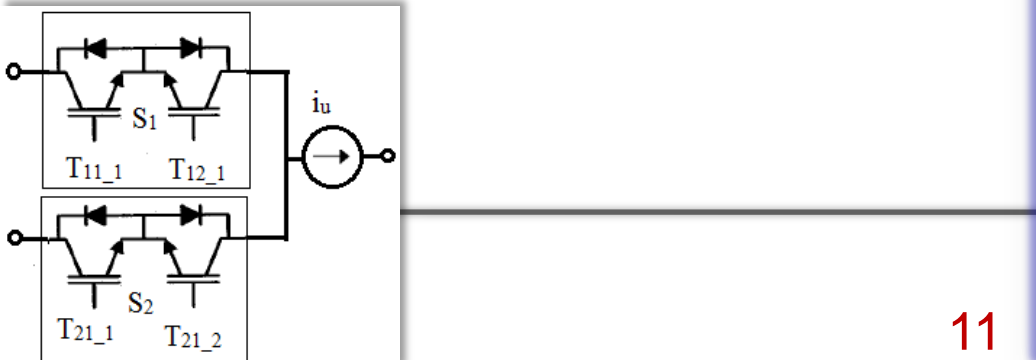


Methods of Commutation

- 1) Multi Step Current Commutation (Requiring direction of Output Current)

- 2) Dead Time Commutation

(Requiring Snubber Circuit)



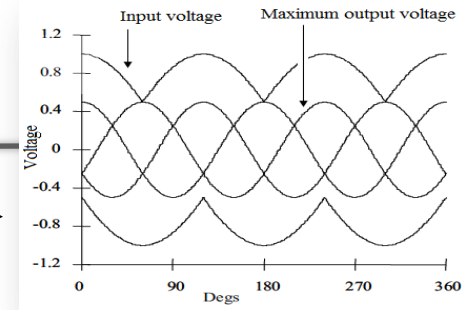
Modulation Techniques of Matrix Converters

1) Venturini Method

2) Modified Venturini Method

3) Scalar Method

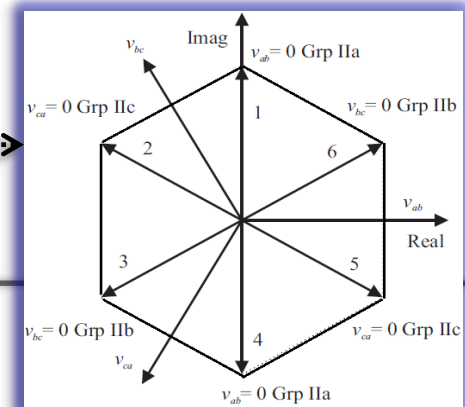
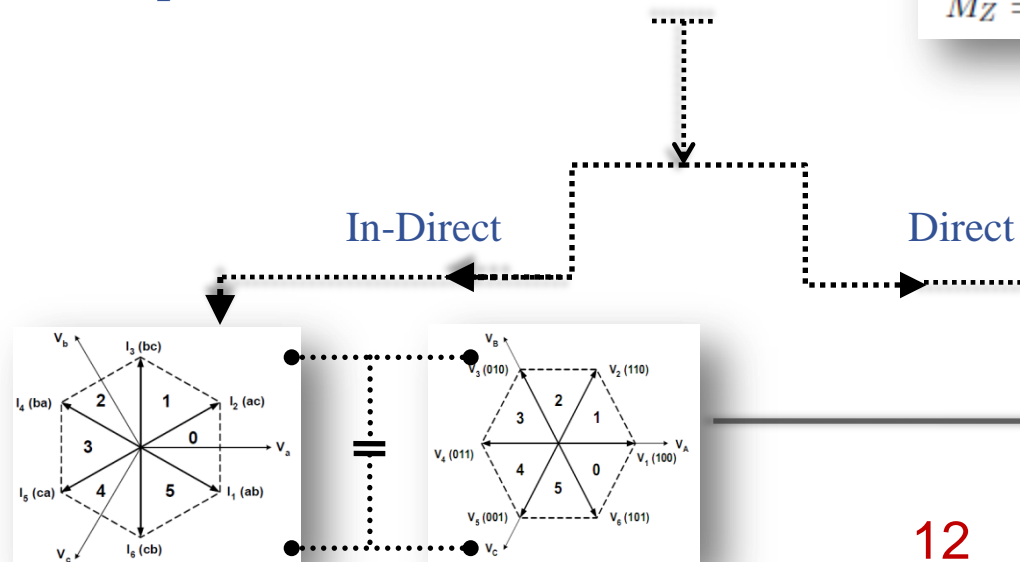
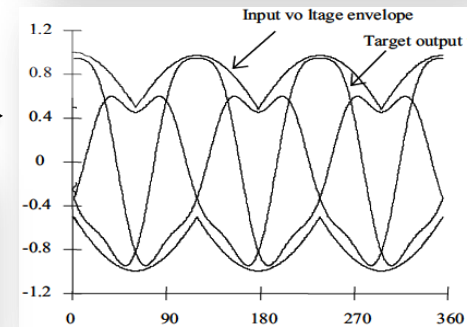
4) Space Vector PWM Method



$$M_Y = \frac{(V_{o\alpha} - V_Z)V_Y}{1.5V_i m^2}$$

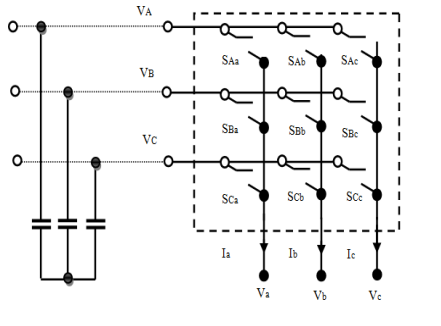
$$M_X = \frac{(V_{o\alpha} - V_Z)V_X}{1.5V_i m^2}$$

$$M_Z = T_s - (M_Y + M_X)$$

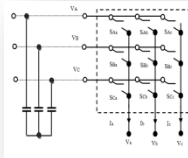


A New PWM Strategy for – Matrix Converters with High Switching Frequency

Minimum Error Switching Strategy (MESS)



A New PWM Strategy for –Matrix Converter For High Switching Frequency Minimum Error Switching Strategy (MESS)



- The **indirect-space vectors** of the MC are used for synthesizing input current and output voltage.
- Switching vectors are selected based on the **minimum computed voltage error** and **minimum computed current error** over every sampling period.
- Important features of the technique are the **simplified modulation**, **lower switching losses** and **inherent mitigation of input unbalance at the output**.
- The technique has a **poor input current THD performance** for lower switching frequencies but it is found that the performance improves with higher switching frequencies

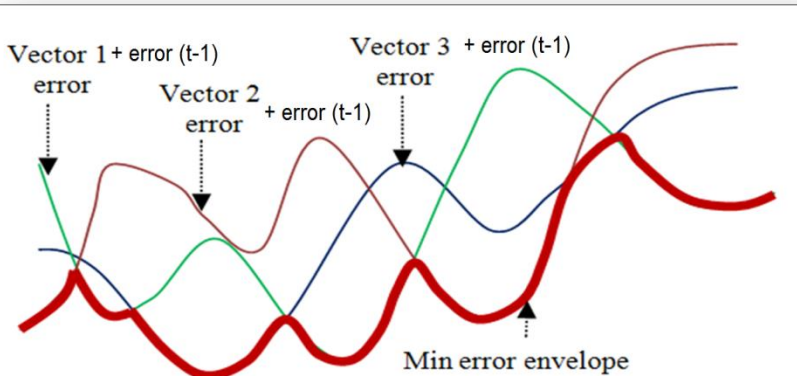
The Idea of MESS Technique

Different from space vector technique the selection of switching space vector over a sampling period is done on the following basis.

Find the errors between the reference signal(expected Output) and the computed outputs on application of all available switching space vector at the beginning of a sampling time.

To all these errors add the previous switching error.

Find the minimum of all these errors – and switch the space vector corresponding to the minimum error.



Mess is applied to both voltage side space vectors and current side space vectors – In Matrix converters

MESS - Algorithm for Matrix Converter

$$V_{mj}(t) = S_{Im} \times V_{DC} i(t), \\ m \in \{1 \rightarrow 8\}, i \in \{+, -\} \text{ & } j \in \{a, b, c\}$$

$$Ve_{mj}(t) = (V_{rj}(t) - V_{mj}(t)) + Ve_{pj}(t)$$

$$I_{mj}(t) = S_{cm}^T \times I_{DC} i(t), \\ m \in \{1 \rightarrow 9\}, i \in \{+, -\} \text{ & } j \in \{A, B, C\}$$

$$Ie_{mj}(t) = (I_{rj}(t) - I_{mj}(t)) + Ie_{pj}(t)$$

$$S_{Ion}(t) = S_{Im} \in \min_{m \rightarrow 1 \dots 8} \sum_{i=a,b,c} |Ve_{mj}(t)|^2$$

$$S_{con}(t) = S_{cm} \in \min_{m \rightarrow 1 \dots 9} \sum_{i=A,B,C} |Ie_{mj}(t)|^2$$

$$Ve_{pj}(t) = Ve_{mj}(t-1) \epsilon S_{Ion}(t-1)$$

$$Ie_{pj}(t) = Ie_{mj}(t-1) \epsilon S_{con}(t-1)$$

..

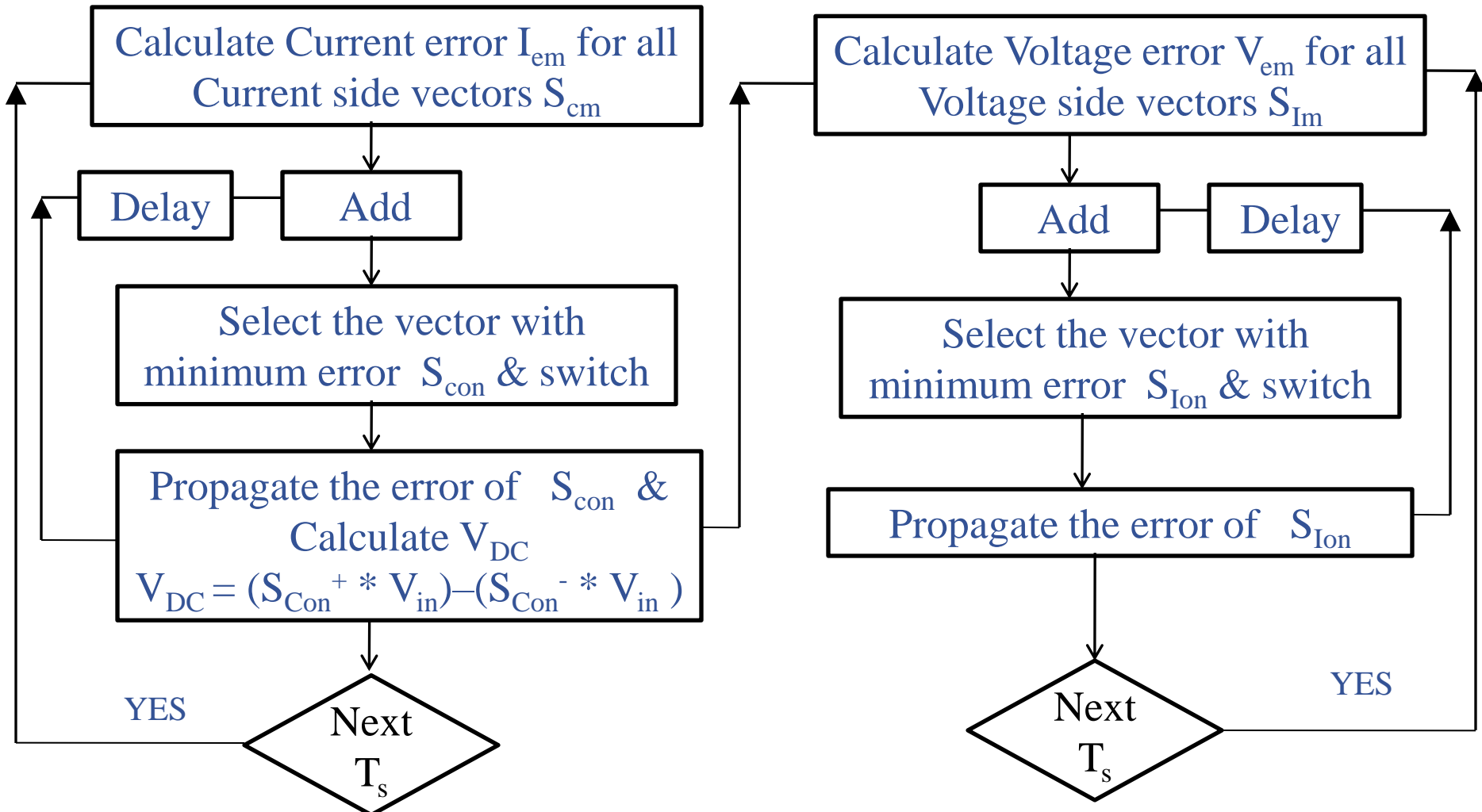
SWITCHING STATES AND INPUT CURRENTS FOR THE CSC				
m	S_{cm}	I_A	I_B	I_C
1	[1 -1 0]	I_{DC}	- I_{DC}	0
2	[1 0 -1]	I_{DC}	0	- I_{DC}
3	[0 1 -1]	0	I_{DC}	- I_{DC}
4	[-1 1 0]	- I_{DC}	I_{DC}	0
5	[-1 0 1]	- I_{DC}	0	I_{DC}
6	[0 -1 1]	0	- I_{DC}	I_{DC}
7	[(1, -1) 0 0]	0	0	0
8	[0 (1, -1) 0]	0	0	0
9	[0 0(1, -1)]	0	0	0

SWITCHING STATES AND OUTPUT VOLTAGE FOR THE FVSI

m	S_{Im}	V_a	V_b	V_c
1	[100]	$\frac{2}{3}V_{DC}$	$-\frac{1}{3}V_{DC}$	$-\frac{1}{3}V_{DC}$
2	[110]	$\frac{1}{3}V_{DC}$	$\frac{1}{3}V_{DC}$	$-\frac{2}{3}V_{DC}$
3	[010]	$-\frac{1}{3}V_{DC}$	$\frac{2}{3}V_{DC}$	$-\frac{1}{3}V_{DC}$
4	[011]	$-\frac{2}{3}V_{DC}$	$\frac{1}{3}V_{DC}$	$\frac{1}{3}V_{DC}$
5	[001]	$-\frac{1}{3}V_{DC}$	$-\frac{1}{3}V_{DC}$	$\frac{2}{3}V_{DC}$
6	[010]	$\frac{1}{3}V_{DC}$	$-\frac{2}{3}V_{DC}$	$\frac{1}{3}V_{DC}$
7	[000]	0	0	0
8	[111]	0	0	0

MESS – Flow Chart for Matrix Converter

Assuming I_{DC} is constant in the FDC Bus

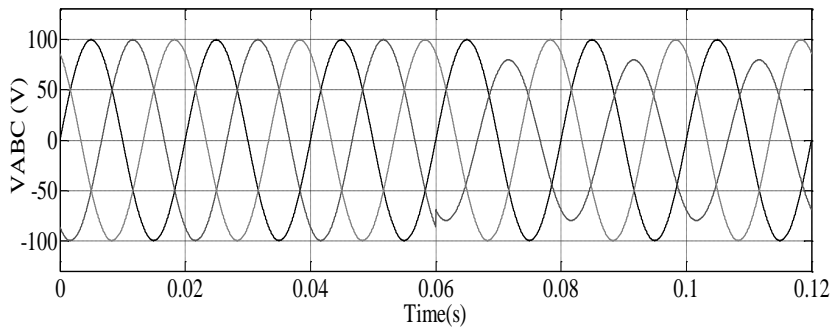


Simulation / Hardware Parameters

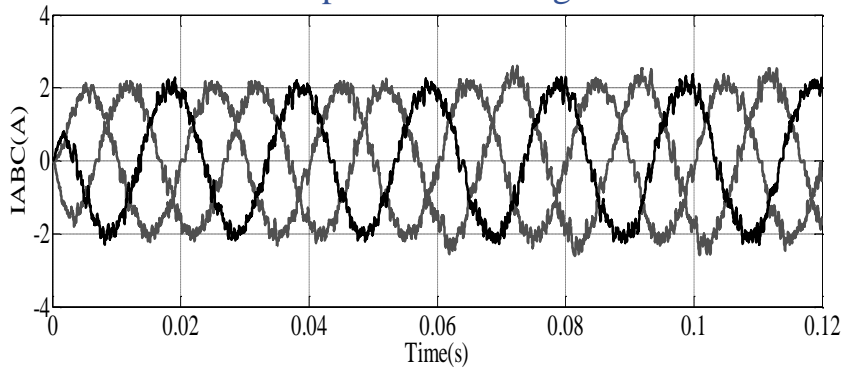
MESS

R-L Load	$R = 20\Omega$, $L = 21mH$
Input phase voltage	100 V
Input voltage frequency	50 Hz
Input filter	$L = 2 mH$, $C = 35 \mu F$, $R_d = 15 \Omega$
Output Voltage frequency	25 Hz
Switching frequency	7 kHz
Modulation Index	0.75

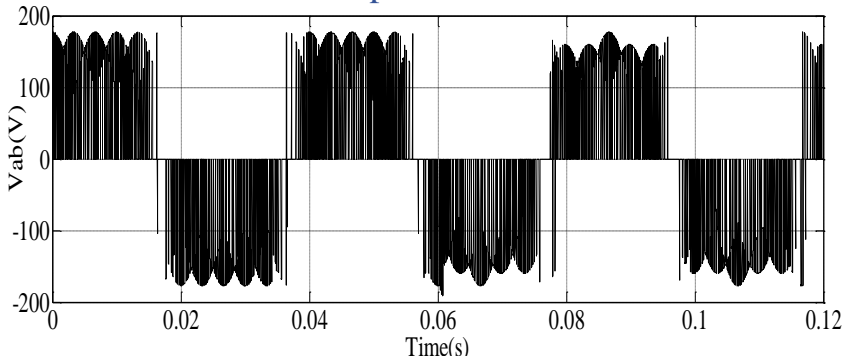
MESS - Simulation Results



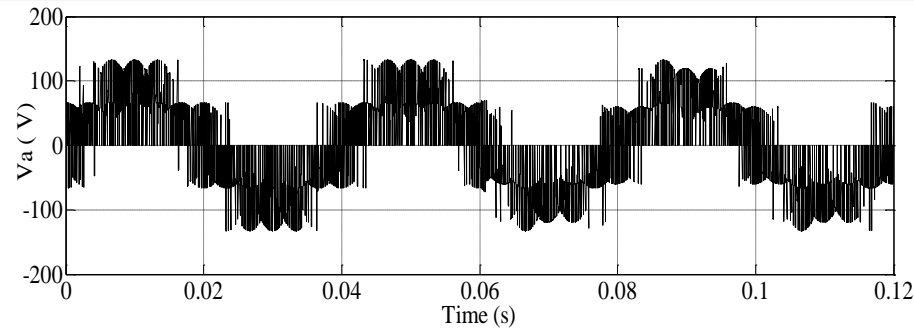
Input Phase Voltage



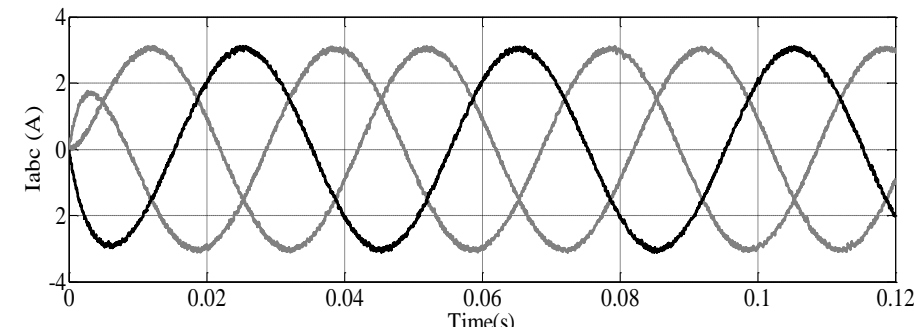
Input Current



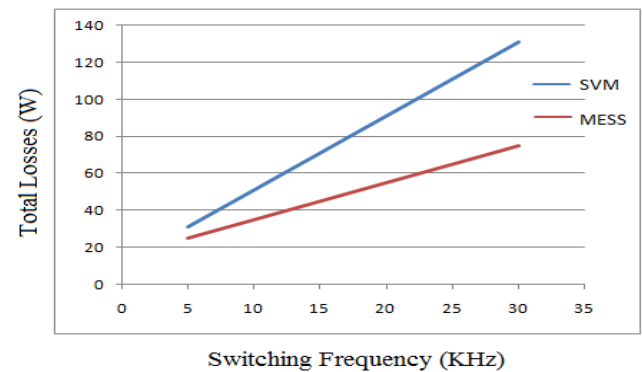
Output Line Voltage



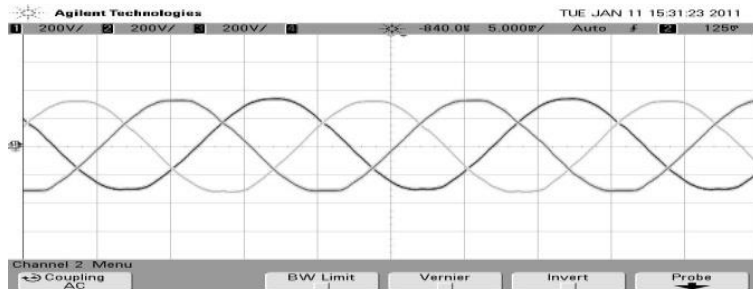
Output Phase Voltage



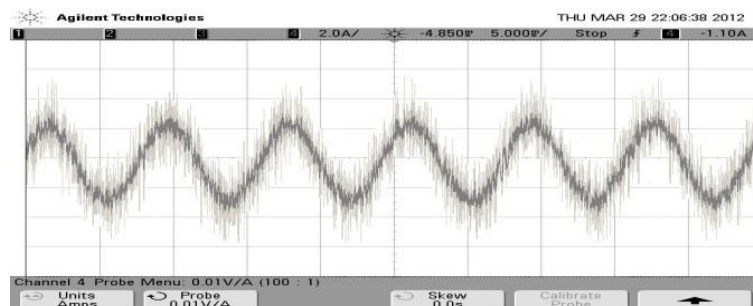
Output Current



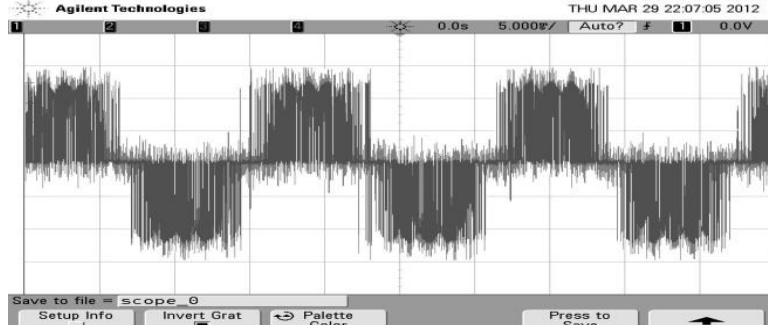
MESS - Experimental Results



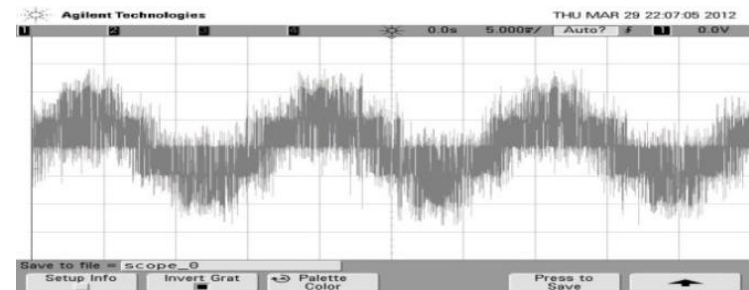
Input Phase Voltage



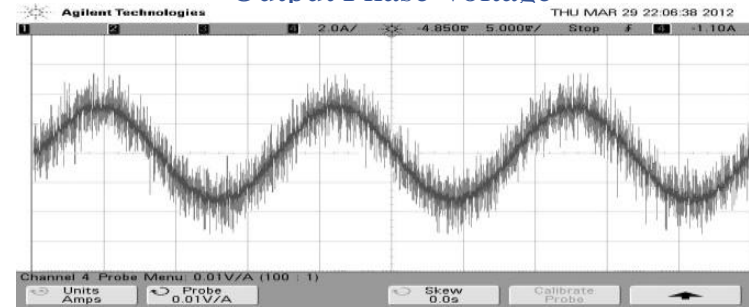
Input Current



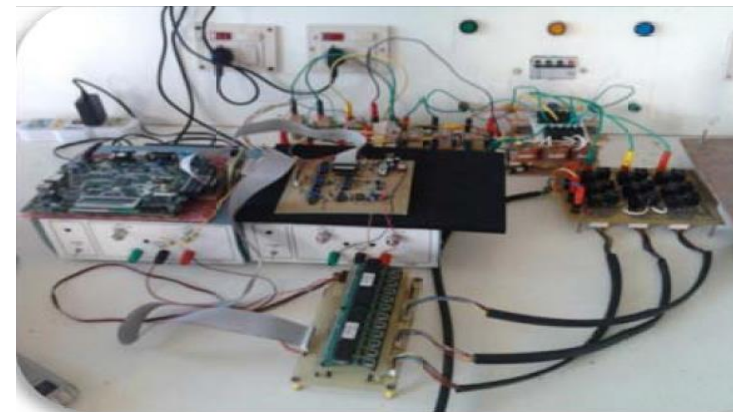
Output Line Voltage



Output Phase Voltage



Output Current

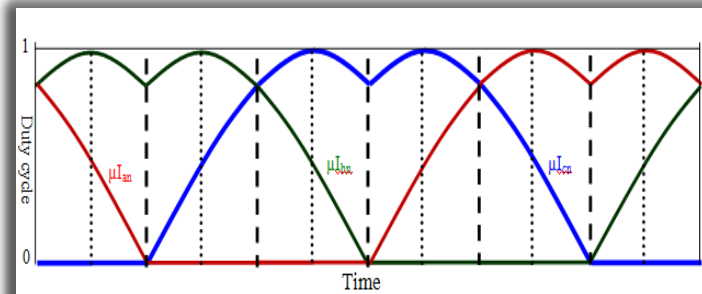
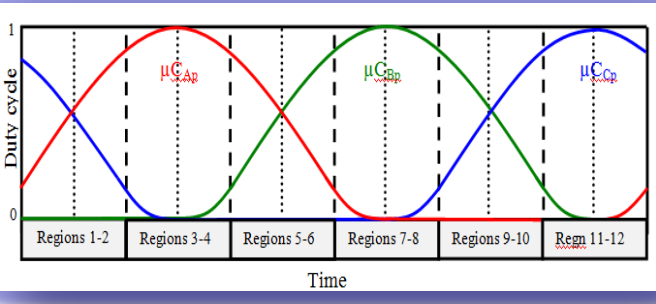


SUMMARY

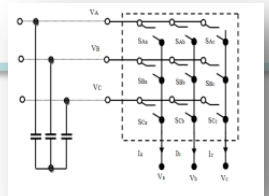
- 1) Literature Review of the work is carried out
- 2) Fundamentals of Matrix converter is reviewed
- 3) A new Minimum error switching strategy (MESS) was proposed
- 4) The highlights such as
 - 1) Simple modulation strategy
 - 2) Lower switching losses
 - 3) Inherent quality to mitigate unbalance at input.
 - 4) Suitable for very high switching frequency are reported
- 5) Demerits such as
 - 1) Higher THD in the input current for lower switching frequency
- 6) Objective & organization of the work

CHAPTER -II

Decoupled Indirect Duty Cycle PWM for Matrix Converter



Decoupled Indirect Duty Cycle PWM Technique for –Matrix Converter



Carrier based and Computation free implementation

The basic idea of the proposed DIDC PWM is to reduce the computations required to calculate the duty cycle as in SVM.

The **duty cycle information**, extracted from the **input voltage signal** through a classic analog circuit directly generates the firing pulses

The proposed **carrier frequency adjustment** method increases the performance of the DIDC PWM technique

- Important features of the technique is the **computation free implementation**

Modeling of decoupled Rectifier & Inverter

Rectifier Modeling

The expected input current at each leg

$$I_A = I_m \sin(\omega_i t + \varphi_i)$$

$$I_B = I_m \sin(\omega_i t + \varphi_i - 120^\circ)$$

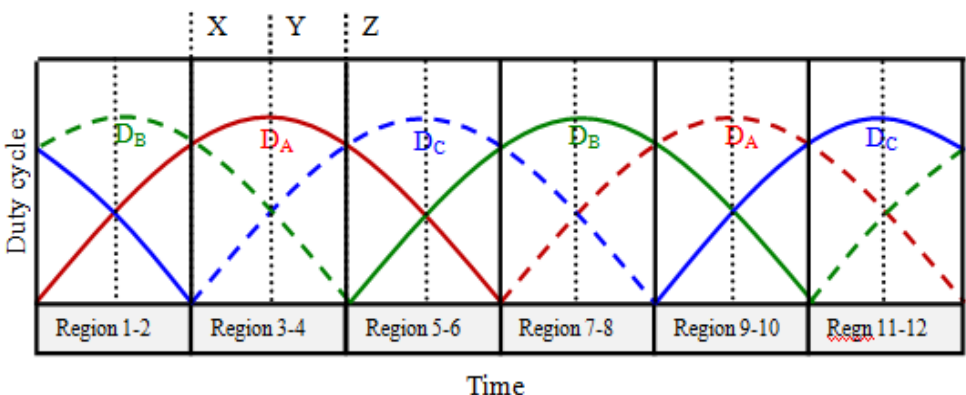
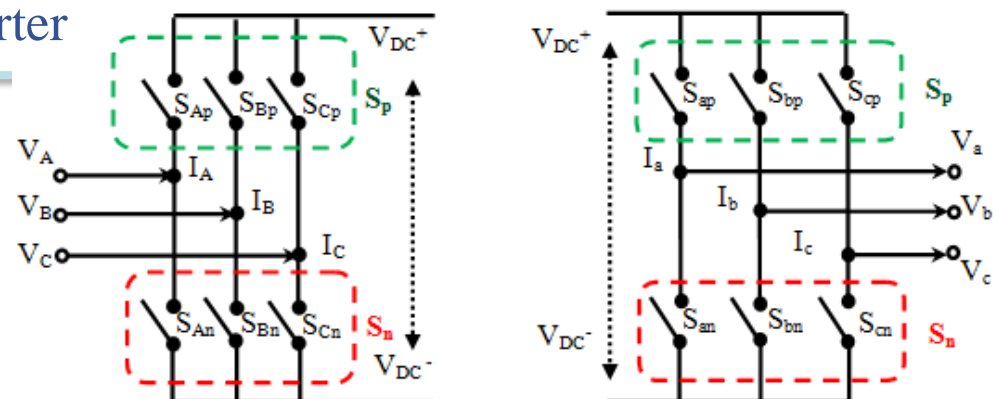
$$I_C = I_m \sin(\omega_i t + \varphi_i + 120^\circ)$$

The duty cycle for each leg

$$D_A = |\sin(\omega_i t + \varphi_i)|$$

$$D_B = |\sin(\omega_i t + \varphi_i - 120^\circ)|$$

$$D_C = |\sin(\omega_i t + \varphi_i + 120^\circ)|$$



Leg with maximum duty cycle	Leg with decreasing duty cycle	Leg with increasing duty cycle
A Phase Leg	B Phase Leg	C Phase Leg
B Phase Leg	C Phase Leg	A Phase Leg
C Phase Leg	A Phase Leg	B Phase Leg

Rectifier Modeling

The duty cycle for each Switch

$$\mu C_{Ap} = (D_A + \sin(\omega_i t + \varphi_i))/2$$

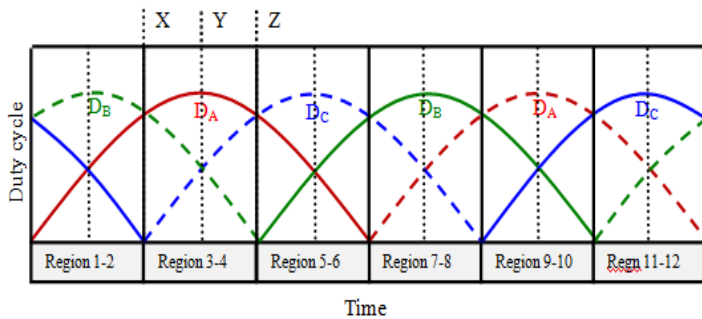
$$\mu C_{Bp} = (D_B + \sin(\omega_i t + \varphi_i - 120^\circ))/2$$

$$\mu C_{Cp} = (D_C + \sin(\omega_i t + \varphi_i + 120^\circ))/2$$

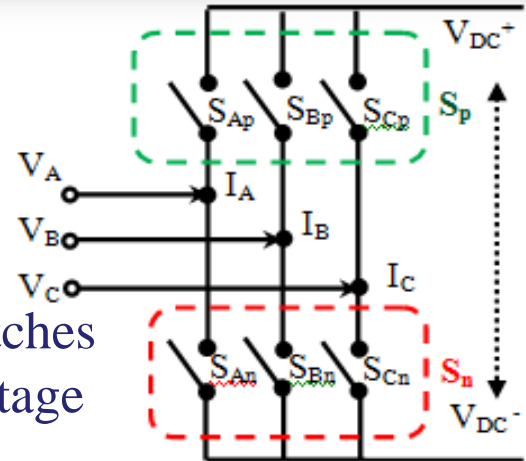
$$\mu C_{An} = (D_A - \sin(\omega_i t + \varphi_i))/2$$

$$\mu C_{Bn} = (D_B - \sin(\omega_i t + \varphi_i - 120^\circ))/2$$

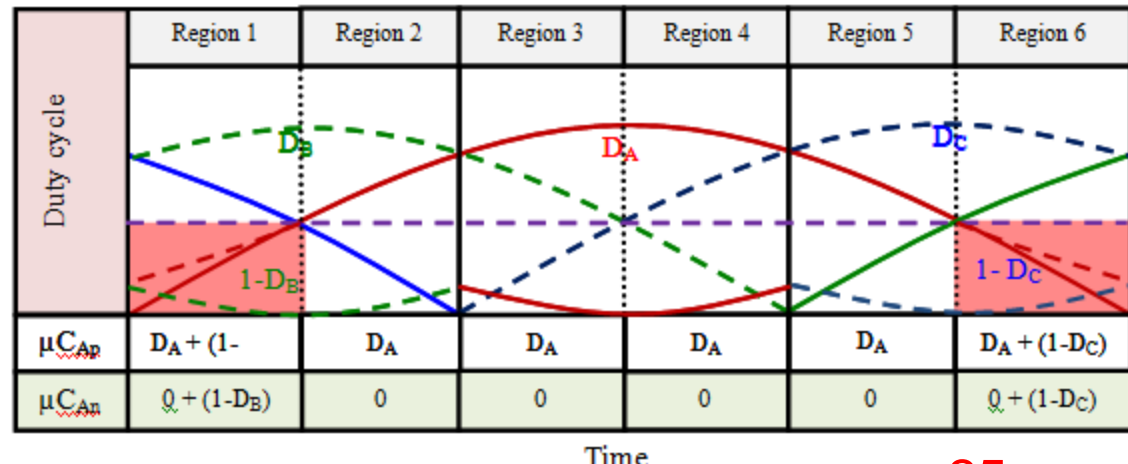
$$\mu C_{Cn} = (D_C - \sin(\omega_i t + \varphi_i + 120^\circ))/2$$



- Rectifier dose not conduct for a time of $(1-D_{max}) * T_S$
- The free-wheeling path is provided by putting ON both switches of leg with the V_{min} to provide a reduced common mode voltage

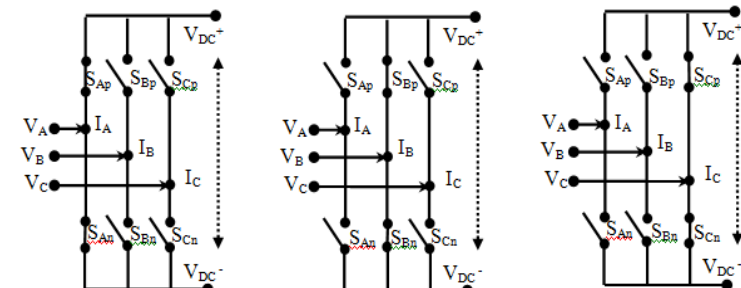


Modified duty cycle of the switches in the leg with minimum Duty cycle is given as



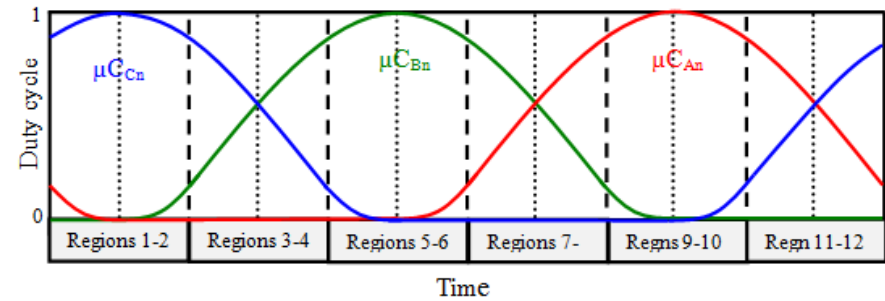
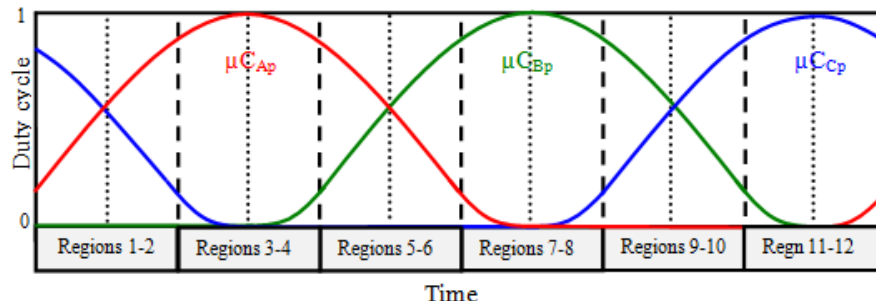
$$\mu C_{Dmin_p}^* = \mu C_{Dmin_p} + (1 - D_{max})$$

$$\mu C_{Dmin_n}^* = \mu C_{Dmin_n} + (1 - D_{max})$$



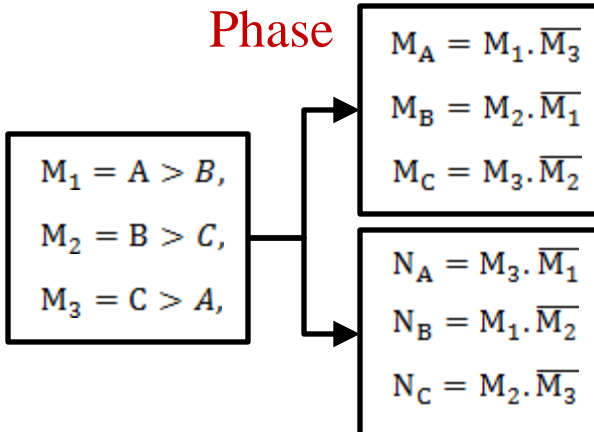
Rectifier Modeling

The modified duty cycle for each Switch in different regions is represented below



Signals generated for producing the Firing pulses

Maximum & Minimum

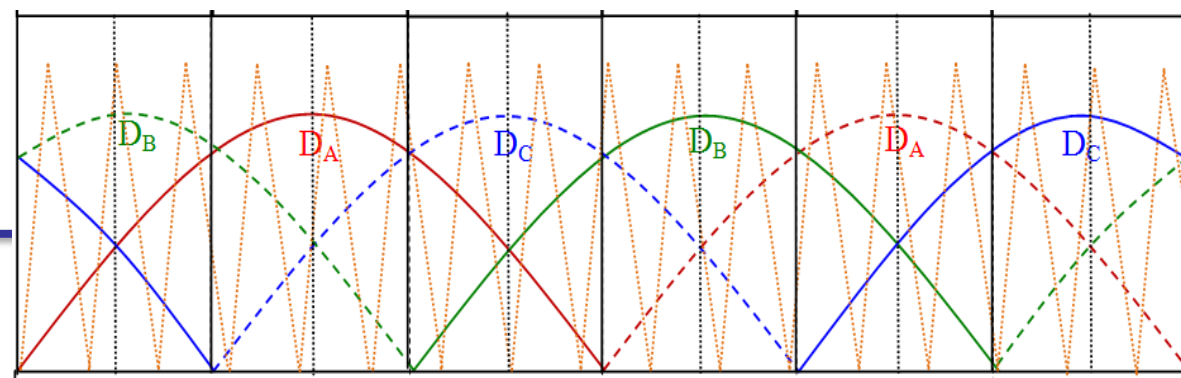


Polarity of the Phase

$$\begin{aligned} P_B &= B > 0, \\ P_A &= A > 0, \\ P_C &= C > 0, \end{aligned}$$

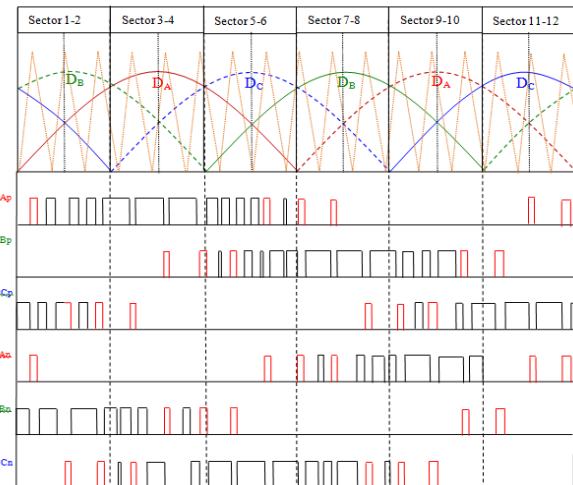
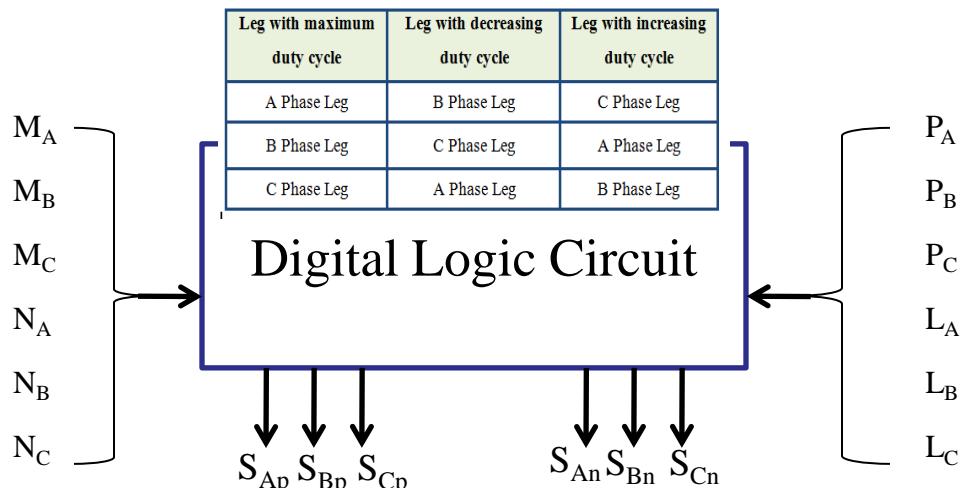
Carrier & Phase Comparator

$$\begin{aligned} L_A &= \text{Trig} < A, \\ L_B &= \text{Trig} < B, \\ L_C &= \text{Trig} < C \end{aligned}$$



Development of the LOGIC circuit

- If a phase is maximum [$M_i=1$], carrier less than the phase voltage [$L_i=1$] and positive [$P_i=1$] then the switch S_{ip} is ON. If $M_i=1$ and $L_i = 1$ and $[P_i=0]$ (i.e.) negative then the switch S_{in} is ON.
- If $L_j=1$ and $P_j=1$, the switch S_{jp} is ON else if $L_j=1$ and $P_j=0$, the switch S_{jn} is ON.
- If $P_k=1$, $L_j=0$ and $L_i=1$, the switch S_{kp} is ON else if $P_k=0$, $L_j=0$ and $L_i=1$ the switch S_{kn} is ON.
- If $L_i= 0$ and $N_j=1$ then switches S_{jp} and S_{jn} are ON else If $L_i= 0$ and $N_k=1$ then switches S_{kp} and S_{kn} are ON.



Inverter Modeling....

The expected output voltage

$$V_a = V_m \sin(\omega_o t + \varphi_o)$$

$$V_b = V_m \sin(\omega_o t + \varphi_o - 120^\circ)$$

$$V_c = V_m \sin(\omega_o t + \varphi_o + 120^\circ)$$

Duty cycle of the Inverter with Sin PWM

$$\mu I_{ap} = (1 + \sin(\omega_o t + \varphi_o))/2$$

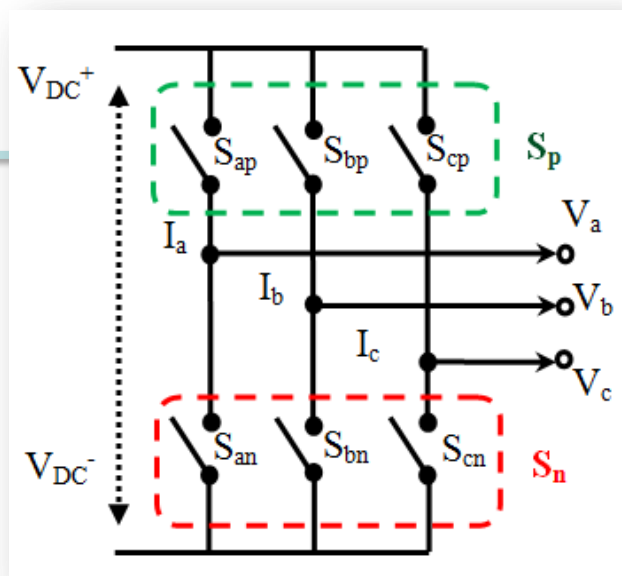
$$\mu I_{bp} = (1 + \sin(\omega_o t + \varphi_o - 120^\circ))/2$$

$$\mu I_{cp} = (1 + \sin(\omega_o t + \varphi_o + 120^\circ))/2$$

DC bus utilization of Sin PWM = $V_{DC}/2$, To increase it by a factor of $2/\sqrt{3}$

The modified Duty cycles are given as

$$D_a = D_b = D_c = 1 - Z_{3c}$$



Constraint of the Inverter arm i

$$\mu I_{ip} + \mu I_{in} = 1$$

The duty cycle for each leg

$$D_a = D_b = D_c = 1$$

Inverter Modeling

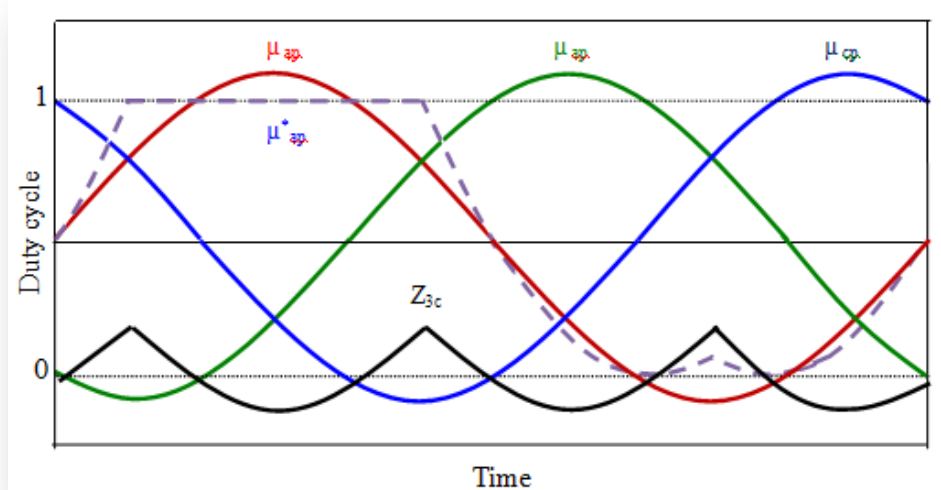
Z_{3c} is the zero sequence third harmonic component

$$Z_{3c} = - \left((1 - 2K_0) + K_0 \mu I_{\max_p} + (1 - K_0) \mu I_{\min_p} \right)$$

K_0 ratio of sharing the two zero vectors V_0 and V_7

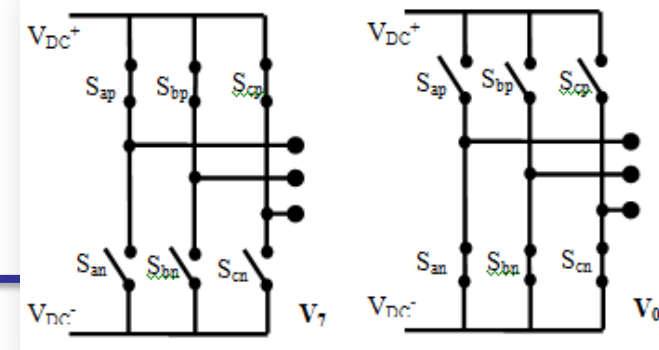
When K_0 is fixed as 1 (only V_7 used) $Z_{3c} = (1 - \mu I_{\max_p})$

Modified duty cycle of the switches is given as



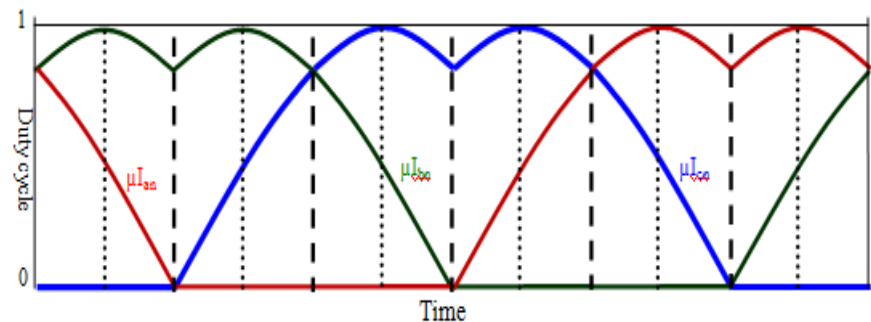
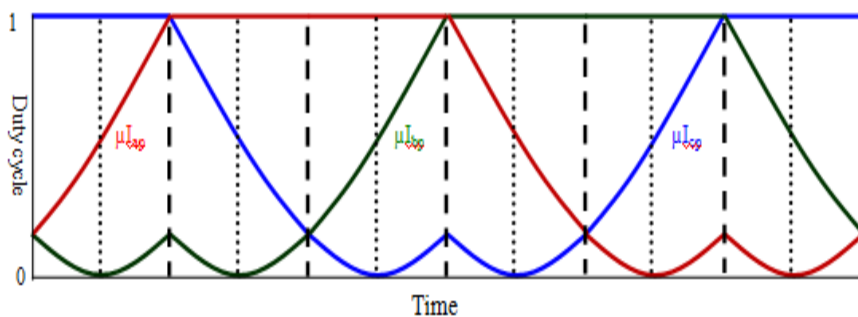
$$\begin{aligned}\mu I_{ap}^* &= ((1 + \frac{2}{\sqrt{3}} \sin(\omega_o t + \varphi_o)) / 2) + Z_{3c} \\ \mu I_{bp}^* &= ((1 + \frac{2}{\sqrt{3}} \sin(\omega_o t + \varphi_o - 120^\circ)) / 2) + Z_{3c} \\ \mu I_{cp}^* &= ((1 + \frac{2}{\sqrt{3}} \sin(\omega_o t + \varphi_o + 120^\circ)) / 2) + Z_{3c}\end{aligned}$$

Two free-wheeling paths

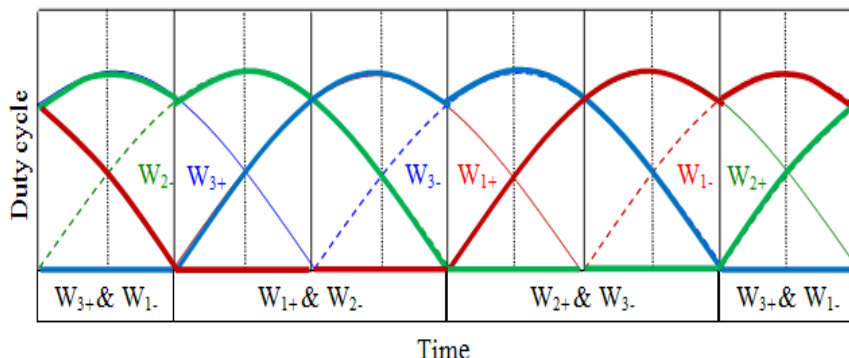


Inverter Modeling

The modified duty cycle for each Switch in different regions is represented below



On superimposing a 3-phase rectified waveform $|W_{123}|$ of the same frequency



Regions Switches	$W_{1+} \& W_{2-}$	$W_{2+} \& W_{3-}$	$W_{3+} \& W_{1-}$
μI_{ap}	1	$(1 - W_2)$	$(1 - W_1)$
μI_{bp}	$(1 - W_2)$	1	$(1 - W_3)$
μI_{cp}	$(1 - W_1)$	$(1 - W_3)$	1
μI_{an}	0	$ W_2 $	$ W_1 $
μI_{bn}	$ W_2 $	0	$ W_3 $
μI_{cn}	$ W_1 $	$ W_3 $	0

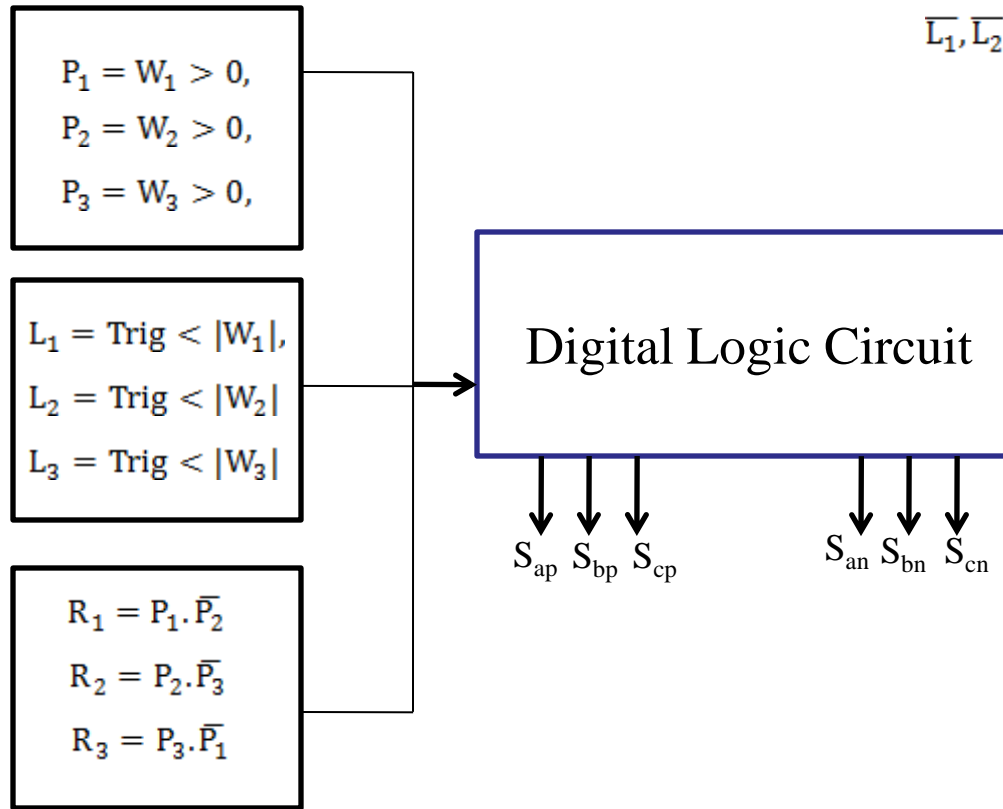
it is observed that the duty cycle of each switch is simply the selected portions of $|W_{123}|$

Three Distinct Regions - Identified

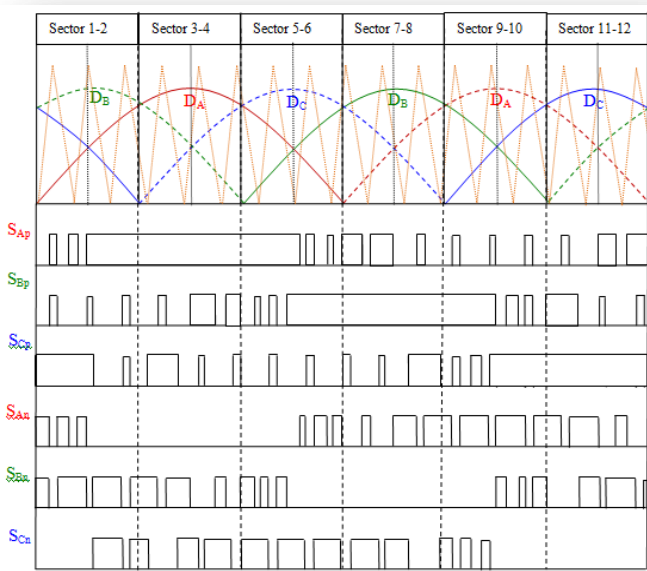
Inverter Modeling

Signals generated for producing the Firing pulses

L_1, L_2, L_3 Proportional $|W_1|, |W_2|, |W_3|$



$\bar{L}_1, \bar{L}_2, \bar{L}_3$ Proportional $|(1 - W_1)|, |(1 - W_2)|, |(1 - W_3)|$

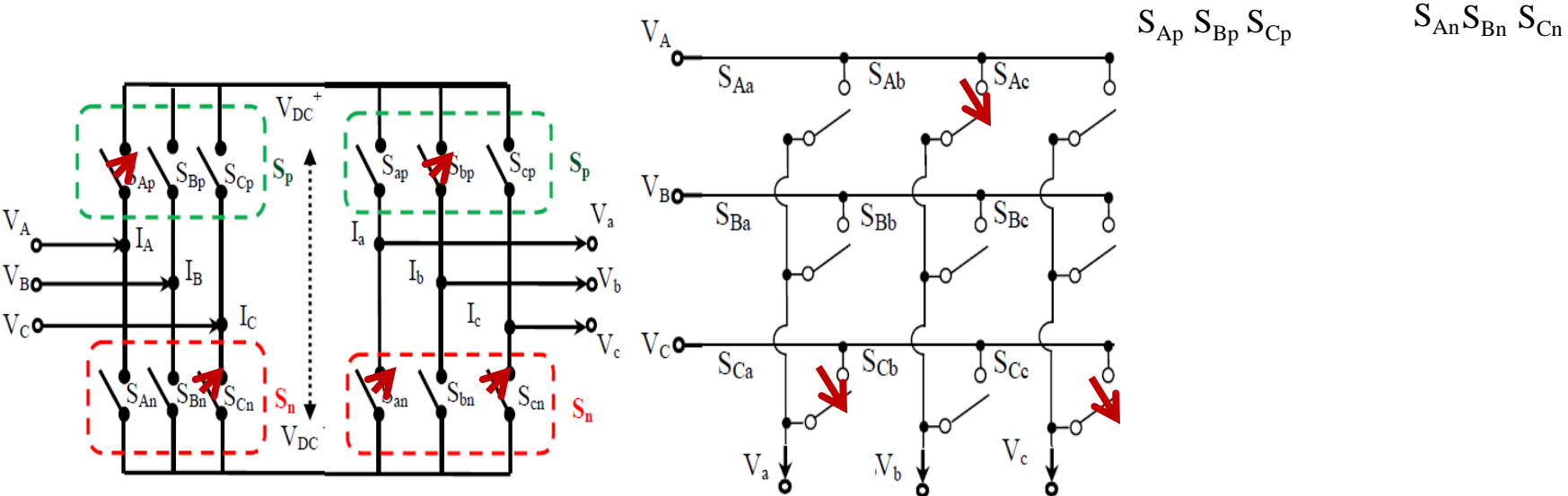
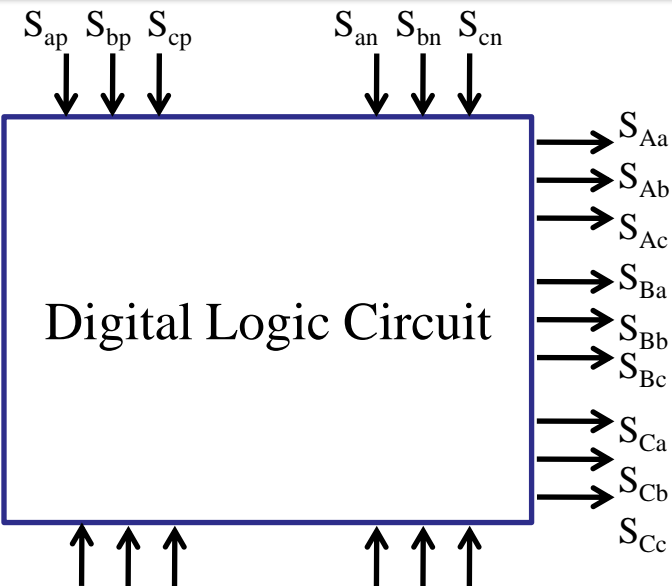


Matrix Converter Switching Signals

Signals generated for producing the Firing pulses

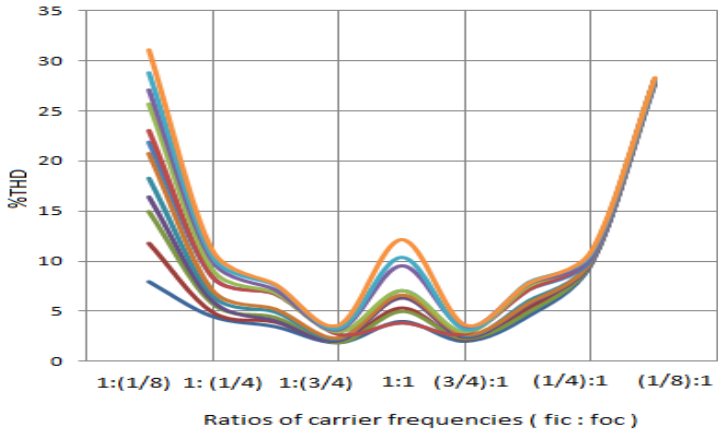
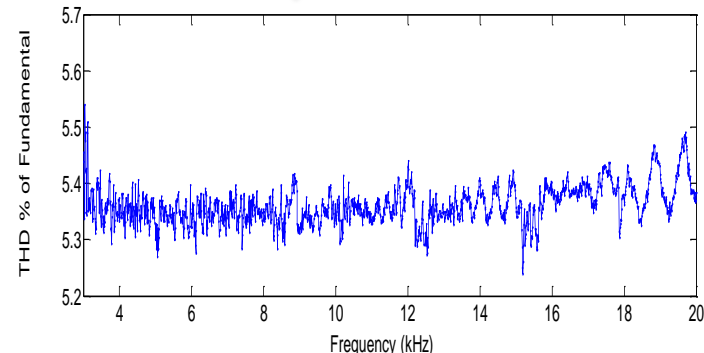
$$\begin{bmatrix} S_{Aa} & S_{Ab} & S_{Ac} \\ S_{Ba} & S_{Bb} & S_{Bc} \\ S_{Ca} & S_{Cb} & S_{Cc} \end{bmatrix} =$$

$$\begin{bmatrix} S_{ap} \cdot S_{Ap} + S_{An} \cdot S_{An} & S_{ap} \cdot S_{Bp} + S_{an} \cdot S_{Bn} & S_{ap} \cdot S_{Cp} + S_{an} \cdot S_{Cn} \\ S_{bp} \cdot S_{Ap} + S_{bn} \cdot S_{An} & S_{bp} \cdot S_{Bp} + S_{bn} \cdot S_{Bn} & S_{bp} \cdot S_{Cp} + S_{bn} \cdot S_{Cn} \\ S_{cp} \cdot S_{Ap} + S_{cn} \cdot S_{An} & S_{cp} \cdot S_{Bp} + S_{cn} \cdot S_{Bn} & S_{cp} \cdot S_{Cp} + S_{cn} \cdot S_{Cn} \end{bmatrix}$$



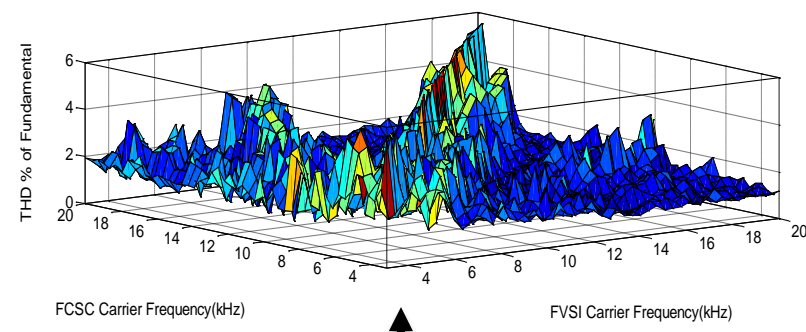
Carrier frequency adjustment technique to improve the THD

THD when $f_{sic} = f_{soc}$ & $f_o = 20$ Hz

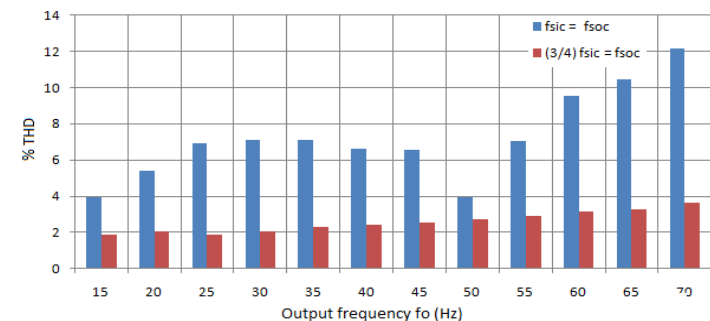


THD for various f_{sic} , f_{soc} , f_o

f_{sic} = input converter switching frequency
 f_{soc} = output converter switching frequency
 f_o = output frequency at the load



THD when $f_{sic} \neq f_{soc}$ & $f_o = 20$ Hz



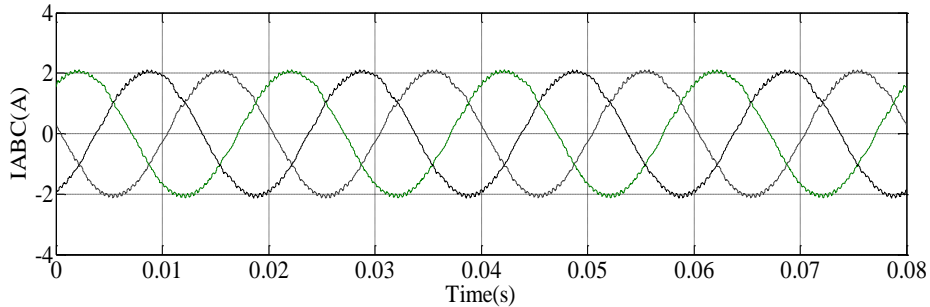
THD for various f_o with a ratio of $\frac{3}{4}$ between f_{sic} & f_{soc}

DIDCPWM - Simulation/ Hardware Parameters

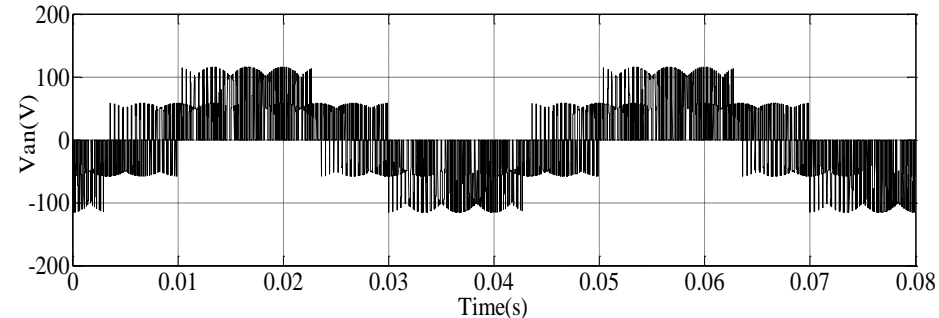
DIDC

R-L Load	$R = 20 \Omega, L = 21 \text{ mH}$
Input Phase Voltage	100 V
Input Voltage Frequency	50 Hz
Input Filter	$L = 2.5 \text{ mH}, C = 10 \mu\text{F}, R_d = 15 \Omega$
Output Voltage Frequency	25 Hz
Modulation Index	0.75
Switching frequency	7 kHz

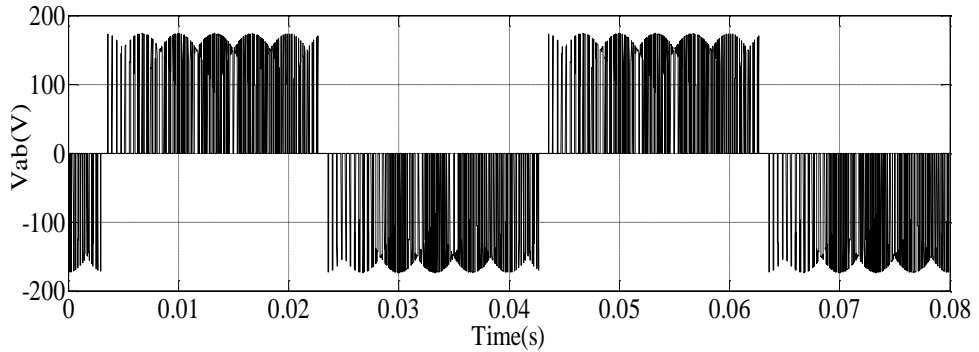
DIDCPWM - Simulation Results



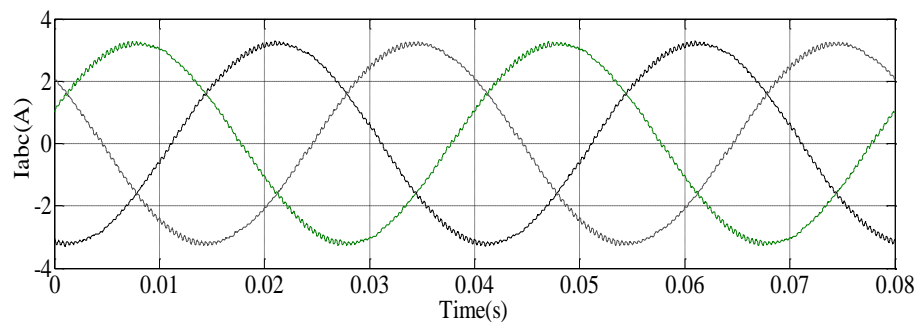
Input Current



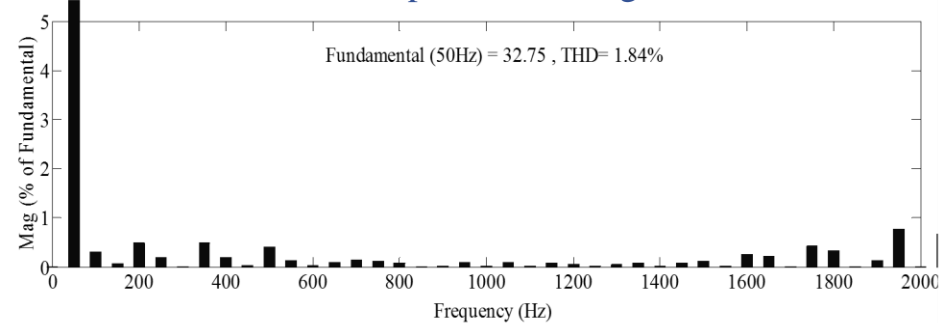
Output Phase Voltage



Output Line Voltage

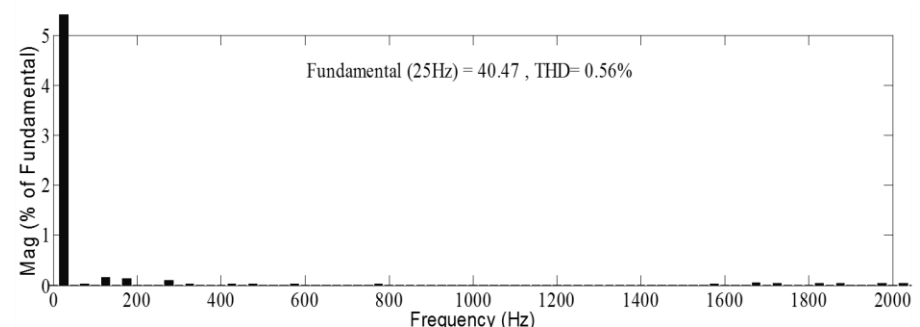


Output Current



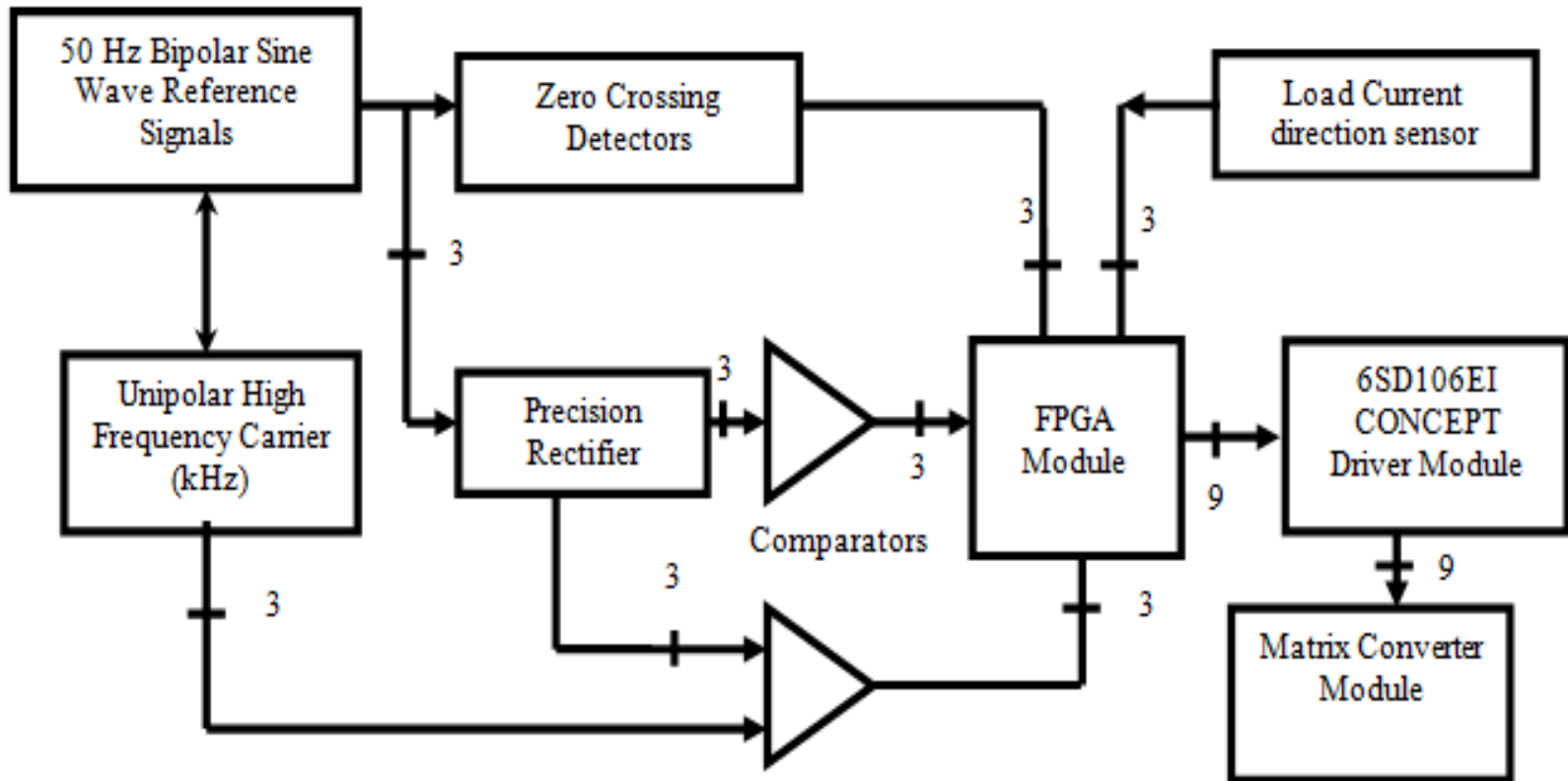
Input Current THD when $f_{s_{ic}} = \frac{3}{4} f_{s_{oc}}$

35

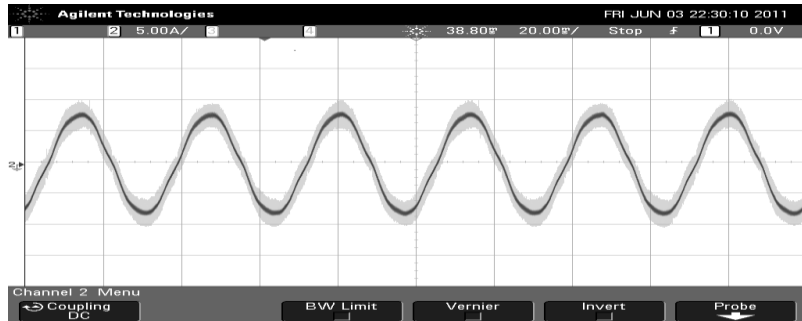


Output Current THD

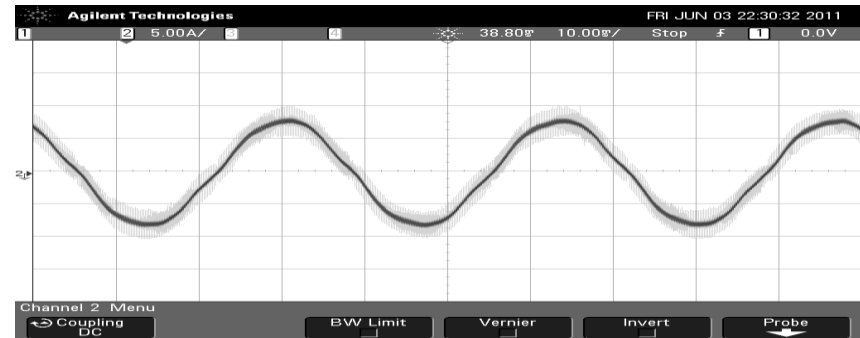
DIDCPWM -Hardware Implementation



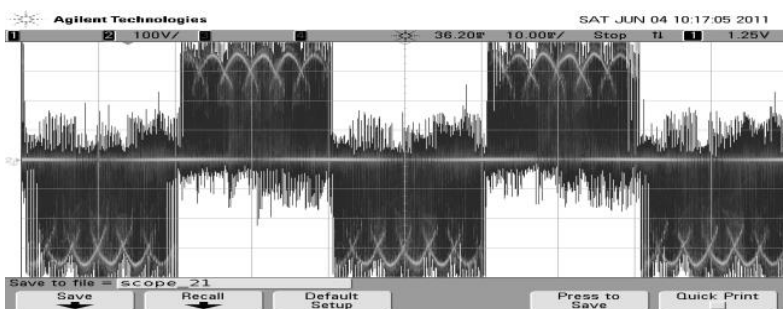
DIDCPWM - Hardware Results



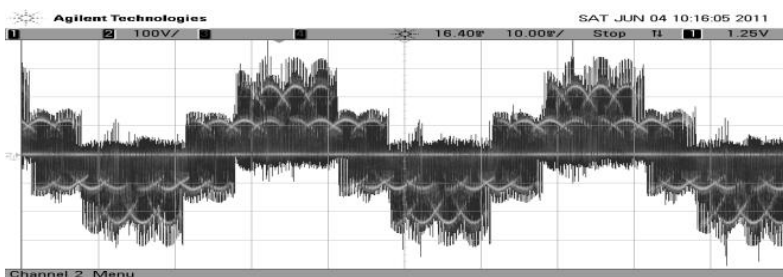
Input Current



Output Current



Output Line Voltage



Output Phase Voltage



Hardware Prototype

SUMMARY

A complete **carrier frequency** technique(DIDC-PWM) for CMC working under unity displacement factor was modeled and proposed

The focus of the technique is to reduce / **eliminate the computations** required to modulate the matrix converters. with superior characteristics

The harmonic content of the input current has been found to be high compared to DSVPWM

A **CFAT** has been proposed to decrease the input current harmonics.

A ratio of **1:3/4** for the input carrier to output carrier frequencies has been identified for the lowest THD under all input output conditions

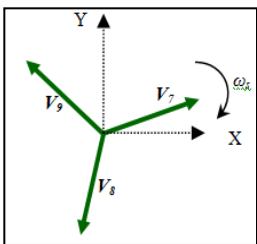
Hardware prototype was developed to show the implementation of the technique



CHAPTER –III

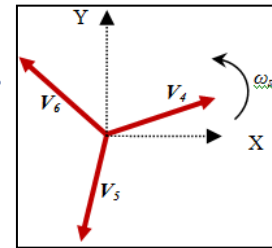
Rotating Space Vector
Modulation (**RSVM**)Strategy
for Matrix Converters to
Eliminate Common Mode
Voltage in Induction
Machines





RSVM Technique for Matrix Converter

Use of the rotating space vector for the elimination of common mode voltage



The MC contains 27 valid direct space vectors. 3 Zero vectors , 18 Standing vectors , 6 Rotating space vectors (RSV).

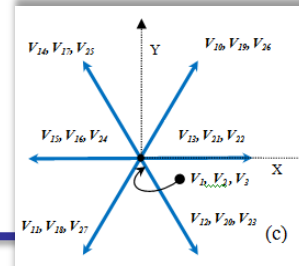
3 RSV's move in the clock wise direction and 3 in the opposite direction.

These 6 RSV's are used for controlling the input power factor along with elimination of common mode voltage

RSV's applied to MC can only eliminate common mode voltage (CMV) in induction machines.

The use of RSV's limits the voltage transfer ratio (VTR) to 0.5

The use of 6-phase matrix converter (PSDSMC)for a 3- phase induction machine with increased voltage transfer ratio for elimination of CMV is proposed.



RSVM Technique for Matrix Converter

$V_a + V_b + V_c = 0$ for balanced input:

if all the inputs are connected to all the outputs CMV is eliminated

3 - Clockwise Rotating Space vectors – Switching pattern

$$\begin{bmatrix} S_{Aa} & S_{Ab} & S_{Ac} \\ S_{Ba} & S_{Bb} & S_{Bc} \\ S_{Ca} & S_{Cb} & S_{Cc} \end{bmatrix} = \begin{bmatrix} 1 & 0 & 0 \\ 0 & 1 & 0 \\ 0 & 0 & 1 \end{bmatrix} \text{ or } \begin{bmatrix} 0 & 0 & 1 \\ 1 & 0 & 0 \\ 0 & 1 & 0 \end{bmatrix} \text{ or } \begin{bmatrix} 0 & 1 & 0 \\ 0 & 0 & 1 \\ 1 & 0 & 0 \end{bmatrix}$$

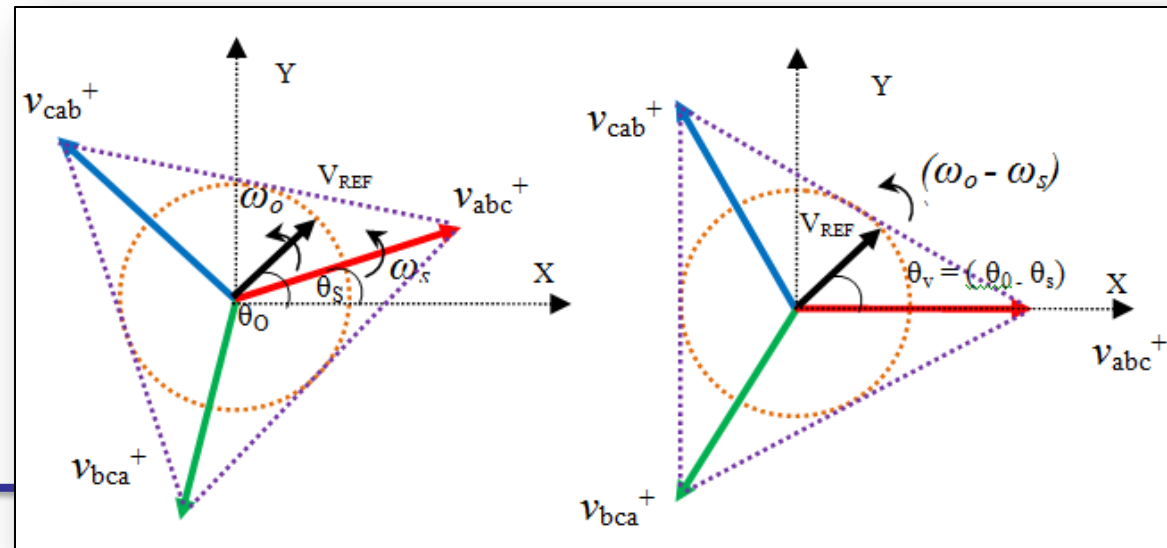
The positions of active switching voltage vectors and reference output voltage vector in space

$$v_{abc}^+ = \frac{3}{2} V_i * e^{j\omega_s t}$$

$$v_{cab}^+ = \frac{3}{2} V_i * e^{j(\omega_s t + \frac{2\pi}{3})}$$

$$v_{bca}^+ = \frac{3}{2} V_i * e^{j(\omega_s t - \frac{2\pi}{3})}$$

$$v_o = \frac{3}{2} V_o * e^{j\omega_0 t}$$



Using Sine law of triangles

Duty cycles of the active and zero vectors are given as

$$\frac{d_\alpha v_\alpha}{\sin(120^\circ - \theta_v)} = \frac{d_\beta v_\beta}{\sin(\theta_v)} = \frac{V_o(\text{REF})}{\sin(60^\circ)}$$

$$d_\alpha = m_v \sin(120^\circ - \theta_v)$$

$$d_\beta = m_v \sin(\theta_v)$$

$$d_0 = 1 - d_\alpha - d_\beta$$

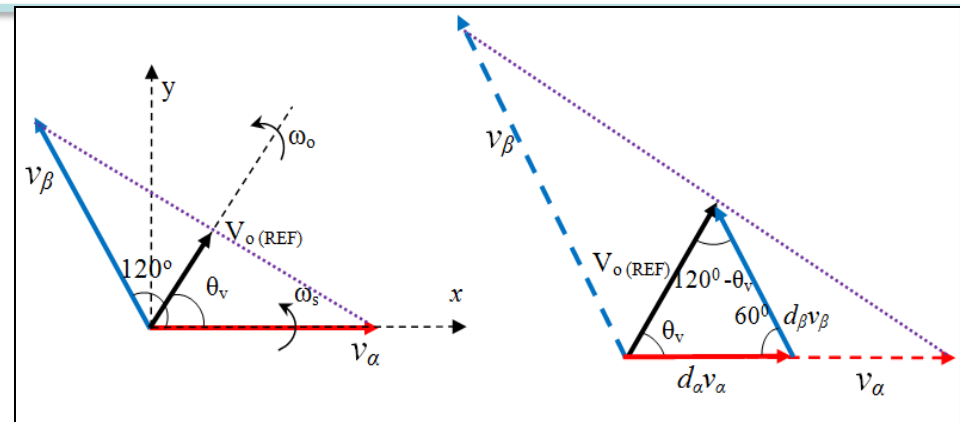
Modified duty cycle of the RSV

$$d_1^+ = d_\alpha' = m_v \sin(120^\circ - \theta_v) + \frac{d_0}{3}$$

$$d_2^+ = d_\beta' = m_v \sin(\theta_v) + \frac{d_0}{3}$$

$$d_3^+ = d_0' = \frac{d_0}{3}$$

$$v_o = d_1^+ v_1 + d_2^+ v_2 + d_3^+ v_3$$



Zero vector synthesis

$$d_m v_{abc}^+ + d_m v_{cab}^+ + d_m v_{bca}^+ = 0$$

Selection of V_1, V_2, V_3 in each sector

S. No.	θ_v	Sector No	Active vectors		
			v_1	v_2	v_3
1	$0^\circ < \theta_v \leq 120^\circ$	1	v_{abc}^+	v_{cab}^+	v_{bca}^+
2	$120^\circ < \theta_v \leq 240^\circ$	2	v_{cab}^+	v_{bca}^+	v_{abc}^+
3	$240^\circ < \theta_v \leq 360^\circ$	3	v_{bca}^+	v_{abc}^+	v_{cab}^+

Method for input power factor control

Using + (or) Clock wise rotating vectors.

The output current vector in space is given as

$$i_{abc}^+ = \frac{3}{2} I_o * e^{j(\omega_0 t - \rho)}$$

$$i_{cab}^+ = \frac{3}{2} I_o * e^{j(\omega_0 t - \rho + \frac{2\pi}{3})}$$

$$i_{bca}^+ = \frac{3}{2} I_o * e^{j(\omega_0 t - \rho - \frac{2\pi}{3})}$$

The Input current vector in space is given as

$$i_s = \frac{3}{2} I_o * e^{j(\omega_s t - \rho)}$$

Using - (or) Anti clock wise rotating vectors.

The output current vector in space is given as

$$i_{acb}^- = \frac{3}{2} I_o * e^{-j(\omega_0 t - \rho)}$$

$$i_{bac}^- = \frac{3}{2} I_o * e^{-j(\omega_0 t - \rho + \frac{2\pi}{3})}$$

$$i_{cba}^- = \frac{3}{2} I_o * e^{-j(\omega_0 t - \rho - \frac{2\pi}{3})}$$

The Input current vector in space is given as

$$i_s = \frac{3}{2} I_o * e^{j(\omega_s t + \rho)}$$

The ratio in which the + & - RSV are used brings the control to input power factor within the range of

$$\cos \rho < \cos \phi < 1$$

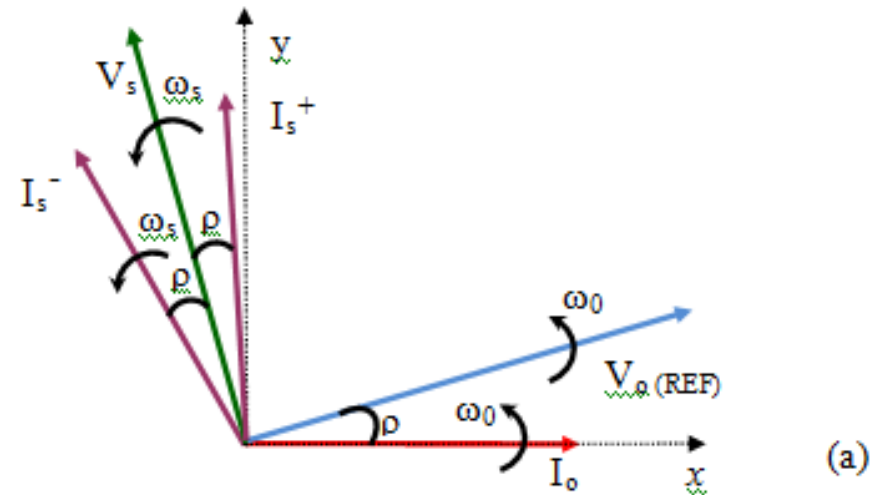
Method for input power factor control

d^+ = Total duty cycle time of + RSV

d^- = Total duty cycle time of - RSV

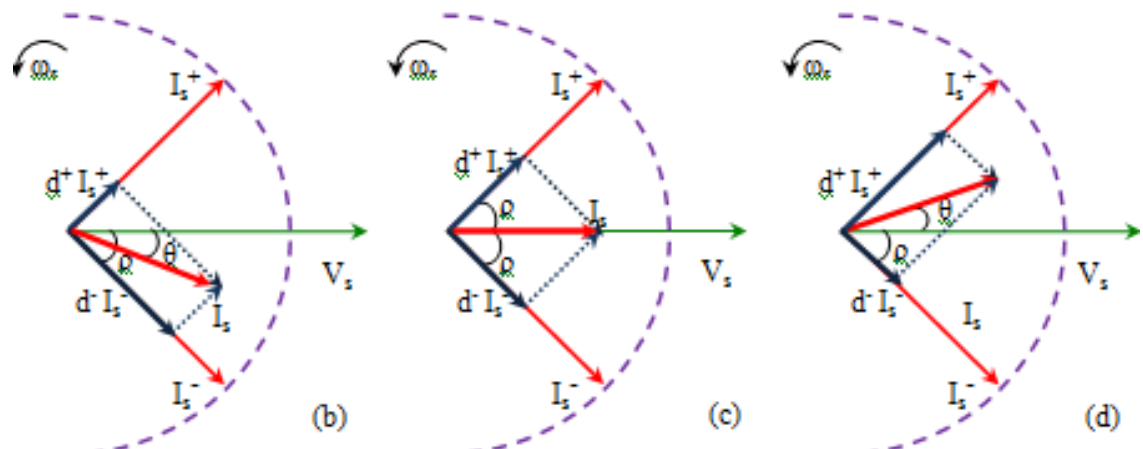
$$d^+ + d^- = 1$$

Vector representation of Input power factor control

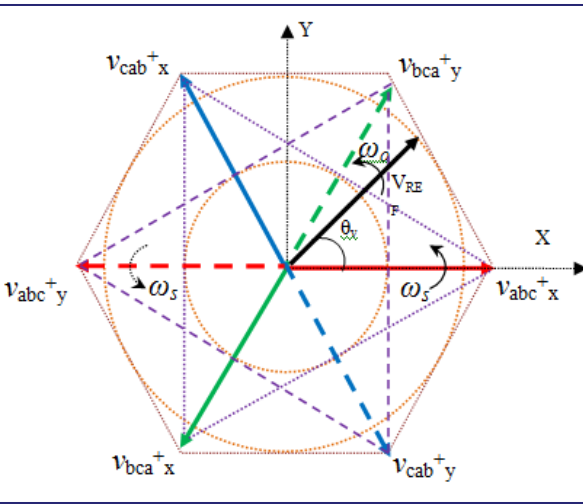


Input power factor θ

$$\theta = \tan^{-1}\{(1 - 2d^+) \tan \rho\}$$

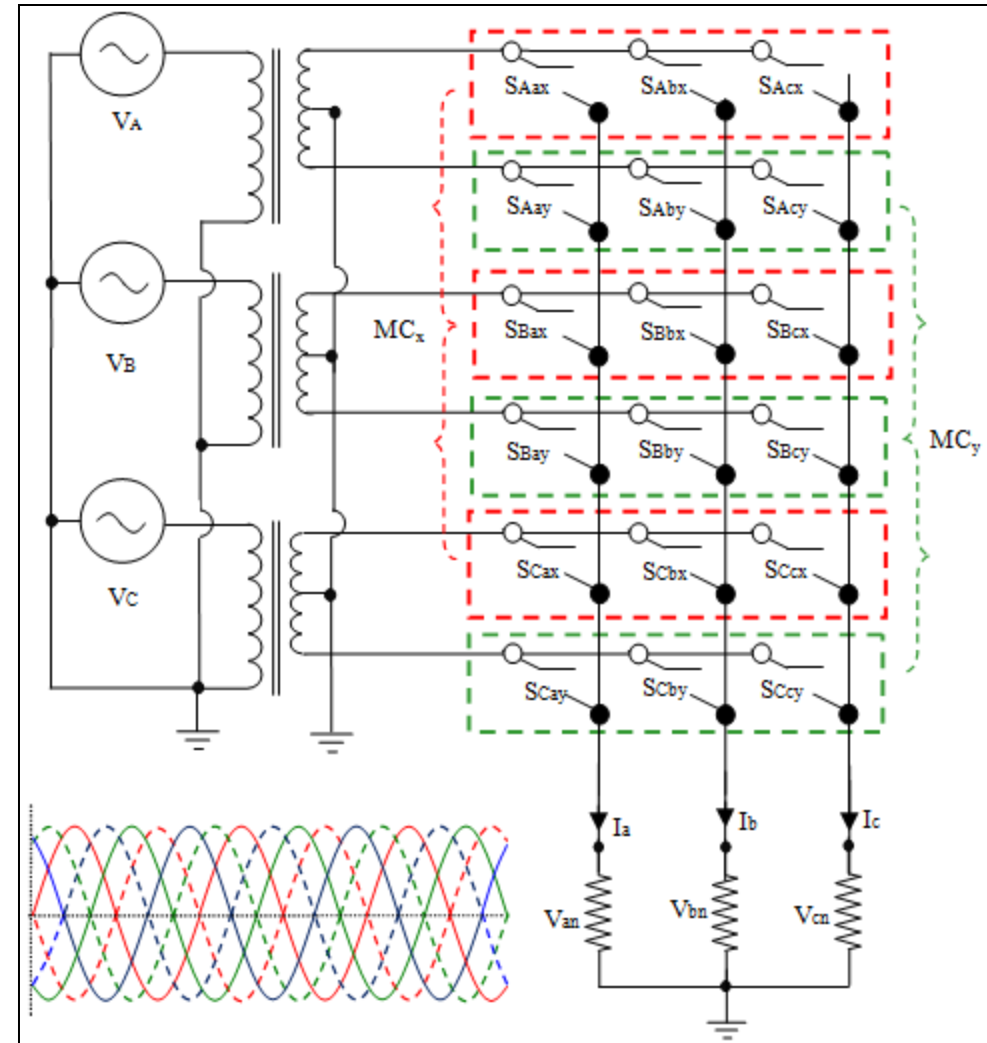
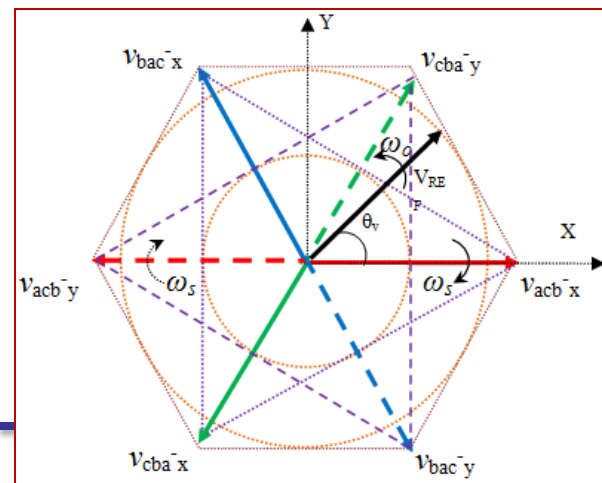


Six phase matrix converter (or) PSDSMC with RSVM to improve the modulation index

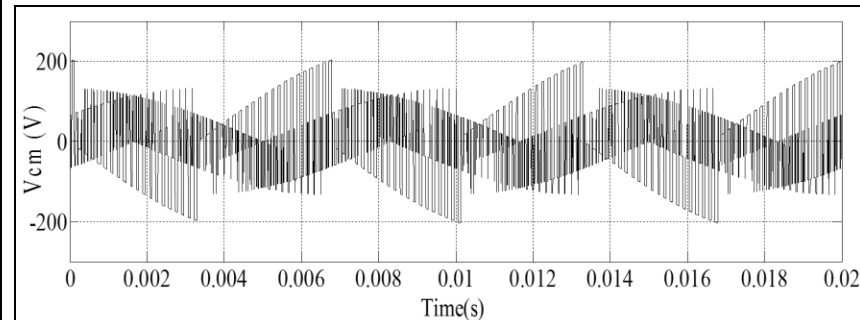
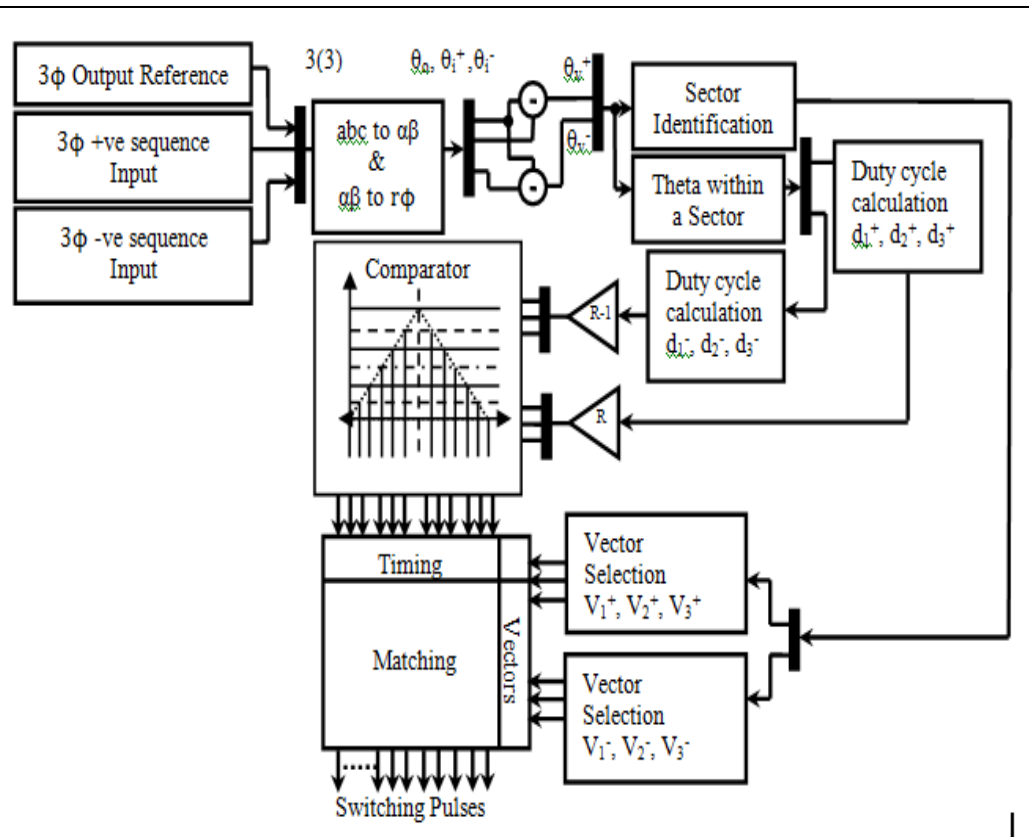


+ RSV of PSDSMC

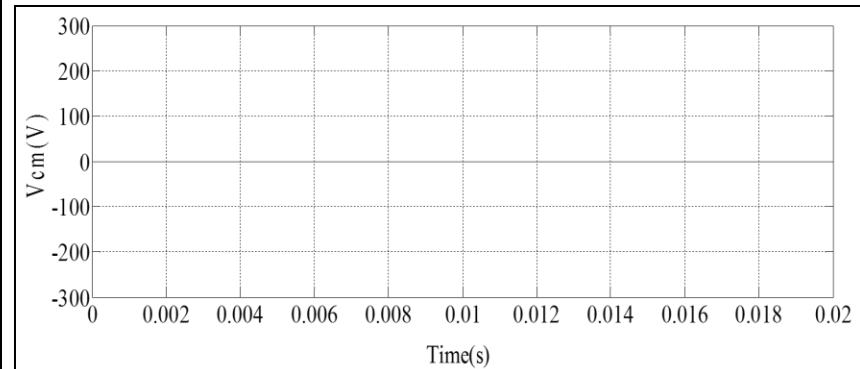
- RSV of PSDSMC



Block diagram of the implementation of RSVM in Matlab / Simulink



CMV with SVPWM technique



CMV with RSVM technique

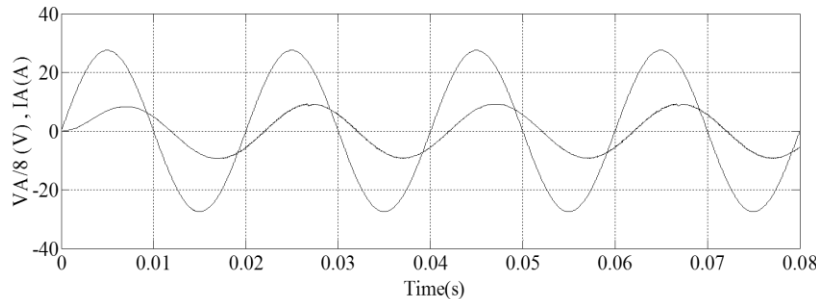
RSVM - Simulation Parameters

RSVM

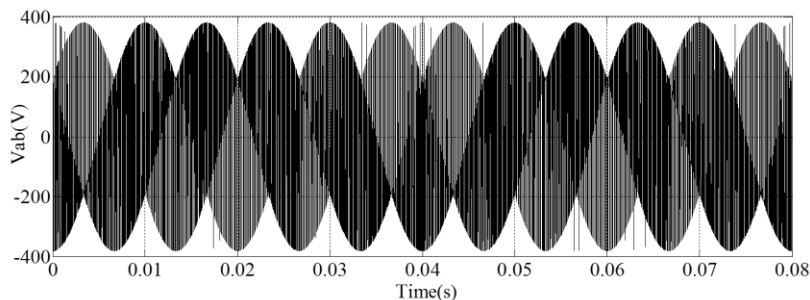
R-L Load	$R = 5 \Omega, L = 12 \text{ mH}$
Input Phase Voltage	220 V
Input Voltage Frequency	50 Hz
Input Filter	$L = 1 \text{ mH}, C = 10 \mu\text{F}, R_d = 15 \Omega$
Output Voltage Frequency	25 Hz
Modulation Index	0.5 – CMC / 0.866 - PSDSMC
Switching frequency	7 kHz

RSVM - Simulation Results for CMC

Without Power factor control

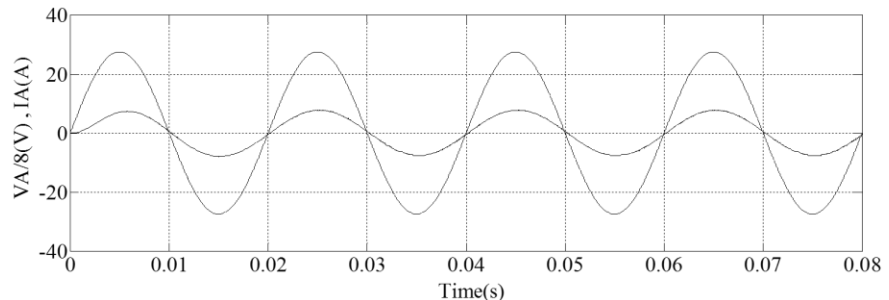


Input Current & Input Voltage

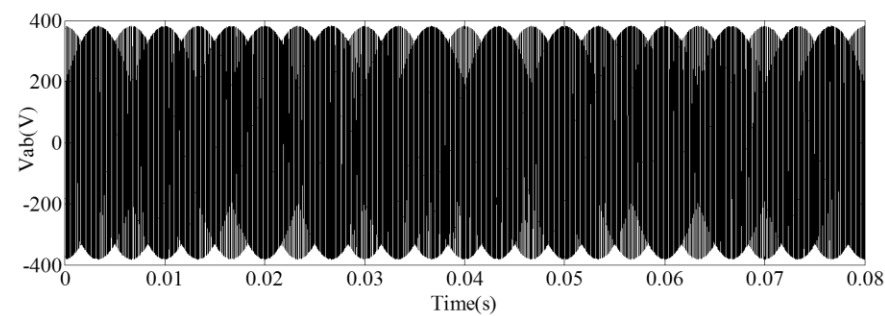


Output Line Voltage

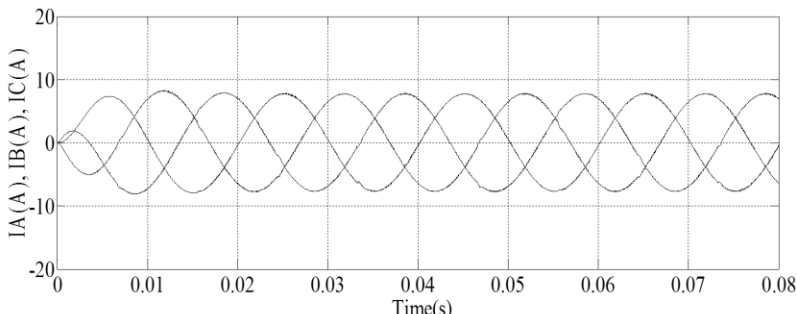
With Power factor control



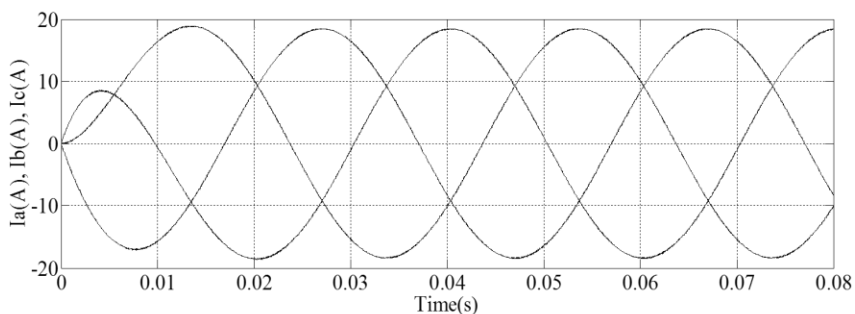
Input Current & Input Voltage



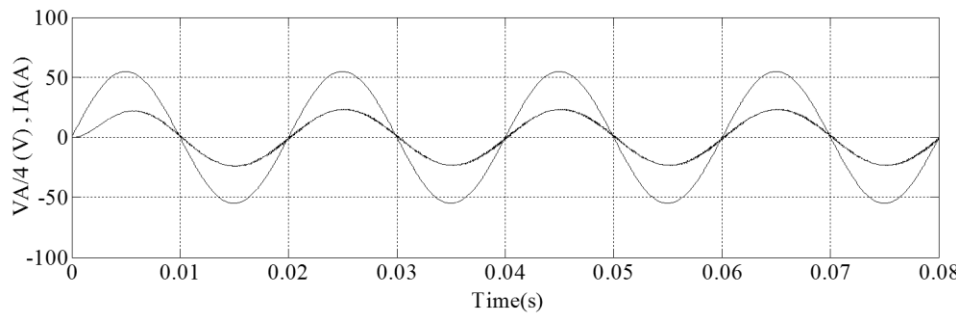
Output Line Voltage



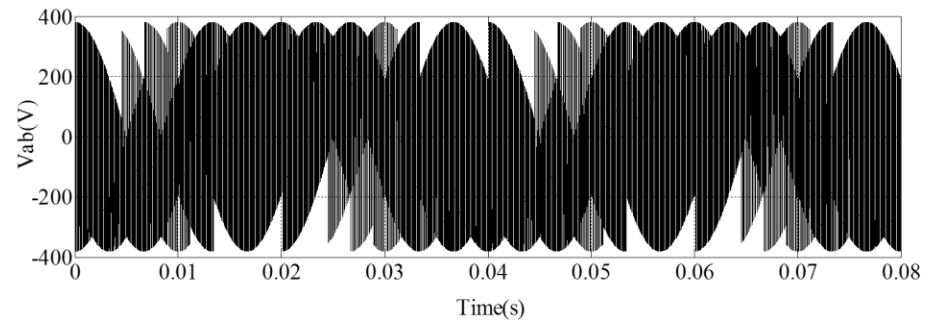
3-phase Input Current



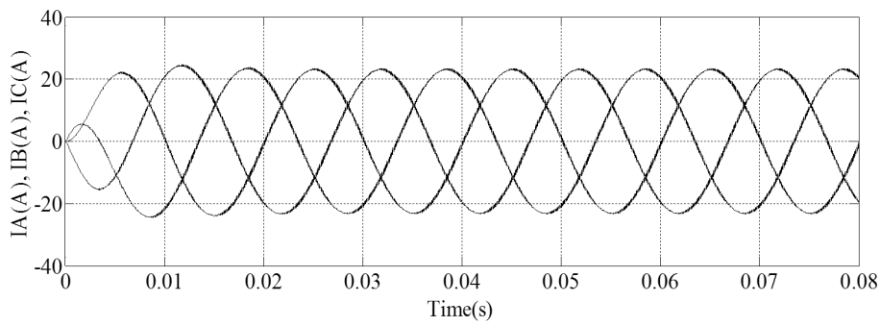
Simulation Results of PSDSMC modulated with RSVM - input power factor controlled



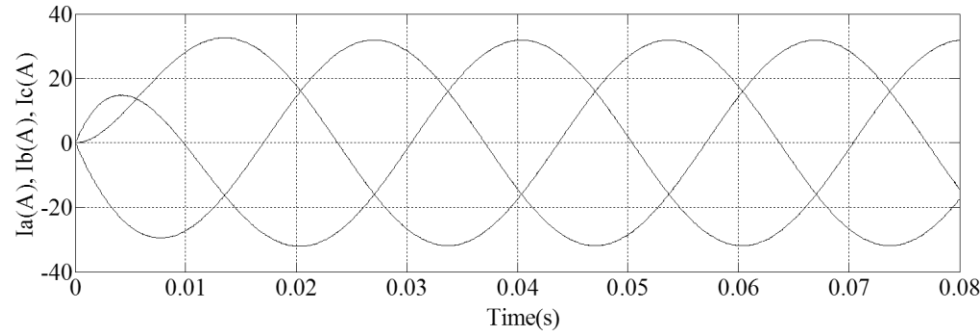
Input Current & Input Voltage



Output Line Voltage



3-phase Input Current



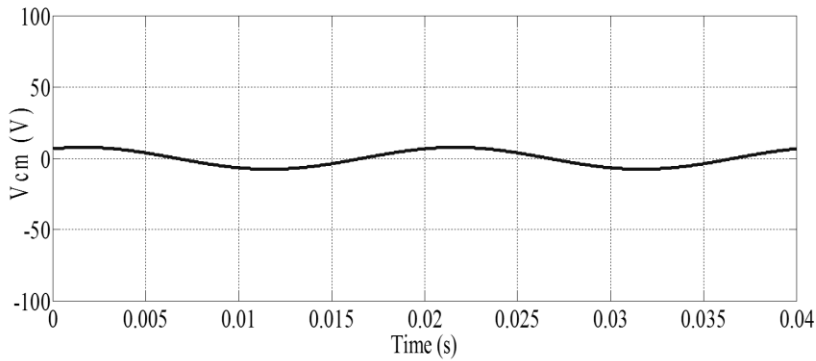
3-phase Output Current

RSVM under unbalance and non-sinusoidal input conditions

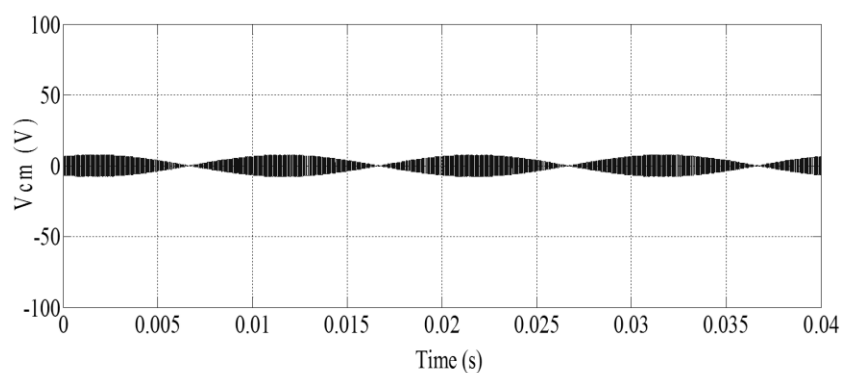
- RSVM dose not eliminate common mode voltage under unbalanced conditions
- RSVM generates a low frequency CMV proportional to the unbalance in case of both CMC & PSDSMC
- With non-homopolar harmonics the response of the RSVM is unaffected.
- Inputs containing homopolar harmonics the technique fails to eliminate CMV

RSVM – with non –sinusoidal input Conditions

An unbalance of 4.3% in the B phase

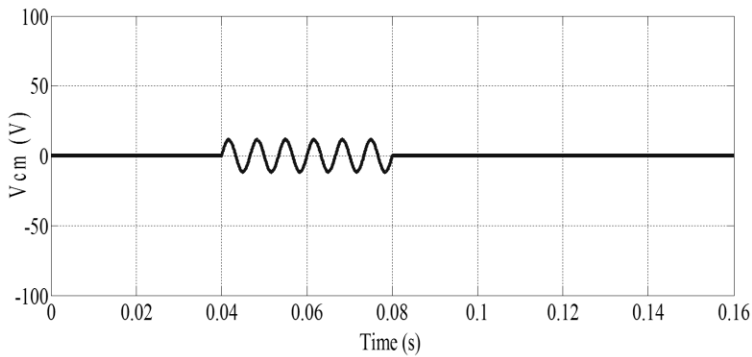


CMV of CMC with RSVM

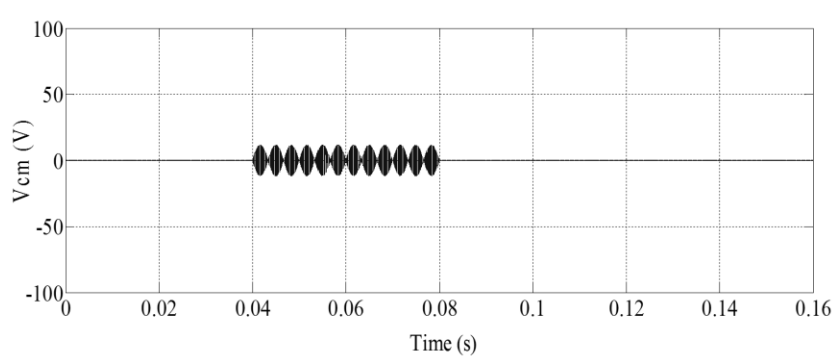


CMV of PDMC with RSVM

3rd harmonic injected from 0.04 s to 0.08 s & 2nd harmonic injected from 0.08 s to 0.12 s



CMV of CMC with RSVM



CMV of PDMC with RSVM

SUMMARY

The focus of the technique is to **eliminate the common mode voltage** effects in matrix converter

The method to use the **Rotating Space Vectors** for the elimination of common mode voltage with voltage transfer ratio of 0.5 is developed.

The control **of input power factor** in RSVM is addressed

The use of a six phase matrix converter (**PDMC**) and its RSVM technique to improve the voltage transfer ratio by 73% is proposed

The analysis of RSVM technique for **unbalanced and non-sinusoidal** conditions was performed



CHAPTER –IV

Analysis & Simplified Control of Matrix converter under Unbalanced and non- Sinusoidal Input Conditions

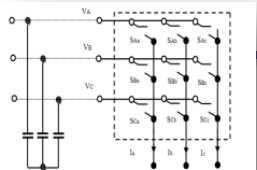


Analysis of the effects of unbalanced inputs in Matrix Converter

Analysis of the Fictitious DC bus Voltage of the Matrix Converter under unbalanced and non sinusoidal input conditions is carried out.

The simplified control based on the signatures present in the fictitious DC bus for matrix converter operated under unbalanced and non sinusoidal inputs is presented

Simulation results are presented to explain the validity of the proposed method.



Effect of Input Unbalance on the Fictitious DC bus

Fourier expression of the Phase voltage is given as

$$V_a = \sum_{i=1}^m V_{a,i} \sin(i\omega_e t + \phi_i)$$

Through the symmetric component method sequence components are derived

The current space vector for Positive Sequence of i^{th} harmonic:

Similarly for Negative Sequence:

The total current space vector f_i

$$f_i = f_i^+ + f_i^-$$

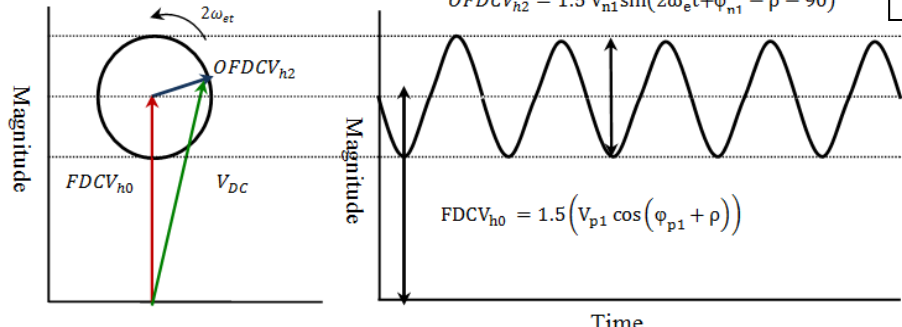
$$f_i^+ = f_{ai}^+ + f_{bi}^+ + f_{ci}^+ = \frac{3}{2} V_{pi} \left(\cos((i-1)\omega_e t + \phi_{pi} + \phi_i + \rho) \right)$$

$$f_i^- = f_{ai}^- + f_{bi}^- + f_{ci}^- = -\frac{3}{2} V_{ni} \left(\cos((i+1)\omega_e t + \phi_{ni} + \phi_i - \rho) \right)$$

Since $f_0 = 0$ for the converter

The fictitious DC bus voltage is given by: $V_{DC_Calc} = \sum_{i=1}^m f_i$

$$V_{DC_Calc} = \frac{3}{2} \left(V_{p1} \cos(\phi_{p1} + \rho) + V_{n1} \sin(2\omega_e t + \phi_{n1} - \rho - 90^\circ) \right)$$



Effect of Oscillations in the Fictitious DC bus on the output voltage

The input unbalance introduces a second harmonic ripple on the Fictitious DC bus

Hence the synthesized output can be expressed as

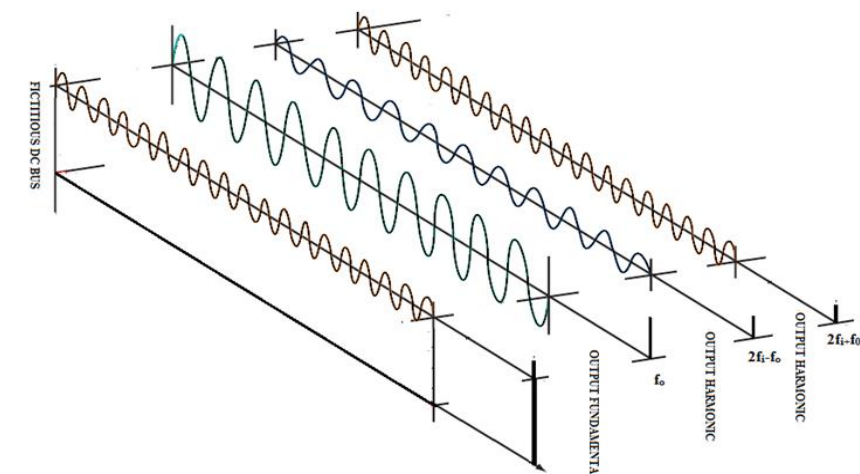
$$V_{\text{out}} = f_{\text{comp}} + H_{\text{comp}}$$

$$f_{\text{comp}} = V_{p1} \cos(\phi_{p1} + \rho) \times \sin(\omega_o t)$$

$$H_{\text{comp}} = V_{n1} (\sin(2\omega_e t + \phi_{n1} - \rho - 90^\circ) \times \sin(\omega_o t))$$

Two lower order harmonics appear at the output voltage

$(2\omega_e + \omega_0) \& (2\omega_e - \omega_0)$



Effect of Oscillations in the Fictitious DC bus on the input current

The input unbalance introduces a second harmonic ripple on the Fictitious DC bus

Hence the synthesized input current can be expressed as

$$I_{in} = I_f + I_h$$

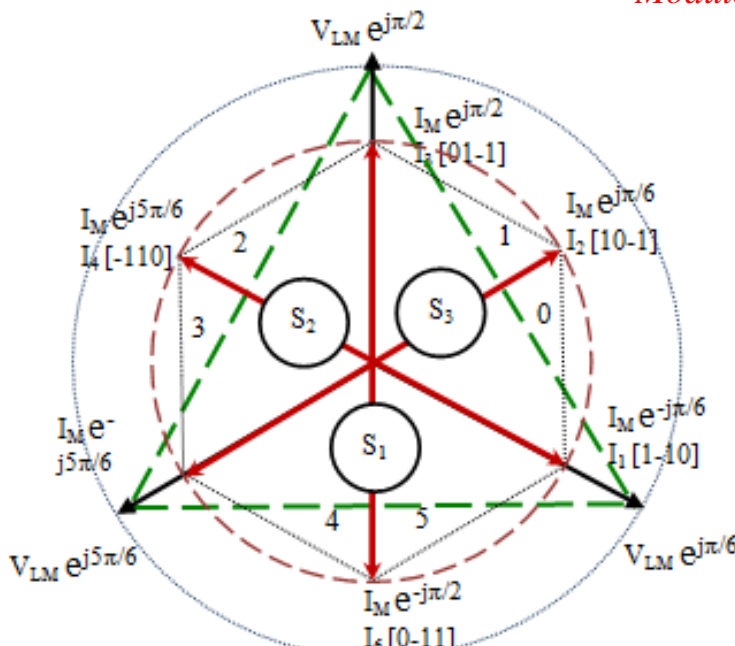
$$I_f = I_{p1} \cos(\phi_{p1} + \rho) \times \sin(\omega_e t)$$

$$I_h = I_{n1} (\sin(2\omega_e t + \phi_{n1} - \rho - 90^\circ) \times \sin(\omega_e t))$$

Lower order third harmonics appear at the input current

$$(2\omega_e + \omega_e) = 3\omega_e$$

Unbalance compensation technique



Line Voltage and Input Current Sectors

Method:

$$V_{DC} = d_{I\alpha} \times |V_1| + d_{I\beta} \times |V_2|$$

$$m_{v,comp} = m_v \times V_{dc,min} / V_{dc}$$

Modulating the switching function of the inverter with the ripple on the DC bus

Voltage and Current Sector Selection

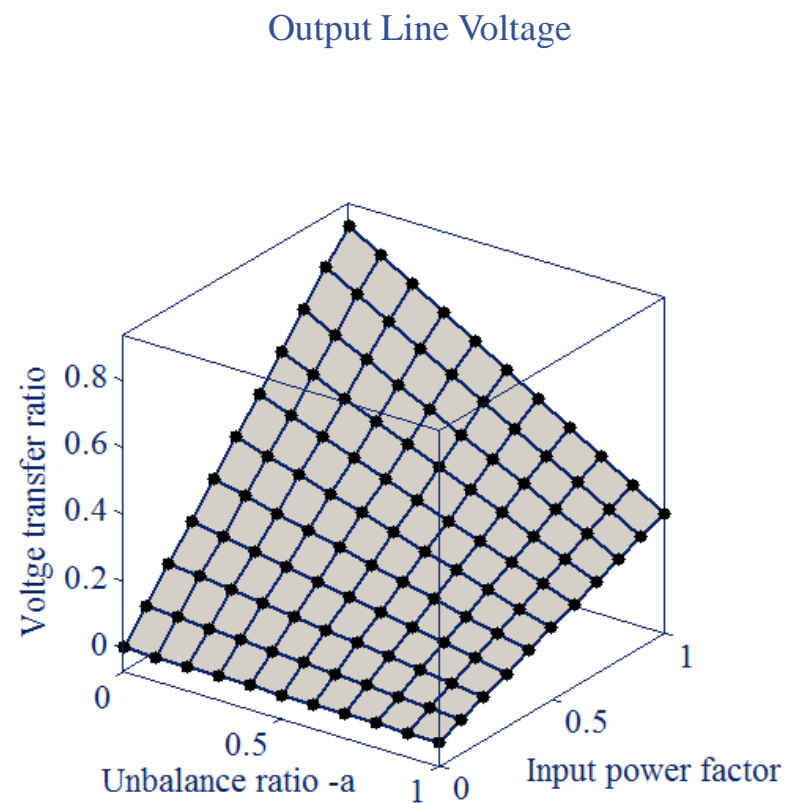
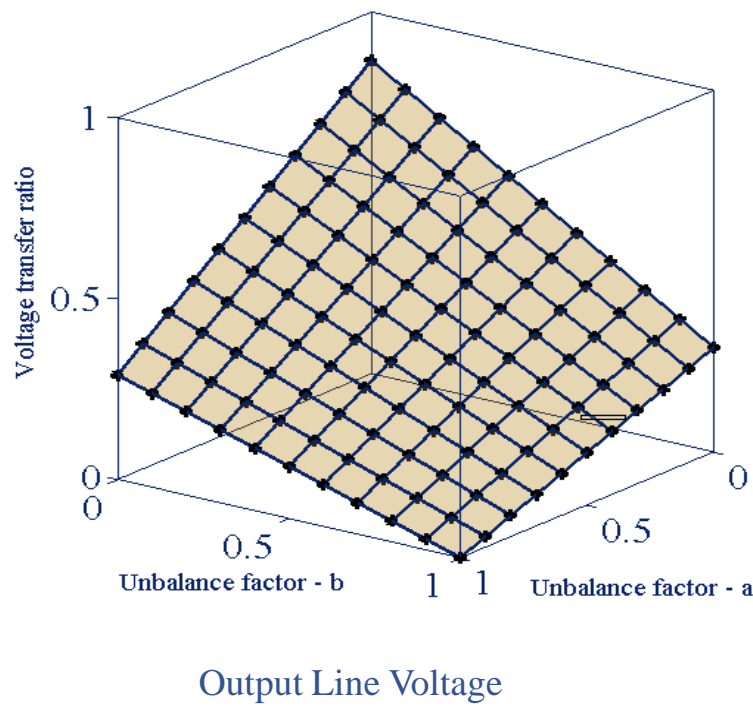
S.No	Voltage Sector	Current Sectors
1	S1	0,3
2	S2	1,4
3	S3	5,2

Methods proposed:

- A sector correspondence between the input current and the line voltage space vector is established for unity displacement factor (UDF)
- The output modulation index (m_i) is modified dynamically based on the computed DC link voltage with Rectifier modulation index ($m_c = 1$).

$V_{dc,min}$ is obtained through a simple memory circuit

RSVM - Simulation Parameters

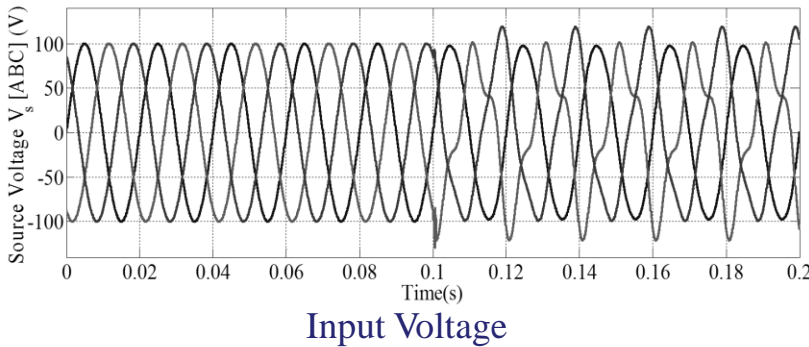


Unbalance Control of Matrix Converter - Simulation Parameters

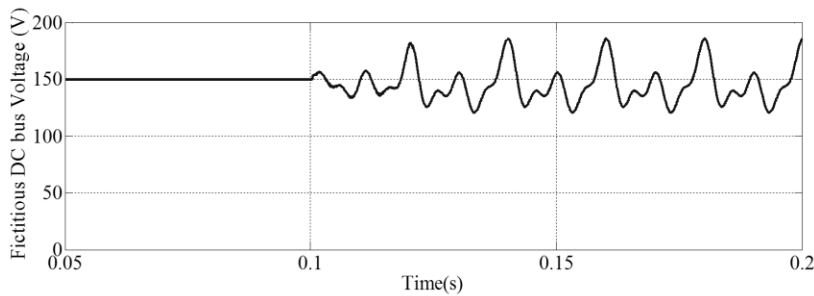
UB

R-L Load	$R_L = 2.7\Omega$, $L_L = 4.77 \text{ mH}$
Input phase voltage	100 V
Input voltage frequency	50 Hz
Input filter	$L = 1 \text{ mH}$, $C = 35 \mu\text{F}$, $R_d = 15\Omega$
Output Voltage frequency	40 Hz
Switching frequency	6 kHz
Unbalance at the input	10% unbalance in B-phase + 2 nd and 3 rd harmonics

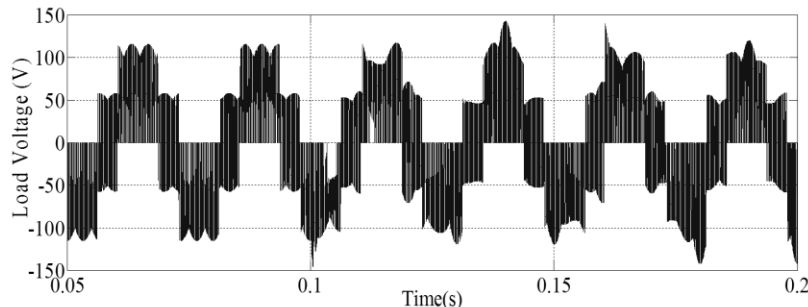
Simulation results – unbalance compensation technique



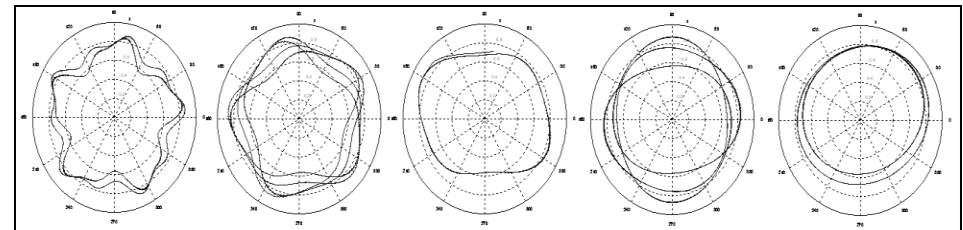
Input Voltage



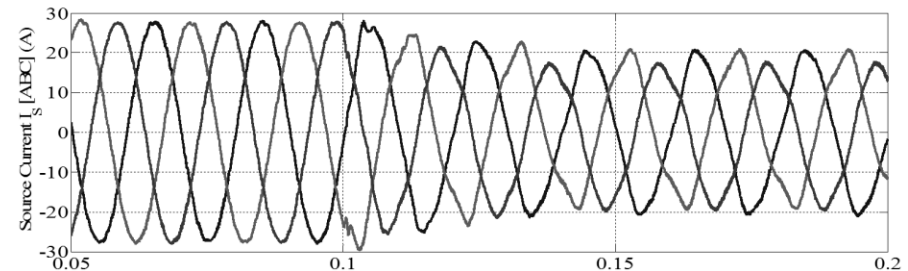
Fictitious DC bus Voltage



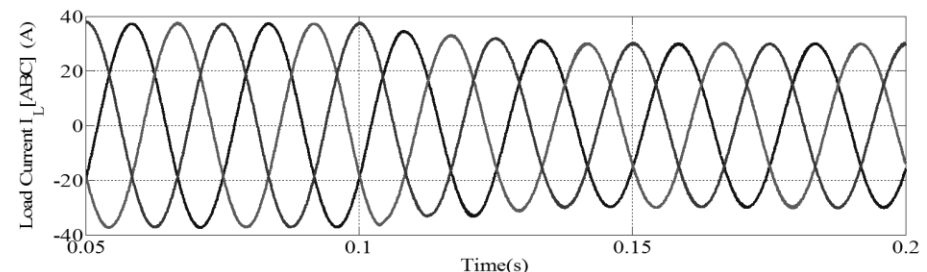
Output phase Voltage



Modified $m_{v,comp}$ for (a) $f=20\text{Hz}$, (b) $f=40\text{Hz}$, (c) $f=50\text{Hz}$,
(d) $f=75\text{Hz}$, & (e) $f=100\text{Hz}$



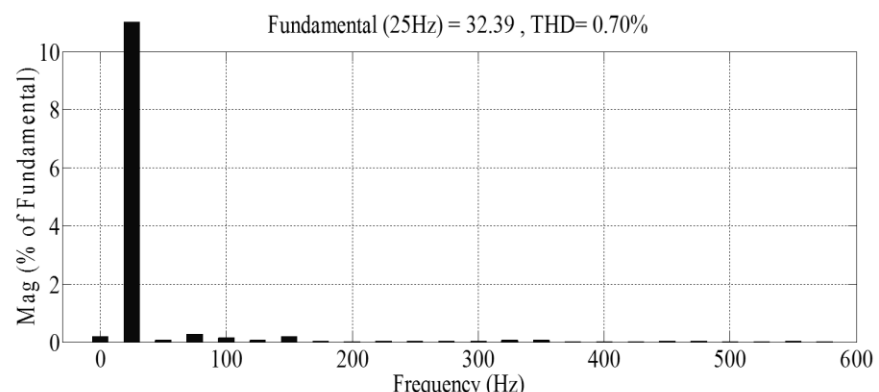
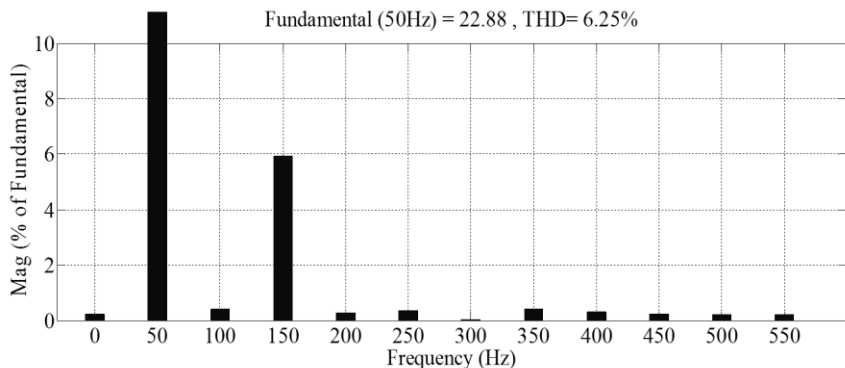
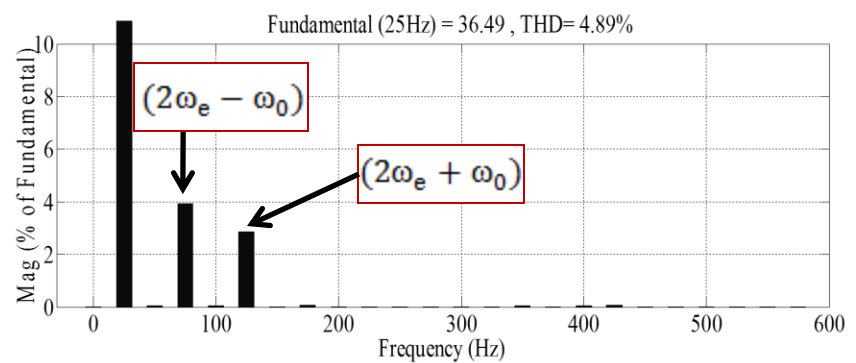
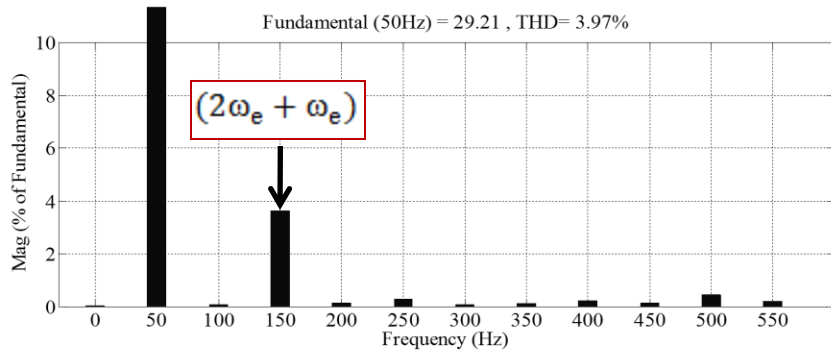
Input Current



Output Current

Harmonic characteristics - Simulation results

Input Voltage 50 Hz , Output Voltage 25 Hz



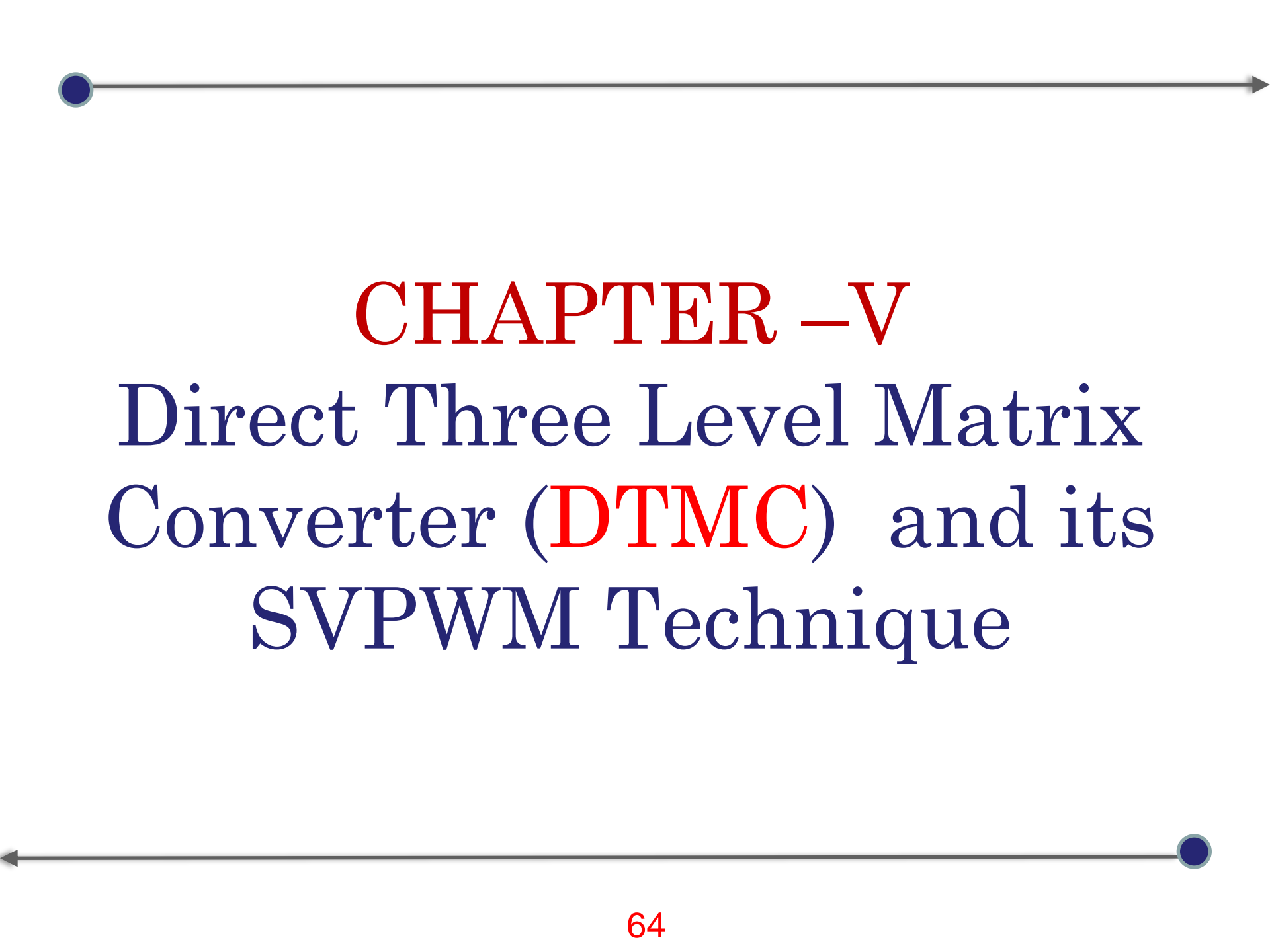
SUMMARY

Analysis of the effects of unbalance in the input voltage on the Fictitious DC bus, Input Current & Output Voltage was carried out.

It was found that the Fictitious DC bus appeared with oscillations under unbalance.

A Simple Compensation based on the Oscillations in the Fictitious DC bus was proposed

The Simulation results of the Matlab – Simulink model was presented



CHAPTER –V

Direct Three Level Matrix Converter (**DTMC**) and its SVPWM Technique

Direct Three Level Matrix Converter

Introduction

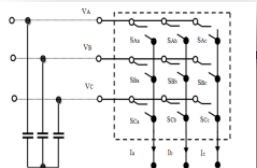
To Introduce the **topology** of Direct three level matrix converter.

Introduce the Development of **Space vector technique** for Direct three level matrix converter.

Explain the method of **neutral current balancing** and **reduction of THD** using **virtual vectors & nearest three vectors**.

Development of switching loss model

Simulation results and hardware results of the prototype .



Direct Three Level Matrix Converter

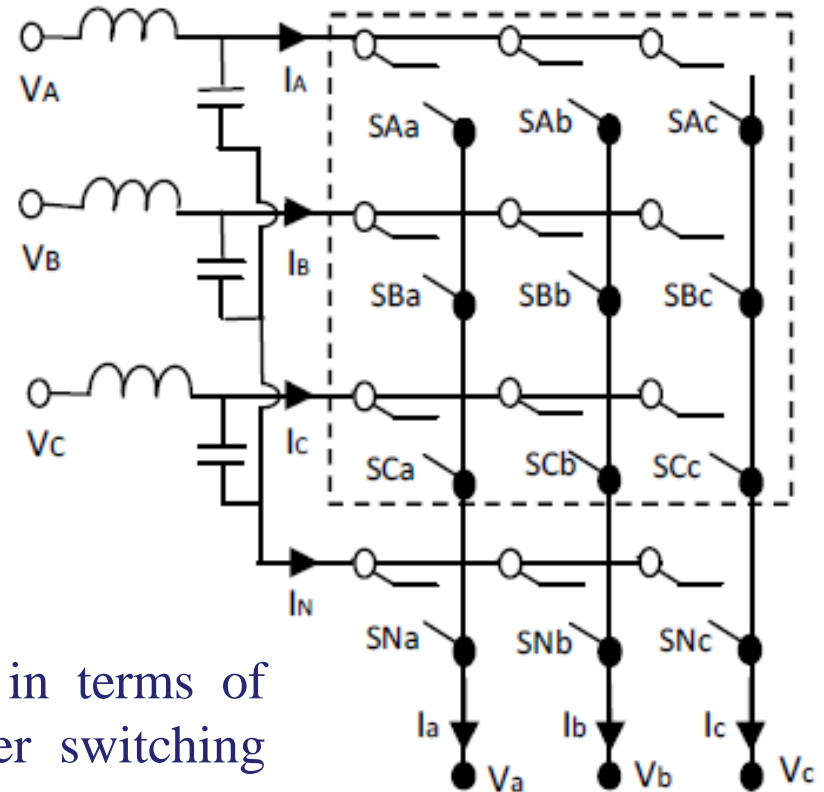
Topology

DTMC

The DTMC provides three levels of voltage by tapping the input filter neutral point with three additional switches

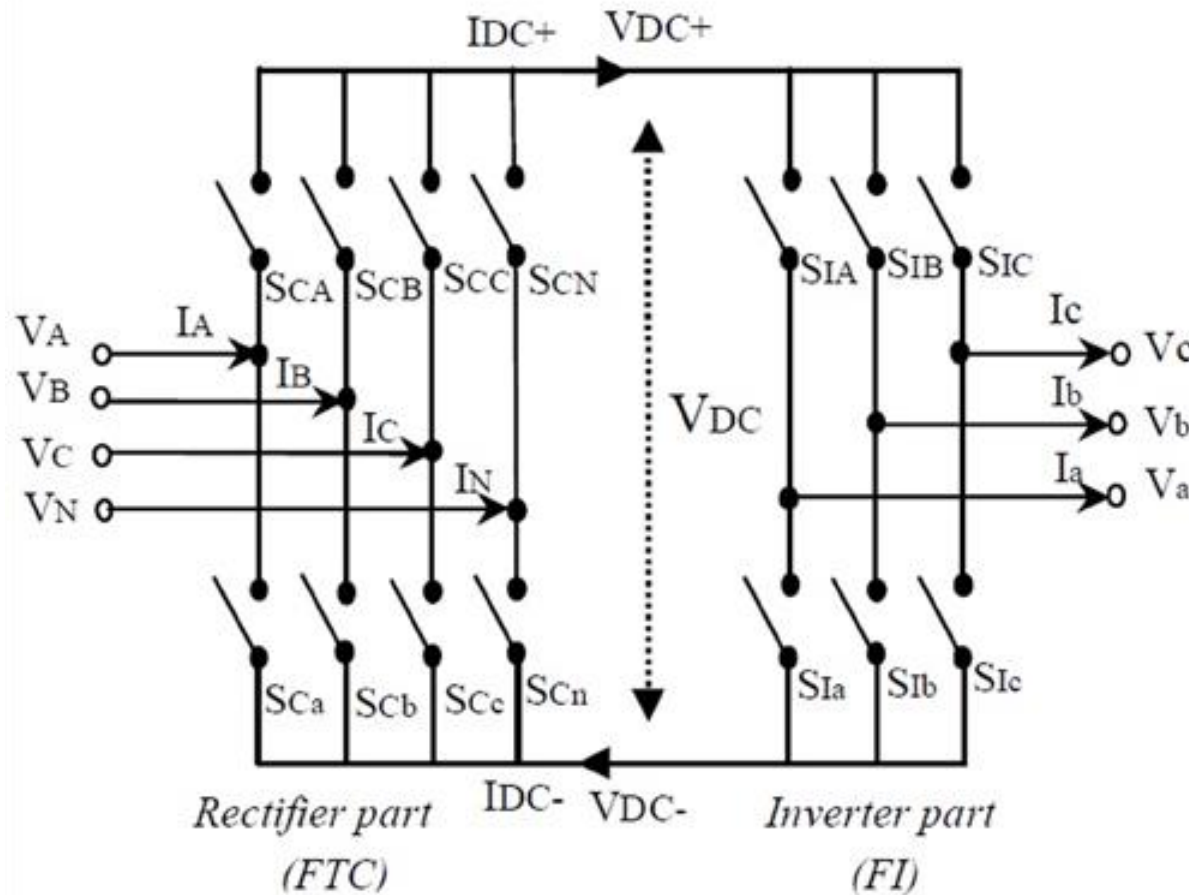
- 1) *The input line voltage*
- 2) *The input phase voltage*
- 3) *The zero voltage*

DTMC is an advancement to the CMC in terms of considerable reduction in THD and lower switching stresses.



EQUIVALENT STRUCTURE FOR SPACE VECTOR DEVELOPMENT OF DTMC

DTMC

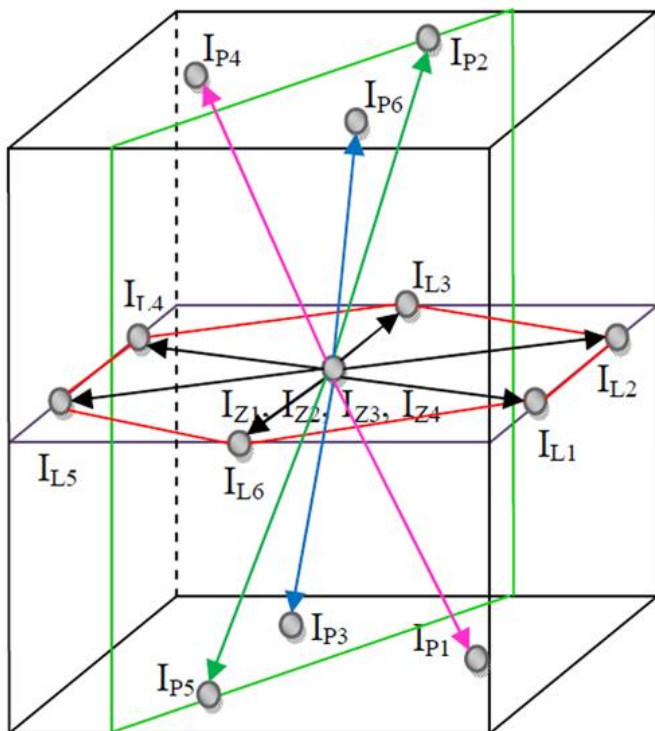
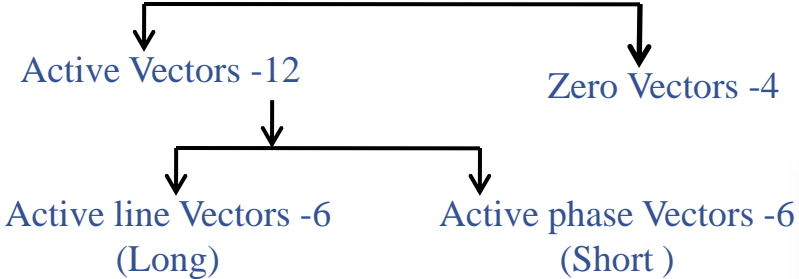


Fictitious three level converter and Fictitious inverter pair

CONVERTER SIDE SPACE VECTOR DEVELOPMENT

DTMC

Space Vectors - 16



$$I_{IN} = \frac{2}{3}(I_a + I_b \cdot e^{j\frac{2\pi}{3}} + I_c \cdot e^{j\frac{4\pi}{3}})$$

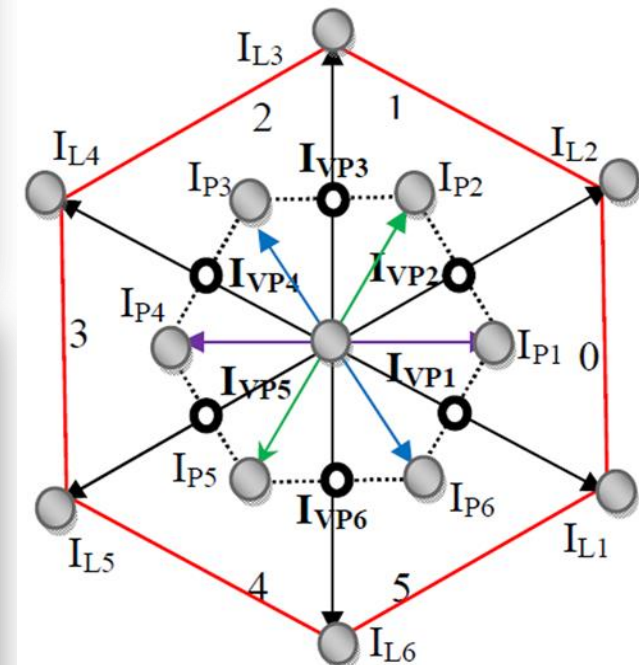
Type	Vector	$\begin{bmatrix} S_{CA} & S_{CB} & S_{CC} \\ S_{Ca} & S_{Cb} & S_{Cc} \end{bmatrix}$	I_A	I_B	I_C	$I_N = I_0$	I_{in}	$\angle I_{in}$	V_{DC}
Active line vector	$I_{L1}[AB]$	$\begin{bmatrix} 1 & 0 & 00 \\ 0 & 1 & 00 \end{bmatrix}$	$+I_{DC}$	$-I_{DC}$	0	0	$\sqrt{3}I_{DC}$	330°	V_{AB}
	$I_{L2}[AC]$	$\begin{bmatrix} 1 & 0 & 00 \\ 0 & 0 & 10 \end{bmatrix}$	$+I_{DC}$	0	$-I_{DC}$	0	$\sqrt{3}I_{DC}$	30°	V_{AC}
	$I_{L3}[BC]$	$\begin{bmatrix} 0 & 1 & 00 \\ 0 & 0 & 10 \end{bmatrix}$	0	$+I_{DC}$	$-I_{DC}$	0	$\sqrt{3}I_{DC}$	90°	V_{BC}
	$I_{L4}[BA]$	$\begin{bmatrix} 0 & 1 & 00 \\ 1 & 0 & 00 \end{bmatrix}$	$-I_{DC}$	$+I_{DC}$	0	0	$\sqrt{3}I_{DC}$	150°	V_{BA}
	$I_{L5}[CA]$	$\begin{bmatrix} 0 & 0 & 10 \\ 1 & 0 & 00 \end{bmatrix}$	$-I_{DC}$	0	$+I_{DC}$	0	$\sqrt{3}I_{DC}$	210°	V_{CA}
	$I_{L6}[CB]$	$\begin{bmatrix} 0 & 0 & 10 \\ 0 & 1 & 00 \end{bmatrix}$	0	$-I_{DC}$	$+I_{DC}$	0	$\sqrt{3}I_{DC}$	270°	V_{CB}
Active phase vector	$I_{P1}[AN]$	$\begin{bmatrix} 1 & 0 & 00 \\ 0 & 0 & 01 \end{bmatrix}$	$+I_{DC}$	0	0	$-I_{DC}$	I_{DC}	0°	V_{AN}
	$I_{P2}[NC]$	$\begin{bmatrix} 0 & 0 & 01 \\ 0 & 0 & 10 \end{bmatrix}$	0	0	$-I_{DC}$	$+I_{DC}$	I_{DC}	60°	V_{NC}
	$I_{P3}[BN]$	$\begin{bmatrix} 0 & 1 & 00 \\ 0 & 0 & 01 \end{bmatrix}$	0	$+I_{DC}$	0	$-I_{DC}$	I_{DC}	120°	V_{BN}
	$I_{P4}[NA]$	$\begin{bmatrix} 0 & 0 & 01 \\ 1 & 0 & 00 \end{bmatrix}$	$-I_{DC}$	0	0	$+I_{DC}$	I_{DC}	180°	V_{NA}
	$I_{P5}[CN]$	$\begin{bmatrix} 0 & 0 & 10 \\ 0 & 0 & 01 \end{bmatrix}$	0	0	$+I_{DC}$	$-I_{DC}$	I_{DC}	240°	V_{CN}
	$I_{P6}[NB]$	$\begin{bmatrix} 0 & 0 & 01 \\ 0 & 1 & 00 \end{bmatrix}$	0	$-I_{DC}$	0	$+I_{DC}$	I_{DC}	300°	V_{NB}
Zero Vector	I_z	$\begin{bmatrix} 1 & 0 & 00 \\ 1 & 0 & 00 \end{bmatrix}, \begin{bmatrix} 0 & 1 & 00 \\ 0 & 1 & 00 \end{bmatrix}, \begin{bmatrix} 0 & 0 & 10 \\ 0 & 0 & 10 \end{bmatrix}, \begin{bmatrix} 0 & 0 & 01 \\ 0 & 0 & 01 \end{bmatrix}$				0			0

VIRTUAL VECTORS & PRINCIPLE OF NEUTRAL CURRENT BALANCING.

DTMC

Switching Time	Applied Vectors	I_A	I_B	I_C	I_N	V_{DC}
$\frac{T_s}{2}$	I_{P6}	0	$-I_{DC}$	0	$+I_{DC}$	V_{NB}
$\frac{T_s}{2}$	I_{P1}	$+I_{DC}$	0	0	$-I_{DC}$	V_{AN}
T_s	$I_{VP1} = \frac{1}{2}I_{P6} + \frac{1}{2}I_{P1}$	$+\frac{1}{2}I_{DC}$	$-\frac{1}{2}I_{DC}$	0	0	$\frac{1}{2}V_{AB}$

Vector	Sharing Vectors	I_A	I_B	I_C	$I_N = I_0$	I_{in}	$\angle I_{in}$	V_{DC}
$I_{VP1}[AN]$	I_{P6}, I_{P1}	$+\frac{1}{2}I_{DC}$	$-\frac{1}{2}I_{DC}$	0	0	$\frac{\sqrt{3}}{2}I_{DC}$	330°	$\frac{1}{2}V_{AB}$
$I_{VP2}[NC]$	I_{P1}, I_{P2}	$+\frac{1}{2}I_{DC}$	0	$-\frac{1}{2}I_{DC}$	0	$\frac{\sqrt{3}}{2}I_{DC}$	30°	$\frac{1}{2}V_{AC}$
$I_{VP3}[BN]$	I_{P2}, I_{P3}	0	$+\frac{1}{2}I_{DC}$	$-\frac{1}{2}I_{DC}$	0	$\frac{\sqrt{3}}{2}I_{DC}$	90°	$\frac{1}{2}V_{BC}$
$I_{VP4}[NA]$	I_{P3}, I_{P4}	$-\frac{1}{2}I_{DC}$	$+\frac{1}{2}I_{DC}$	0	0	$\frac{\sqrt{3}}{2}I_{DC}$	150°	$\frac{1}{2}V_{BA}$
$I_{VP5}[CN]$	I_{P4}, I_{P5}	$-\frac{1}{2}I_{DC}$	0	$+\frac{1}{2}I_{DC}$	0	$\frac{\sqrt{3}}{2}I_{DC}$	210°	$\frac{1}{2}V_{CA}$
$I_{VP6}[NB]$	I_{P5}, I_{P6}	0	$-\frac{1}{2}I_{DC}$	$+\frac{1}{2}I_{DC}$	0	$\frac{\sqrt{3}}{2}I_{DC}$	270°	$\frac{1}{2}V_{CB}$

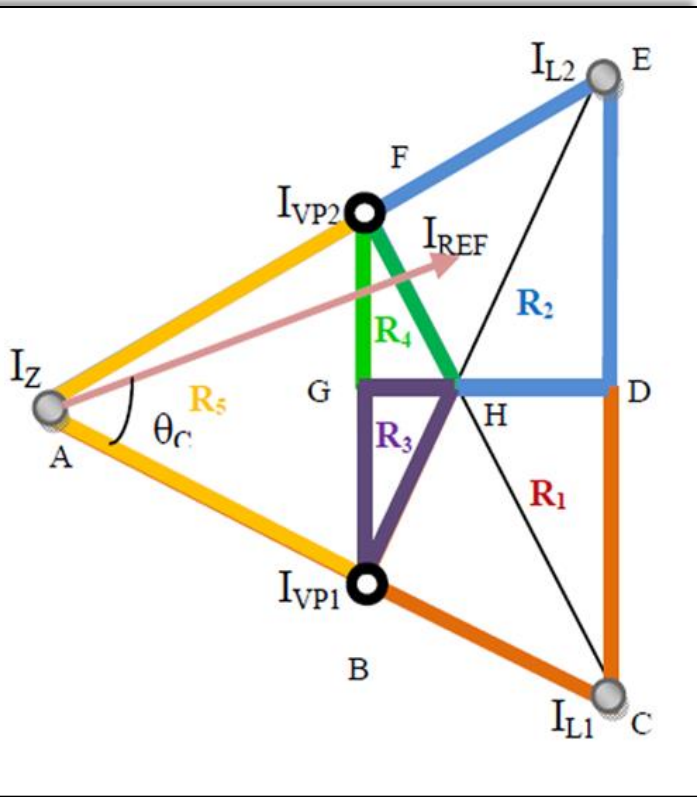


Virtual Vector Distribution

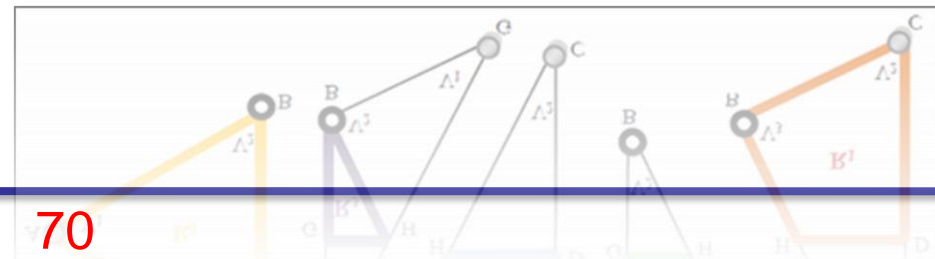
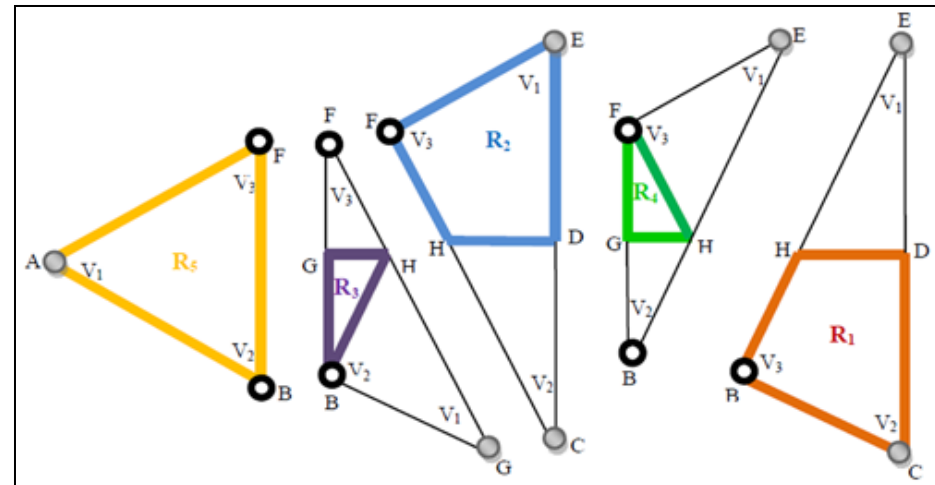
PRINCIPAL OF NEAREST THREE VECTORS

DTMC

Reduction Of Voltage Stresses In Matrix Converter

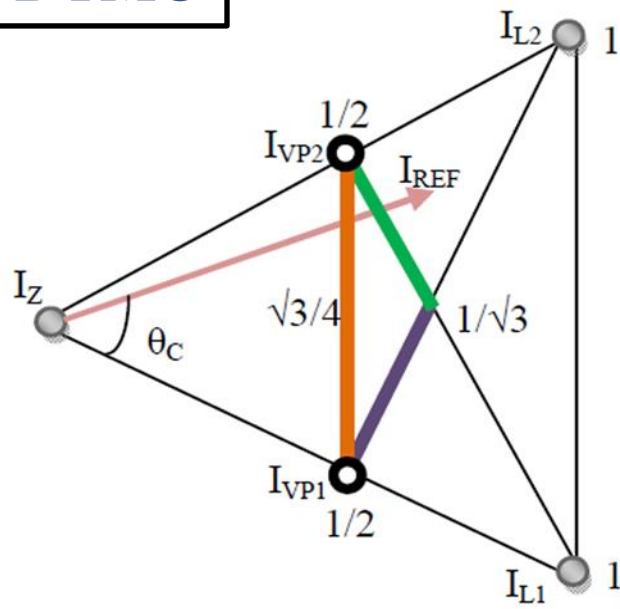


DIFFERENT REGIONS OF SPACE VECTOR SPACE.



IDENTIFICATION OF THE REGION IN WHICH THE REFERENCE VECTOR LIES

DTMC



- $\frac{\sqrt{3}}{4} \operatorname{cosec}(60^\circ + \theta_c) ; 0^\circ < \theta_c < 60^\circ$
- $\frac{1}{2} \sec(60^\circ - \theta_c) ; 30^\circ < \theta_c < 60^\circ$
- $\frac{1}{2} \sec(\theta_c) ; 0^\circ < \theta_c < 30^\circ$

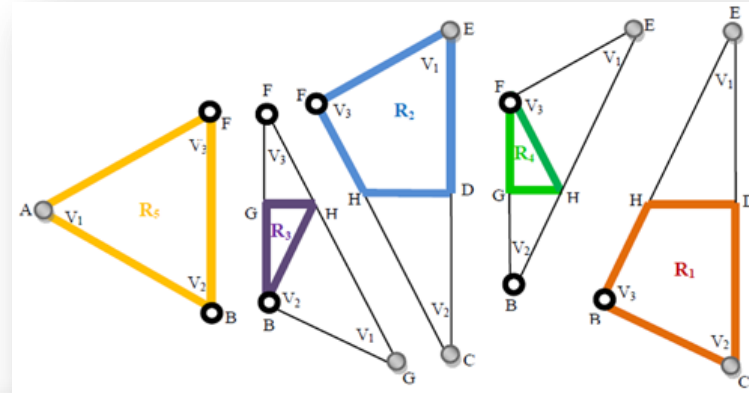
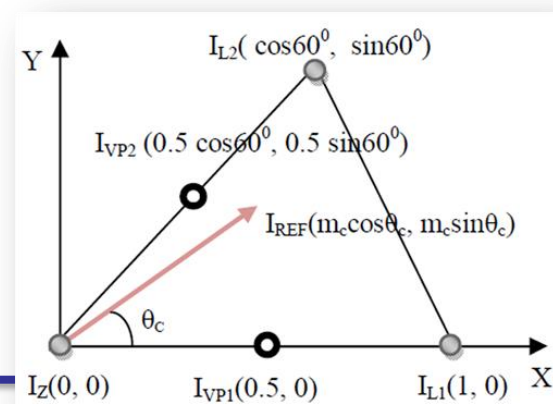
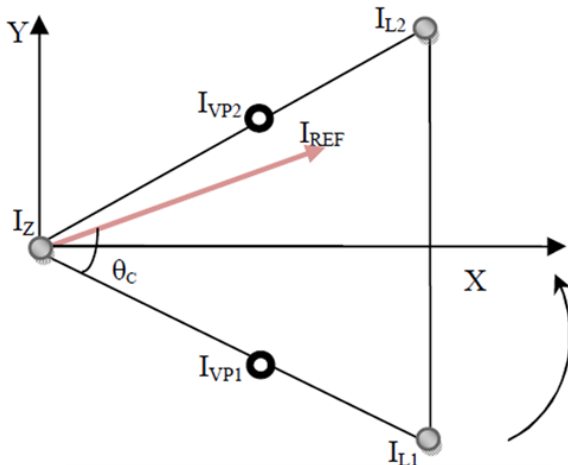
Sl.No	Region	Conditions
1	R_1	$m_c > \frac{1}{2} \sec(\theta_c) ; 0^\circ < \theta_c < 30^\circ$
2	R_2	$m_c > \frac{1}{2} \sec(60^\circ - \theta_c) ; 30^\circ < \theta_c < 60^\circ$
3	R_3	$\frac{\sqrt{3}}{4} \operatorname{cosec}(60^\circ + \theta_c) < m_c \leq \frac{1}{2} \sec(\theta_c) ; 0^\circ < \theta_c < 30^\circ$
4	R_4	$\frac{\sqrt{3}}{4} \operatorname{cosec}(60^\circ + \theta_c) < m_c \leq \frac{1}{2} \sec(60^\circ - \theta_c) ; 30^\circ < \theta_c < 60^\circ$
5	R_5	$m_c \leq \frac{\sqrt{3}}{4} \operatorname{cosec}(60^\circ + \theta_c) ; 0^\circ < \theta_c < 60^\circ$

DUTY CYCLE OF ACTIVE AND VIRTUAL VECTORS FOR DIFFERENT REGIONS

DTMC

$$\begin{bmatrix} x_1 & x_2 & x_3 \\ y_1 & y_2 & y_3 \\ 1 & 1 & 1 \end{bmatrix} \begin{bmatrix} d_1 \\ d_2 \\ d_3 \end{bmatrix} = \begin{bmatrix} X \\ Y \\ 1 \end{bmatrix}$$

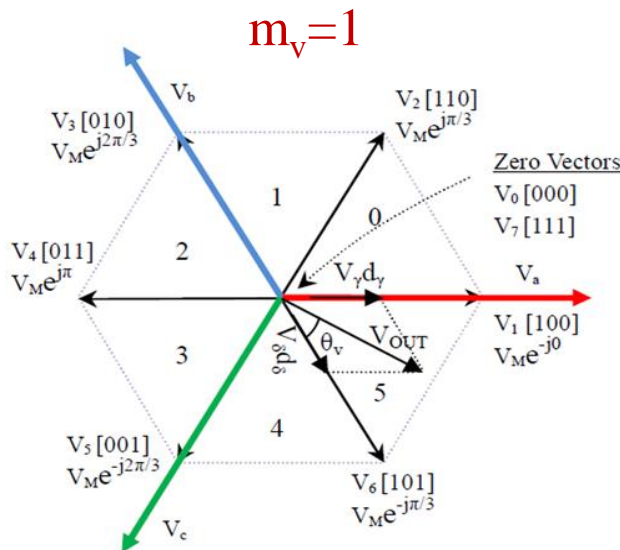
$$X = m_c * \cos \theta_c \text{ & } Y = m_c * \sin \theta_c$$



Region	Duty Cycle		
	$d_{v1}(V1)$	$d_{v2}(V2)$	$d_{v3}(V3)$
R ₁ (BCDH)	$\frac{2}{\sqrt{3}} m_c \sin(\theta_c)$	$2 m_c \cos(\theta_c) - 1$	$2 - \frac{4}{\sqrt{3}} m_c \sin(60^\circ + \theta_c)$
R ₂ (FEDH)	$2 m_c \sin(30^\circ + \theta_c) - 1$	$\frac{2}{\sqrt{3}} m_c \sin(60^\circ - \theta_c)$	$2 - \frac{4}{\sqrt{3}} m_c \sin(60^\circ + \theta_c)$
R ₃ (BGH)	$\frac{4}{\sqrt{3}} m_c \sin(60^\circ + \theta_c) - 1$	$\frac{4}{\sqrt{3}} m_c \sin(60^\circ - \theta_c)$	$2 - 4 m_c \cos(\theta_c)$
R ₄ (FHG)	$\frac{4}{\sqrt{3}} m_c \sin(60^\circ + \theta_c) - 1$	$2 - 4 m_c \sin(30^\circ + \theta_c)$	$\frac{4}{\sqrt{3}} m_c \sin \theta_c$
R ₅ (ABF)	$1 - \frac{4}{\sqrt{3}} m_c \sin(60^\circ + \theta_c)$	$\frac{4}{\sqrt{3}} m_c \sin(60^\circ - \theta_c)$	$\frac{4}{\sqrt{3}} m_c \sin \theta_c$

INVERTER SIDE SPACE VECTOR – CONVENTIONAL SPACE VECTOR

DTMC



In order to decrease the THD to a greater extent
Zero vectors of the Inverter side is not used.

With the elimination of zero vectors the duty cycles for active vectors are recomputed

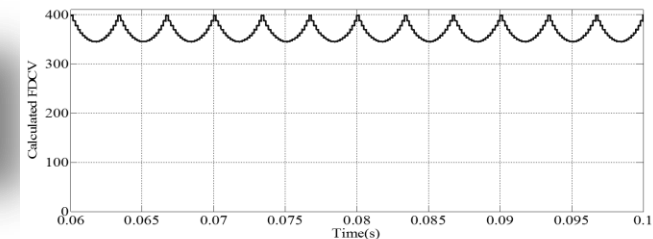
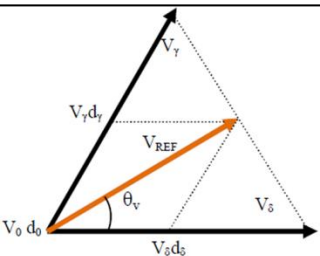
This increases the output voltage vector

$$d'_{\gamma} = \frac{d_{\gamma}}{d_{\gamma} + d_{\delta}} \quad \& \quad d'_{\delta} = \frac{d_{\delta}}{d_{\gamma} + d_{\delta}}$$

$$V'_{OUT} = d'_{\gamma} V_{\gamma} + d'_{\delta} V_{\delta} = \frac{V_{OUT}}{d_{\gamma} + d_{\delta}}$$

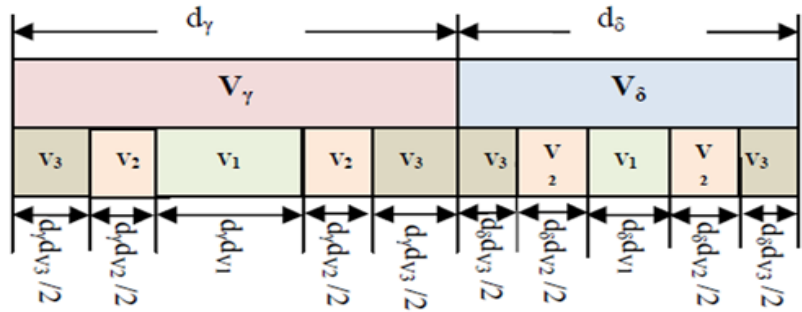
This increase is compensated by varying m_c
dynamically

$$m_c = \frac{\sqrt{3}}{2} m_{DTMC} (d_{\gamma} + d_{\delta})$$

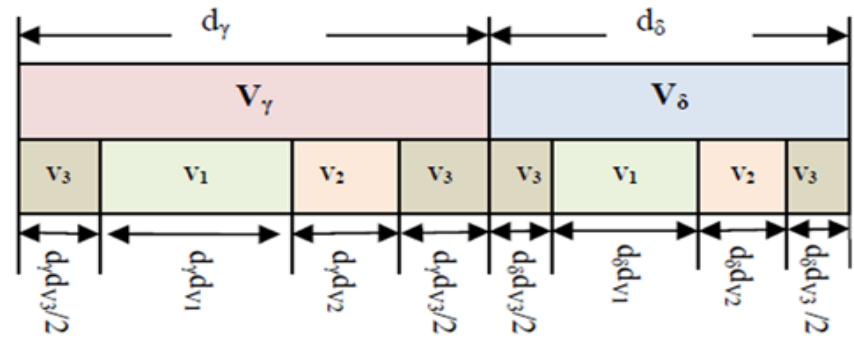


DISTRIBUTION OF CONVERTER / INVERTER DUTY CYCLES

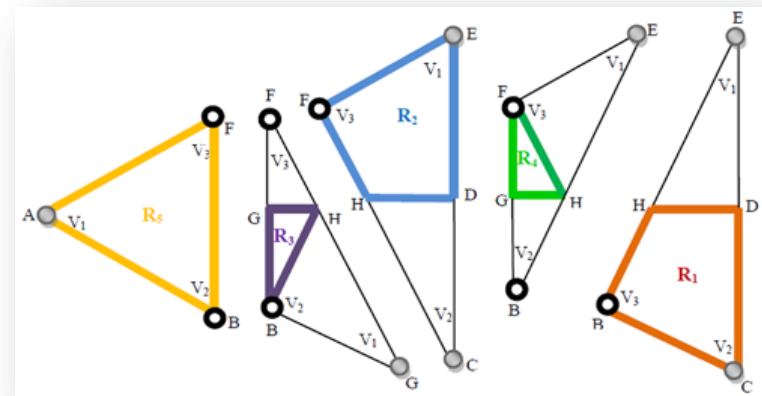
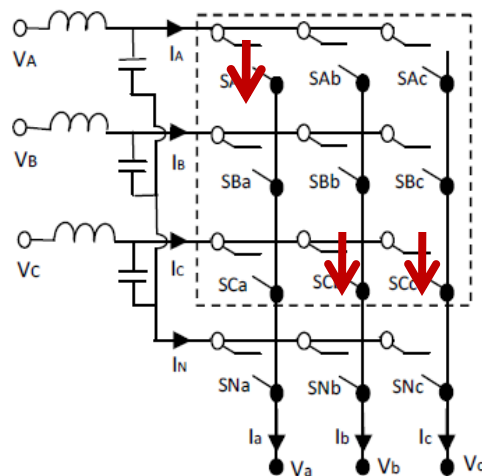
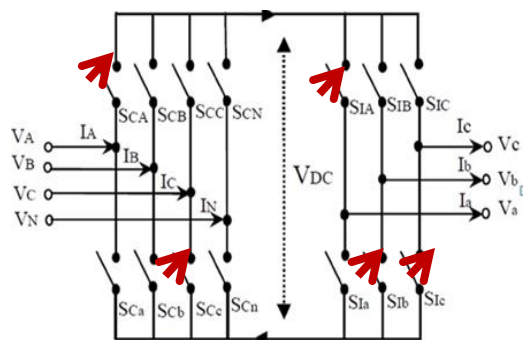
DTMC



Switching Pattern of DTMC for R_1 and R_2



Switching Pattern of DTMC for R_3, R_4 and R_5



SWITCHING LOSS MODELLING – CMC

CMC

Conduction Losses Equations

$$C_{\text{Losses}}(v_d, i_L) = v_{d_{IGBT}}(i_L) * i_L + v_{d_{DIODE}}(i_L) * i_L$$

$$E_C(v_d, i_L) = \int_0^{T_s} C_{\text{Losses}}(v_d, i_L) dt$$

$$C_{L\text{-Avg}} = \frac{1}{T} \int_0^T C_{\text{Losses}}(t) dt$$

$$v_{d_{IGBT}}(i_L) = x + y * i_L^z$$

$$v_{d_{DIODE}}(i_L) = m + n * i_L^k$$

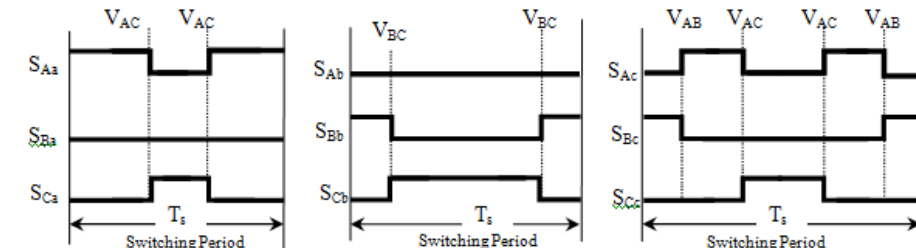
Switching Losses Equations

$$E_{sw}(v_{\text{Block}}, i_L) = E_{swR} * v_{\text{Block}} * i_L / V_R * i_R$$

$$S_{\text{Losses}}(v_d, i_L) = \left(\frac{E_{on}}{T_{on}} + \frac{E_{off}}{T_{off}} + \frac{E_{rr_D}}{T_r} \right) * |v_{xy}| * i_L / V_R * i_R$$

Switching Events in voltage & current sector 1 - CMC

Switch transition	$S_1 \rightarrow S_2$	$S_2 \rightarrow S_1$	$S_1 \rightarrow S_2$	$S_2 \rightarrow S_1$
	I_{out}^+			
V_{in}^+	E_{off}	$E_{on} + E_{rr_D}$	$E_{on} + E_{rr_D}$	E_{off}
V_{in}^-	$E_{on} + E_{rr_D}$	E_{off}	E_{off}	$E_{on} + E_{rr_D}$



$$E_{sw} = K \cdot (|v_{AC}| \cdot i_a + |v_{BC}| \cdot i_b + (|v_{AB}| + |v_{AC}|) \cdot i_c)$$

In General for any sector

$$E_{sw} = K \cdot (x \cdot i_a + y \cdot i_b + z \cdot i_c)$$

$$\text{Where } K = \frac{E_{on} + E_{Off} + E_{rr}}{V_r I_r}$$

SWITCHING LOSS MODELLING – DTMC

DTMC

Following the Same procedure the Switching Events of DMC was calculated

Commutation events	Converter sector –Y & Inverter sector – X				
	Regions of converter sector				
	R ₁	R ₂	R ₃	R ₄	R ₅
Line voltage commutation	6	6	4/2	2/4	0
Phase voltage commutation	14	14	22	22	20

For Example – The Switching Energy loss for the DTMC for Current Sector -1 , Voltage Sector -1
For different regions of Current sector are given

$$E_{sw,R1} = K \cdot (|v_{AN}| \cdot i_a + (|v_{BC}| + |v_{CN}| + |v_{BN}|) \cdot i_b + (|v_{AB}| + |v_{AC}| + 2|v_{AN}| + |v_{BN}| + |v_{CN}|) \cdot i_c)$$

$$E_{sw,R4} = K \cdot (3|v_{AN}| \cdot i_a + (|v_{CN}| + |v_{BN}|) \cdot i_b + (|v_{AC}| + 3|v_{AN}| + |v_{BN}| + 2|v_{CN}|) \cdot i_c)$$

$$E_{sw,R2} = K \cdot (|v_{AN}| \cdot i_a + (|v_{BC}| + 2|v_{CN}|) \cdot i_b + (|v_{AB}| + |v_{AC}| + 2|v_{AN}| + 2|v_{CN}|) \cdot i_c)$$

$$E_{sw,R5} = K \cdot (2|v_{AN}| \cdot i_a + (|v_{BN}| + 2|v_{CN}|) \cdot i_b + (|v_{BN}| + 2|v_{AN}| + 2|v_{CN}|) \cdot i_c)$$

$$E_{sw,R3} = K \cdot (3|v_{AN}| \cdot i_a + (|v_{BC}| + |v_{CN}| + |v_{BN}|) \cdot i_b + (|v_{AB}| + 3|v_{AN}| + |v_{BN}| + 2|v_{CN}|) \cdot i_c)$$

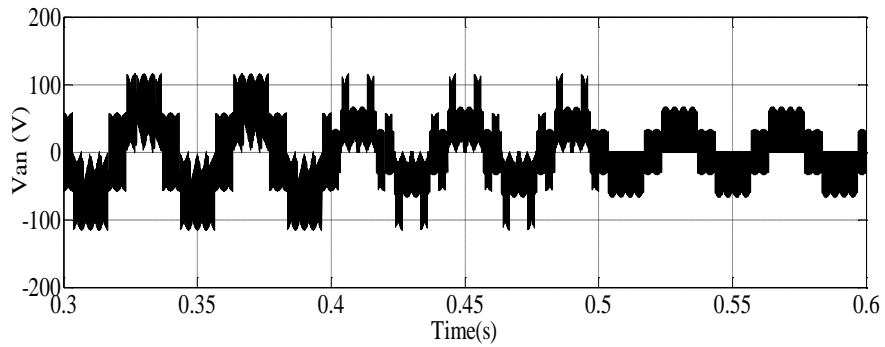
SIMULATION / HARDWARE - PARAMETERS

DTMC

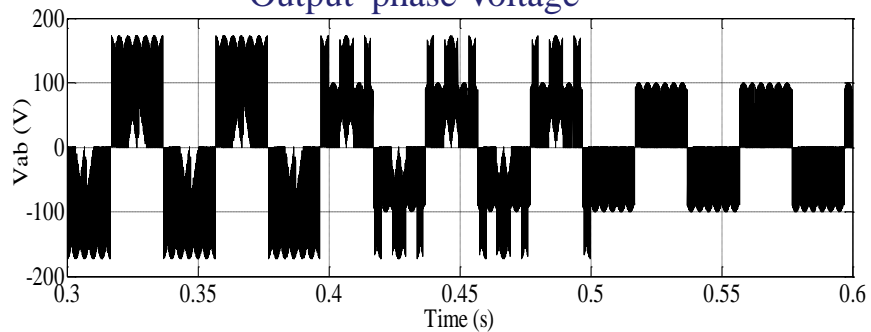
R-L Load	$R = 20\Omega$, $L = 21mH$
Input phase voltage	100 V
Input voltage frequency	50 Hz
Input filter	$L = 2 mH$, $C = 35 \mu F$, $R_d = 15 \Omega$
Output Voltage frequency	25 Hz
Switching frequency	6 kHz
Modulation Index	0.72, 0.5, 0.25

SIMULATION RESULTS

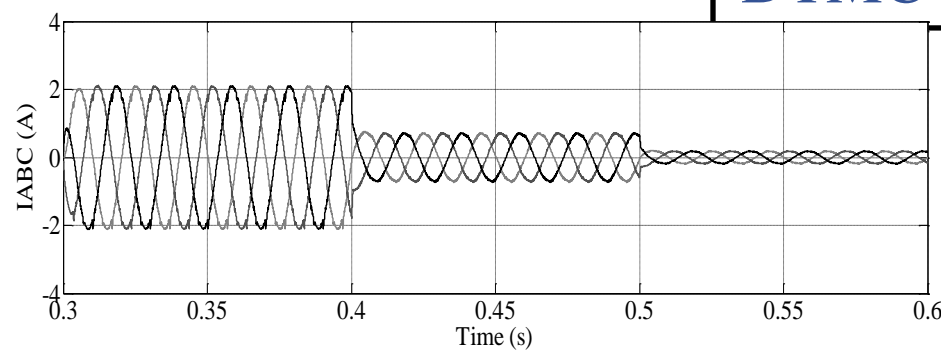
DTMC



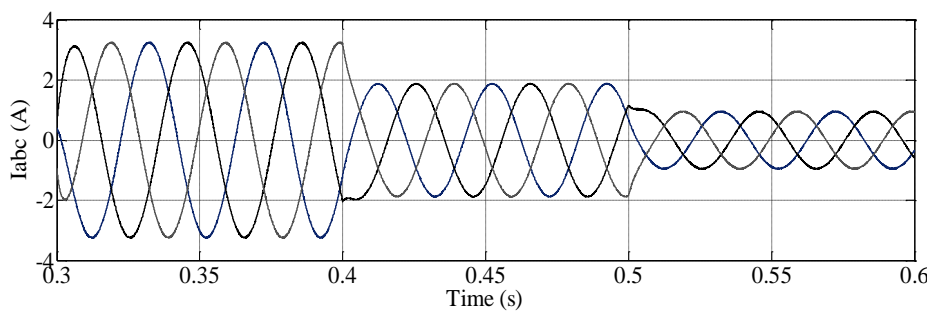
Output phase Voltage



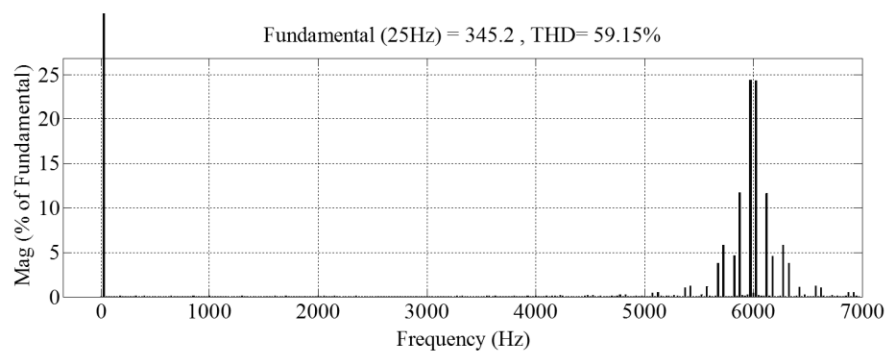
Output line Voltage



Input Current

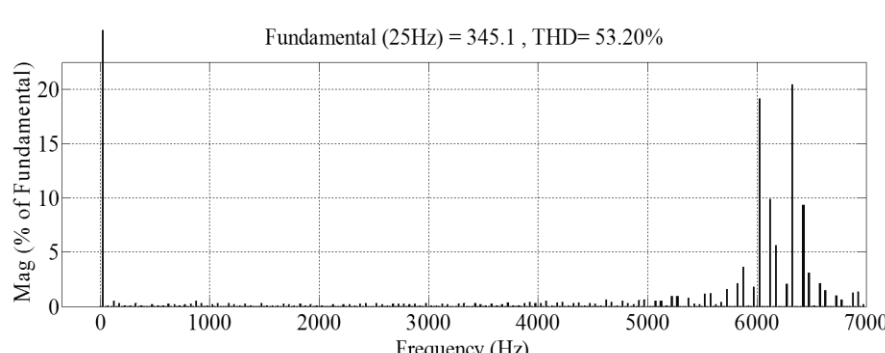


Output Current



Harmonic characteristic of output Voltage for CMC

78



Harmonic characteristic of output Voltage for DTMC

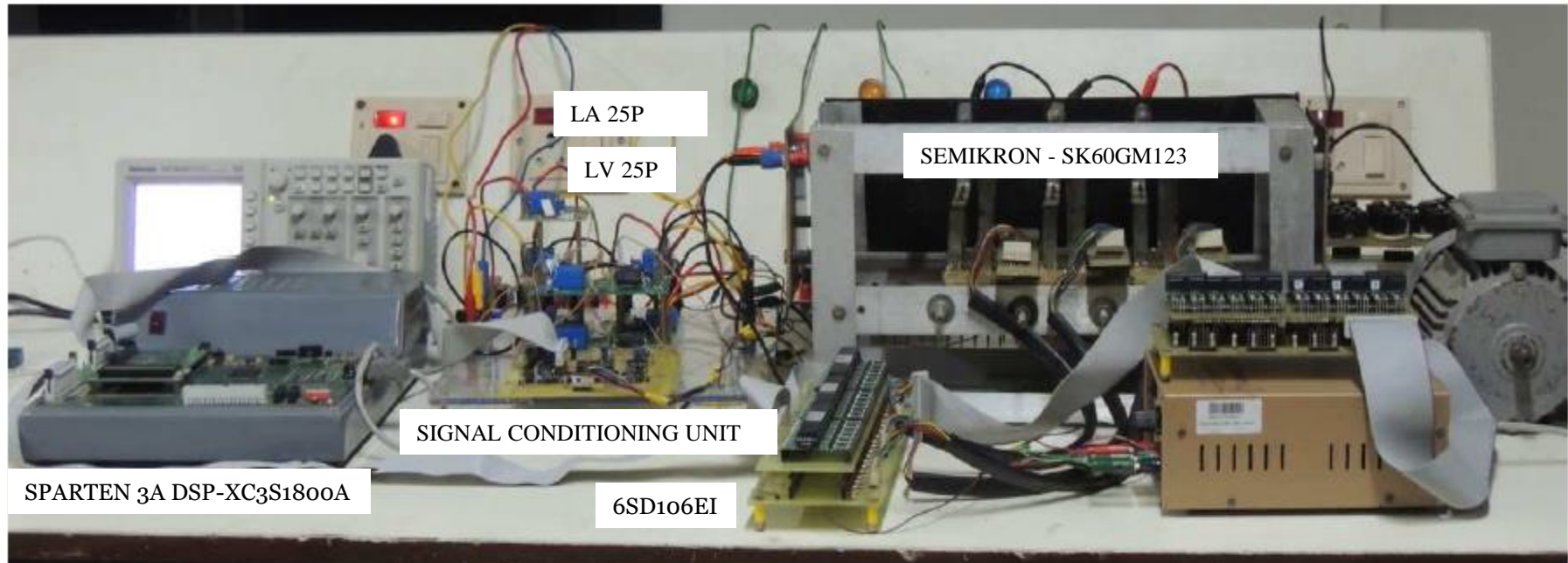
HARDWARE PROTOTYPE

DTMC

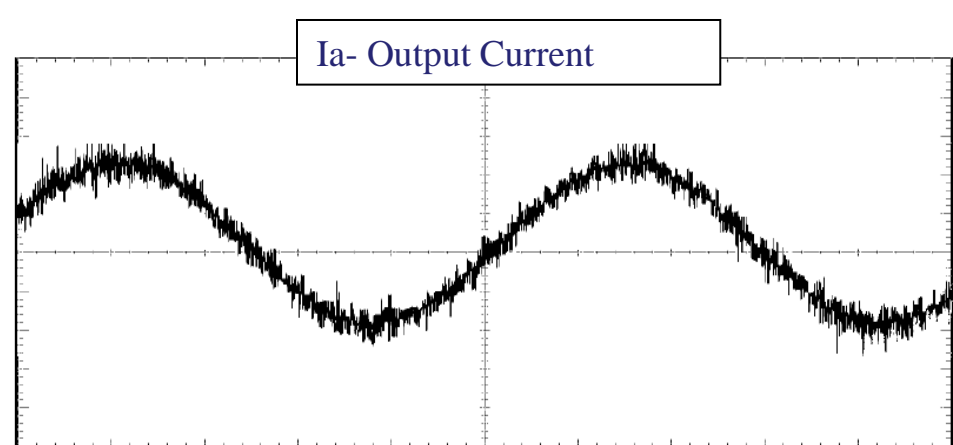
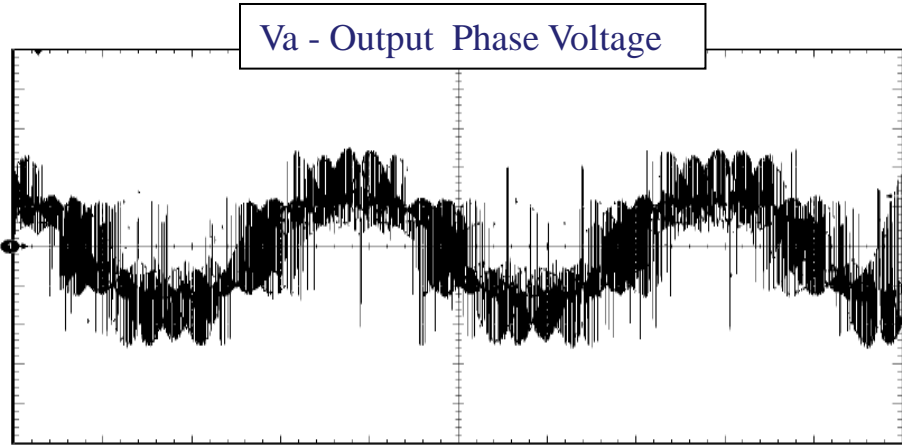
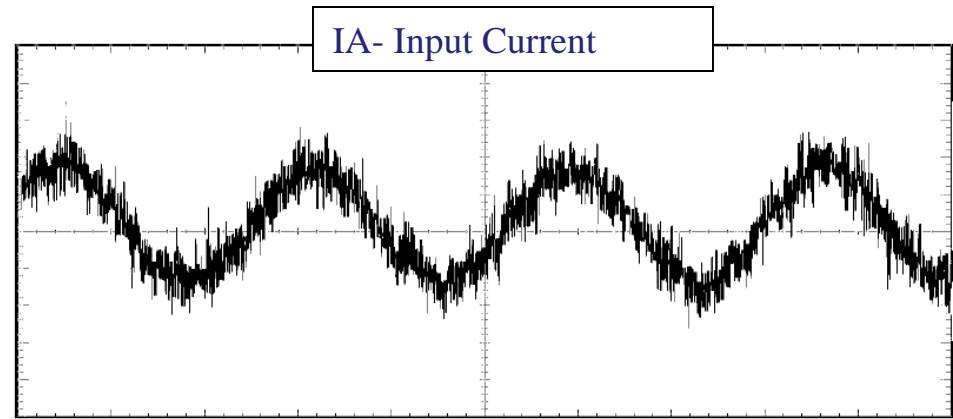
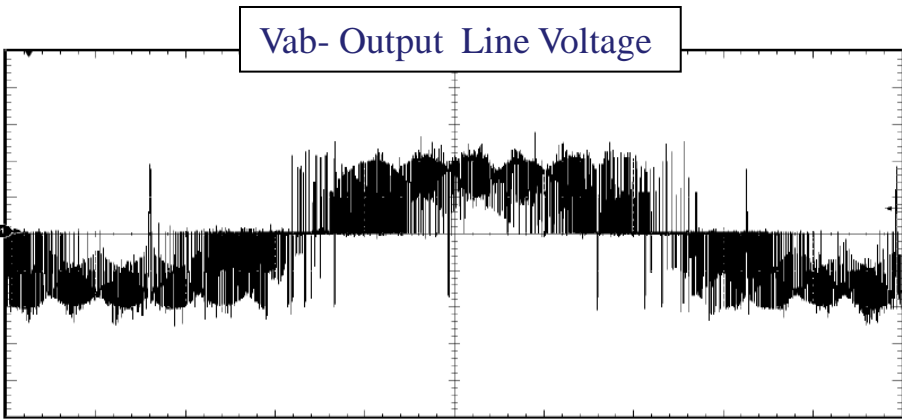
Single Bidirectional Switch – SK60GM123



Direct Three Level Matrix converter setup



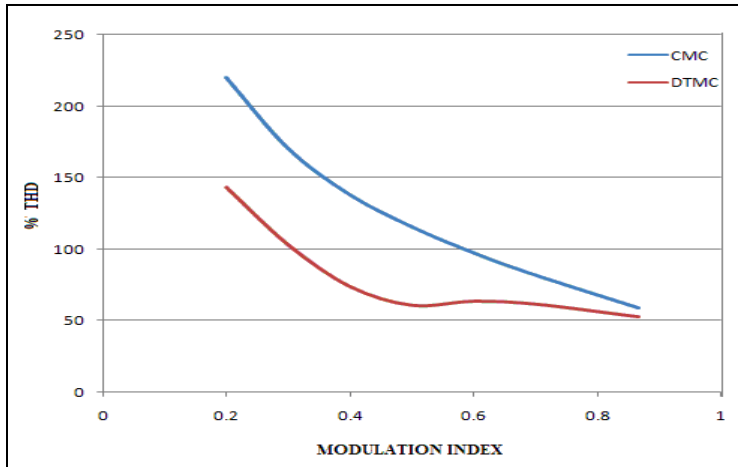
HARDWARE RESULTS



COMPARISION OF CMC & DTMC – THD & LOSSES

DTMC

% THD Vs MI for CMC & DTMC

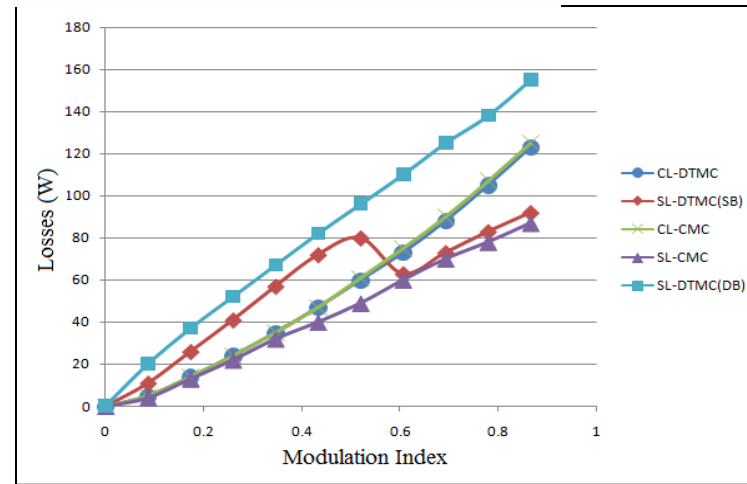


Compared to CMC the THD of DTMC reduces by 10 % and 58% for MI of 0.866 and 0.3

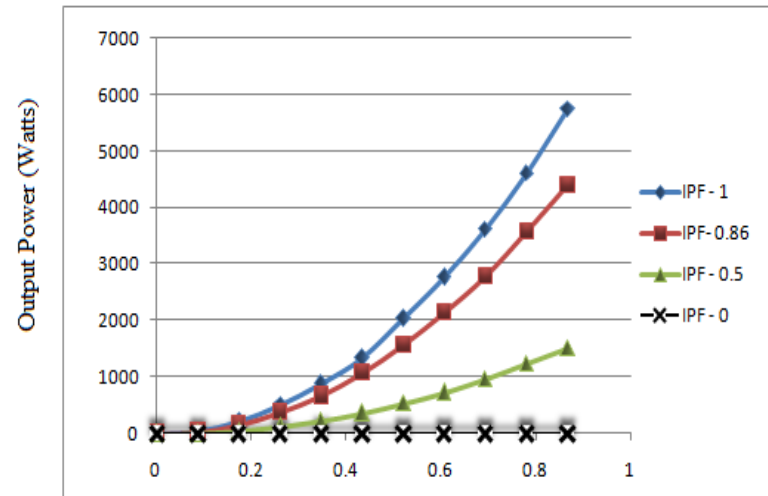
INFERENCE

- 1) At lower modulation indices DTMC has a superior THD performance than CMC
- 2) The switching losses of DTMC is always greater than CMC.
- 3) The output power of the DTMC & CMC both decreases as the input power factor increases.

Losses Vs MI for CMC & DTMC



Output Vs MI (different IPF) for CMC & DTMC



SUMMARY

A topology termed as DTMC with lesser THD compared to CMC is proposed

The Space vector technique for Direct three level matrix converter was developed.

The chapter developed the method of neutral current balancing and reduction of THD using virtual vectors & nearest three vectors.

The switching loss model for DTMC is developed

Simulation results and a hardware results of the prototype is presented.



CHAPTER –VI

Direct Torque Control **(DTC)** of Direct Three Level Matrix Converter

Direct Torque Control (DTC) Characteristics

Advantages:

High - Dynamic Performance

No fixed switching pattern (No modulator Stage)

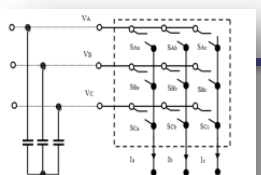
Torque and speed are the directly controlled variable

Non requirement of coordinate transformation

Disadvantages

Higher Current ripple & Torque ripple (Higher switching losses)

Difficulty in controlling Torque and flux at low speed



Direct Torque Control (DTC) Technique

Stator Voltage in Stationary frame of reference

$$V_s^s = R_s i_s^s + \frac{d\psi_s^s}{dt}$$

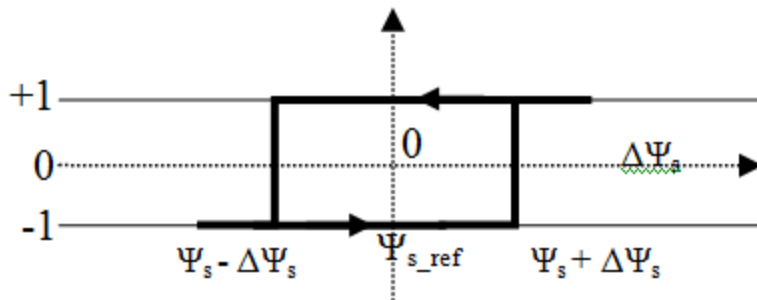
Neglecting stator resistance

$$V_s = \frac{\Delta\psi_s}{\Delta t}$$

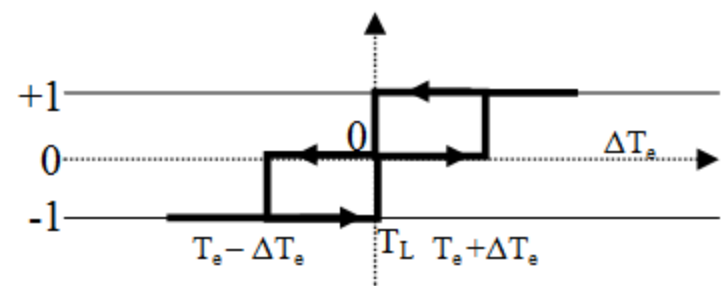
Torque Equation

$$T_e = \frac{3}{2} P |\psi_s| |\psi_r| \sin \theta_{sr}$$

The Torque of the drive can be controlled by the control of flux and flux angle.

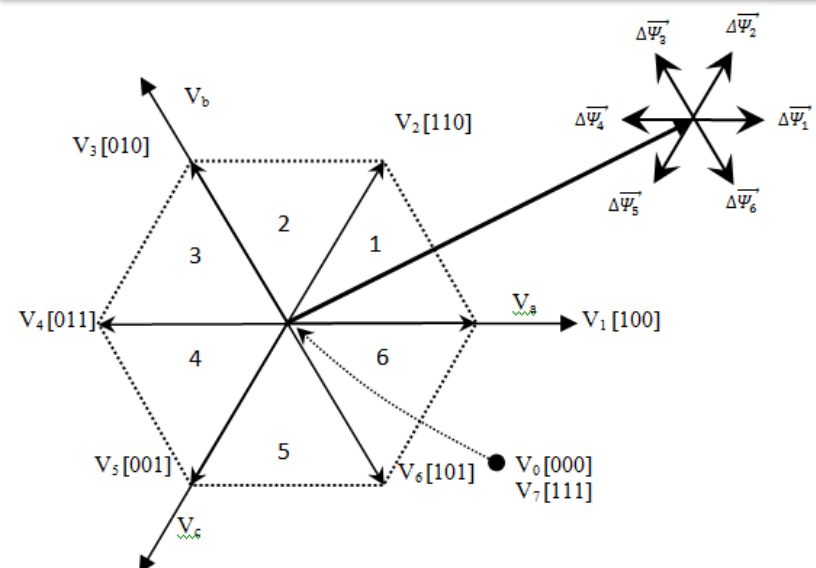


Two level Flux Hysteresis Control



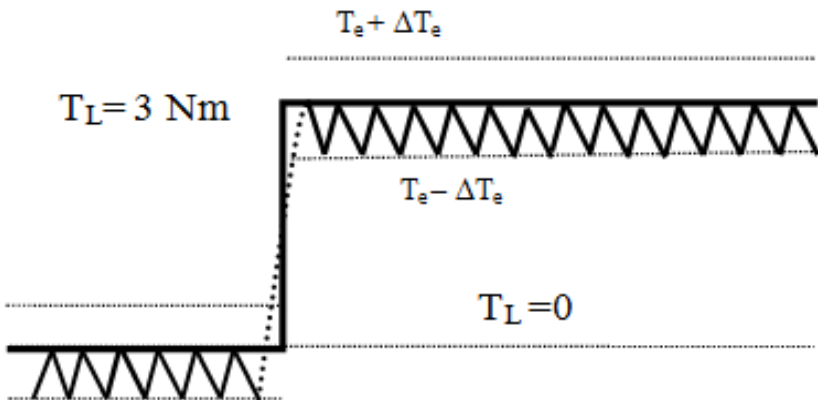
Three level Torque Hysteresis Control

Classical DTC for Inverter



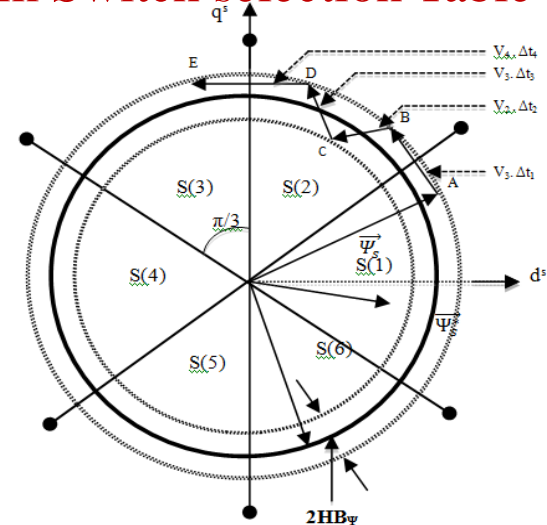
Sector of Ψ	$H_\Psi = -1$			$H_\Psi = 1$		
	$H_T = -1$	$H_T = 0$	$H_T = 1$	$H_T = -1$	$H_T = 0$	$H_T = 1$
1	V_2	V_0	V_6	V_3	V_7	V_5
2	V_3	V_7	V_1	V_4	V_0	V_6
3	V_4	V_0	V_2	V_5	V_7	V_1
4	V_5	V_7	V_3	V_6	V_0	V_2
5	V_6	V_0	V_4	V_1	V_7	V_3
6	V_1	V_7	V_5	V_2	V_0	V_4

Optimum Switch selection Table (OST)



Torque Control

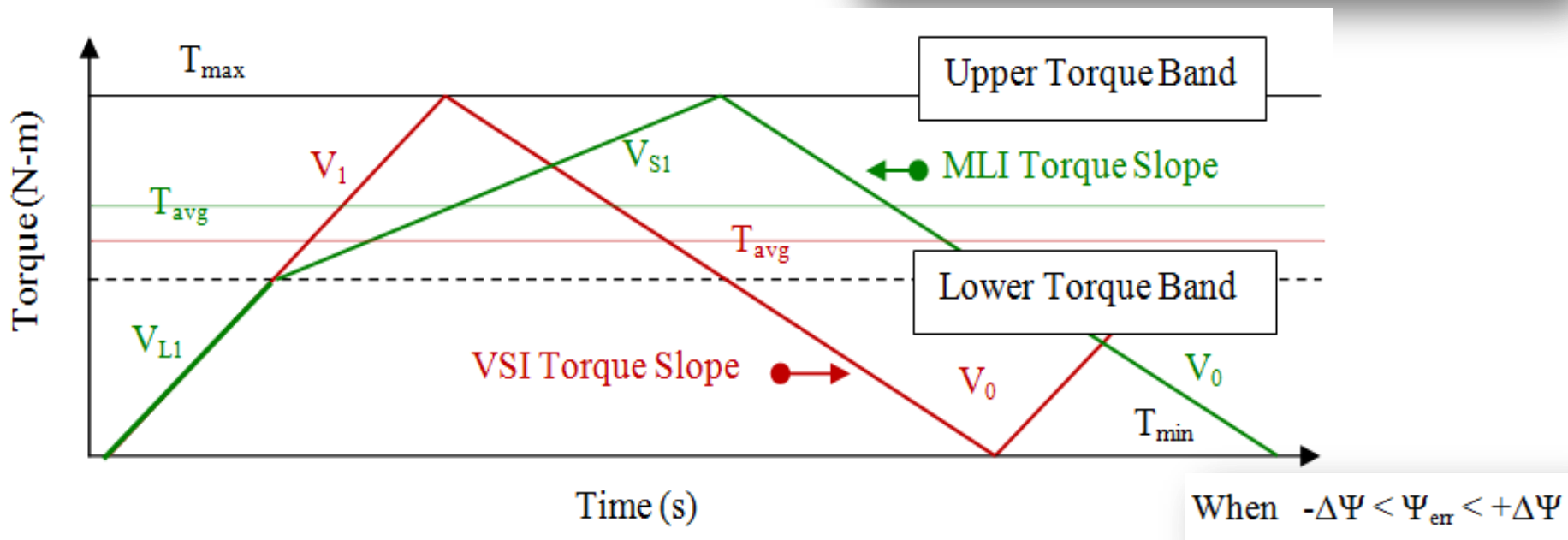
86



Flux Control

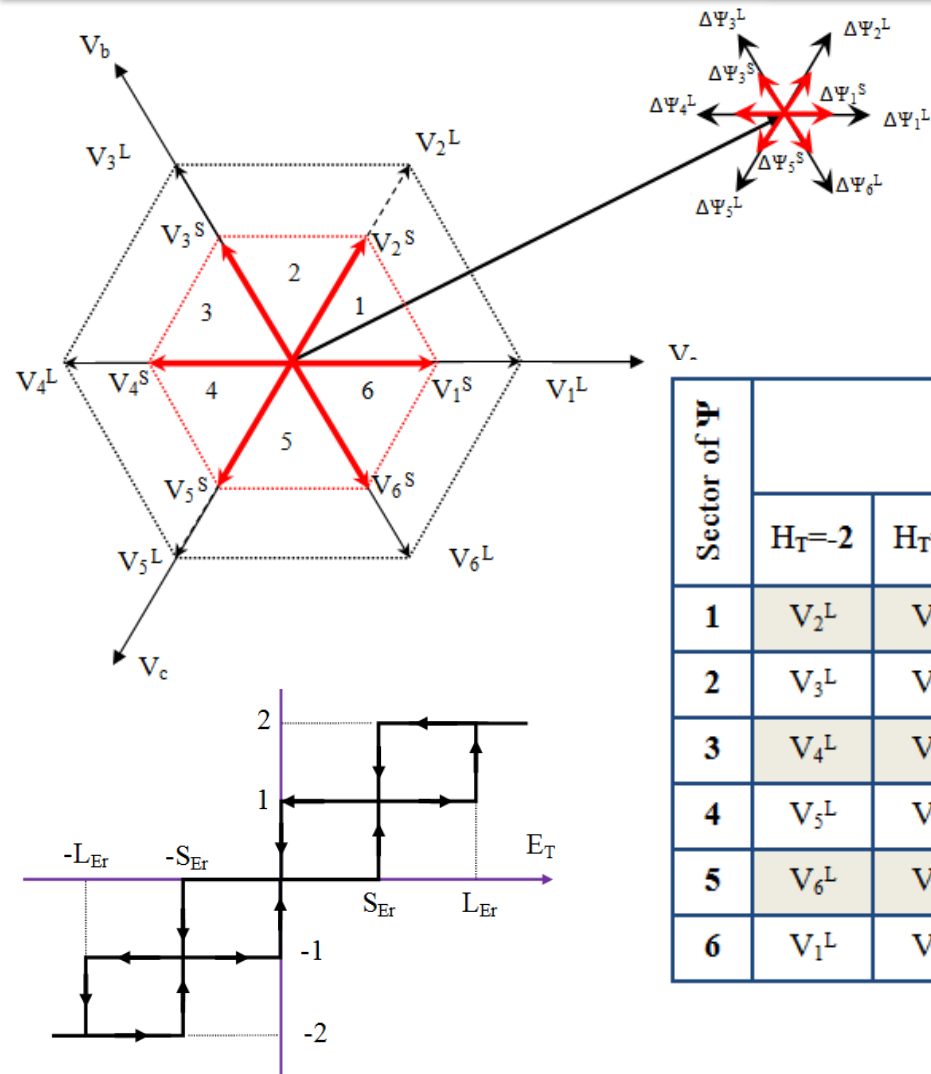
Long & Short Vector for torque ripple Reduction

$$\text{Torque}_{\text{ripple}} = \frac{\text{Torque}_{\text{max}} - \text{Torque}_{\text{min}}}{\text{Torque}_{\text{Average}}}$$



Average Torque of VSI is less than MLI → Hence Torque ripple is minimized

Classical DTC for Multilevel Inverter (MLI)



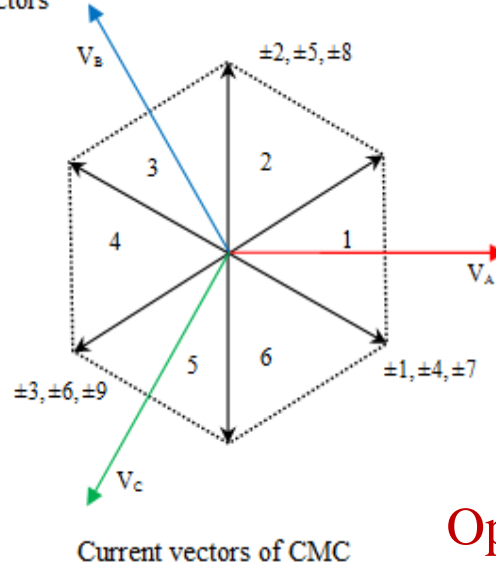
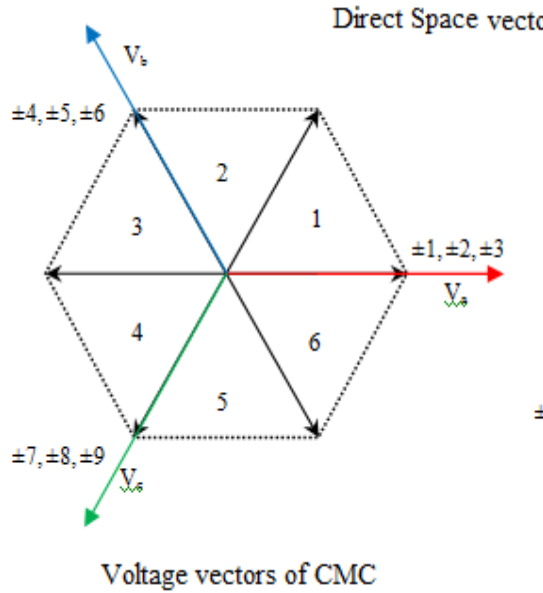
Long Vectors – Torque transitions
Short Vectors – Steady Torque conditions

Sector of Ψ	$H_\Psi = -1$					$H_\Psi = 1$				
	$H_T = -2$	$H_T = -1$	$H_T = 0$	$H_T = 1$	$H_T = 2$	$H_T = -2$	$H_T = -1$	$H_T = 0$	$H_T = 1$	$H_T = 2$
1	V_2^L	V_2^S	V_0	V_6^S	V_6^L	V_3^L	V_3^S	V_0	V_5^S	V_5^L
2	V_3^L	V_3^S	V_7	V_1^S	V_1^L	V_4^L	V_4^S	V_7	V_6^S	V_6^L
3	V_4^L	V_4^S	V_0	V_2^S	V_2^L	V_5^L	V_5^S	V_0	V_1^S	V_1^L
4	V_5^L	V_5^S	V_7	V_3^S	V_3^L	V_6^L	V_6^S	V_7	V_2^S	V_2^L
5	V_6^L	V_6^S	V_0	V_4^S	V_4^L	V_1^L	V_1^S	V_0	V_3^S	V_3^L
6	V_1^L	V_1^S	V_7	V_5^S	V_5^L	V_2^L	V_2^S	V_7	V_4^S	V_4^L

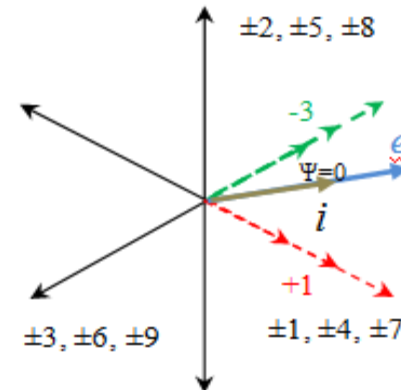
Optimum Switch selection Table (OST)

Five level –Torque Hysteresis controller

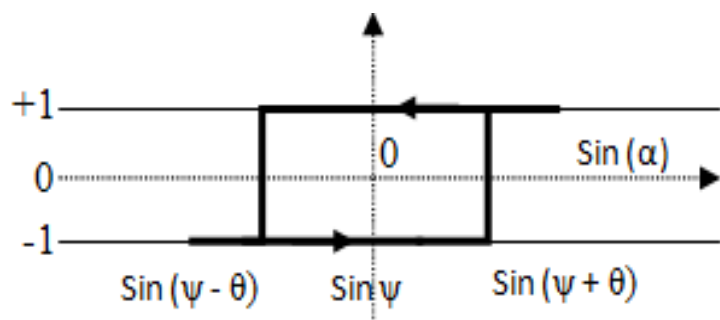
DTC & Input Current Control in CMC



Current Control in CMC



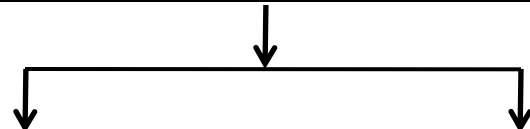
Optimum Switch selection Table (OST)



Input current sector number												
B $_{\Psi}$	1		2		3		4		5		6	
B $_{\Psi}$	+1	-1	+1	-1	+1	-1	+1	-1	+1	-1	+1	-1
V ₁	-3	1	2	-3	-1	2	3	-1	-2	3	1	-2
V ₂	9	-7	-8	9	7	-8	-9	7	8	-9	-7	8
V ₃	-6	4	5	-6	-4	5	6	-4	-5	6	4	-5
V ₄	3	-1	-2	3	1	-2	-3	1	2	-3	-1	2
V ₅	-9	7	8	-9	-7	8	9	-7	-8	9	7	-8
V ₆	6	-4	-5	6	4	-5	-6	4	5	-6	-4	5

Direct Space Vectors of DTMC

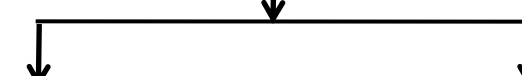
Rotating Space vectors (24)



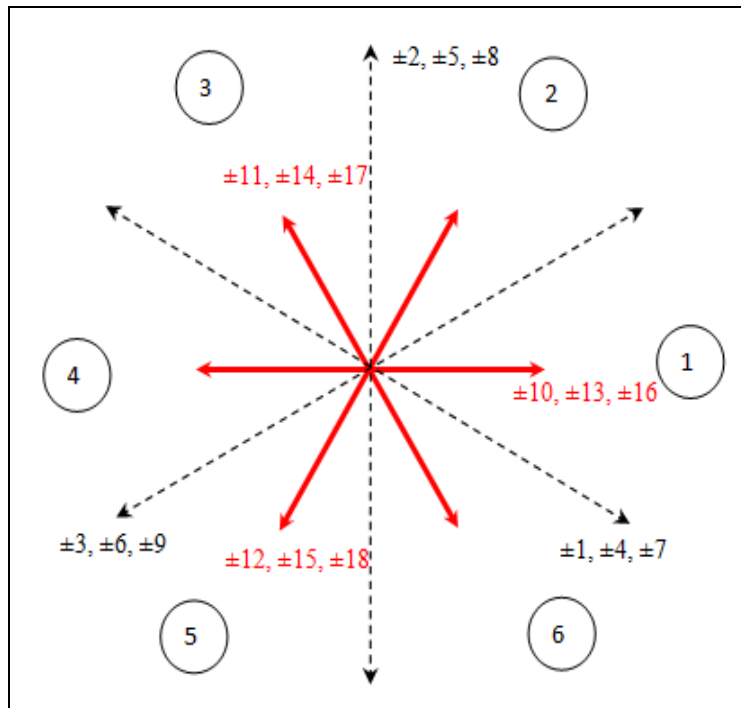
Circular (6)

Elliptical (24)

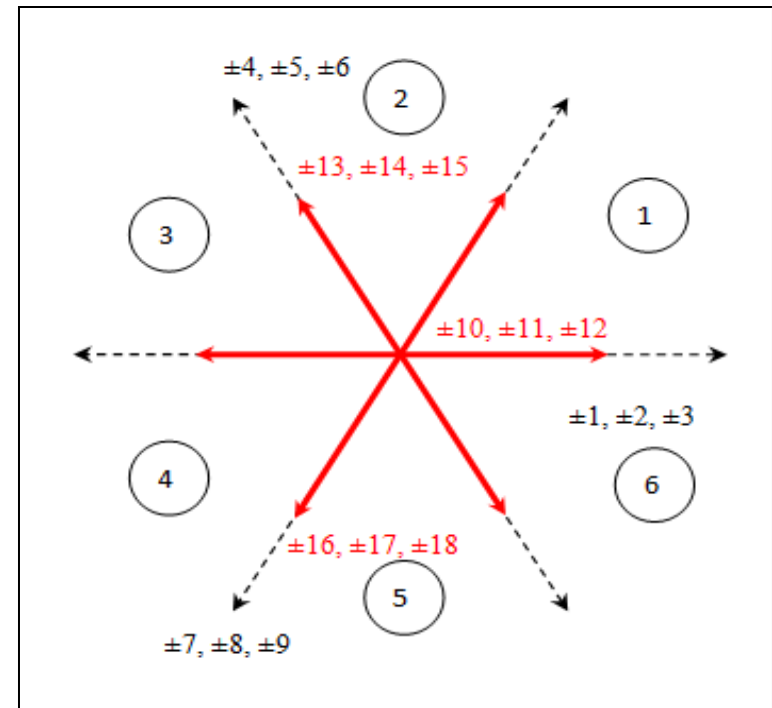
Stationary Space vectors (36)



Zero (4)



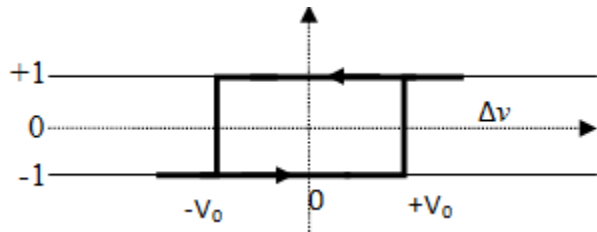
Current Space vectors (L &S)



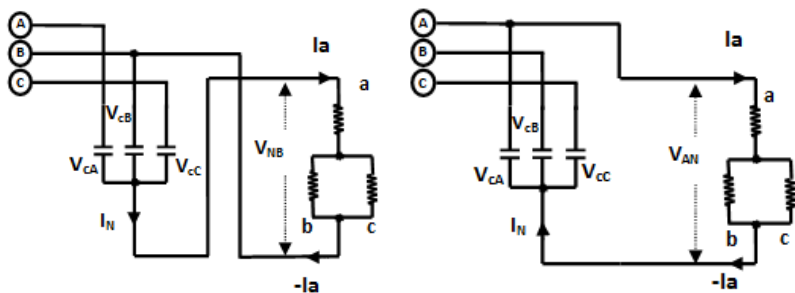
Voltage Space vectors (L &S)

Use of Short Space Vectors of DTMC

$$\Delta v = V_{cA} + V_{cB} + V_{cC}$$



Two level –voltage Hysteresis controller

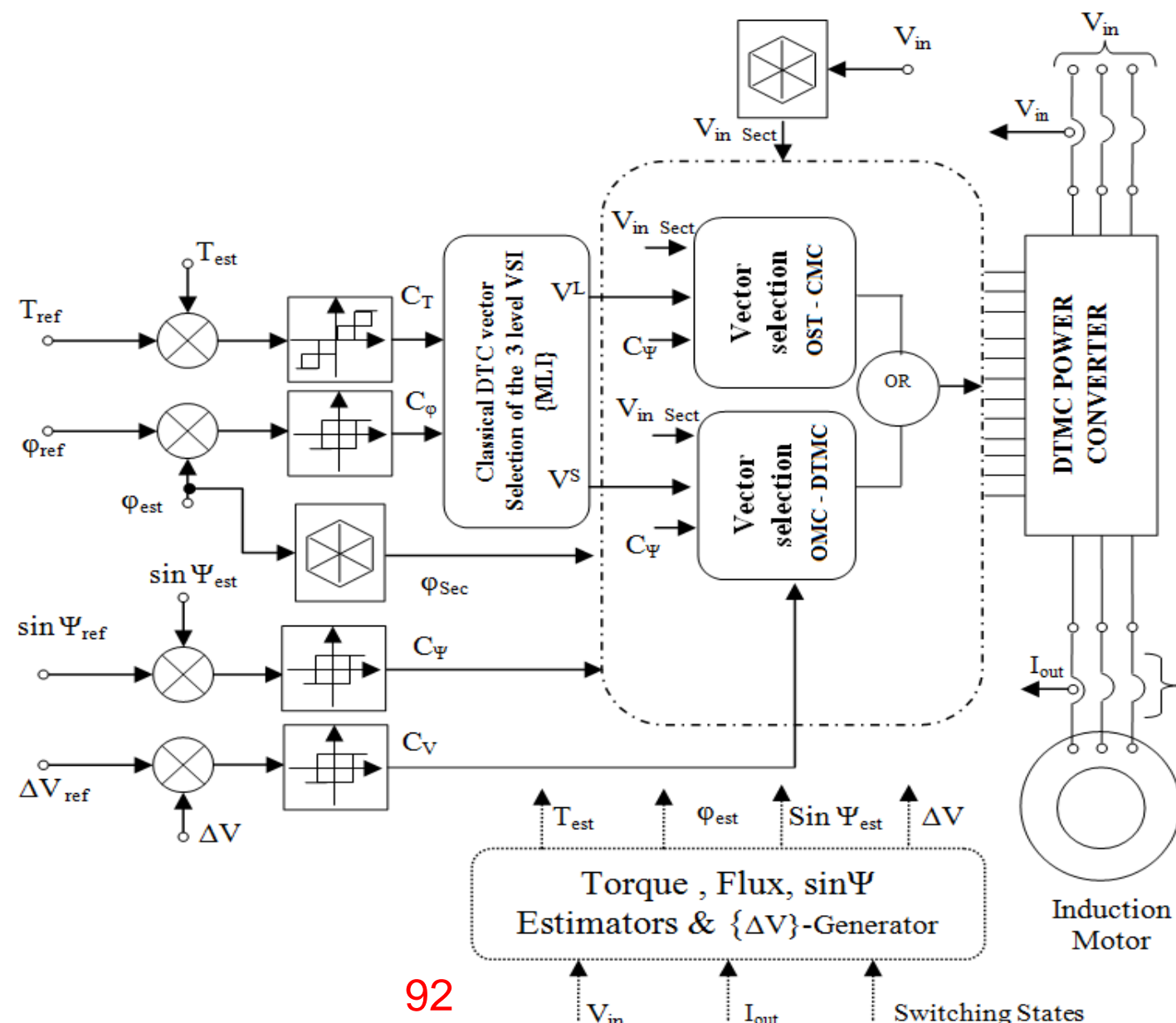


Neutral Current Balancing

Optimum Switch selection Table (OST)

		Input current sector number												
		1	2	3	4	5	6							
V_1^S	$B_\psi \setminus B_v$	+1	+10	+10	-12	-12	+11	-11	-10	-10	+12	+12	-11	-11
		-1	-12	-11	+11	+10	-10	-12	+12	+11	-11	-10	+10	+12
V_2^S	$B_\psi \setminus B_v$	+1	-16	-16	+18	+18	-17	-17	+16	+16	-18	-18	+17	+17
		-1	+18	+17	-17	-16	+16	+18	-18	-17	+17	+16	-16	-18
V_3^S	$B_\psi \setminus B_v$	+1	+13	+13	-15	-15	+14	+14	-13	-13	+15	+15	-14	-14
		-1	-15	-14	+14	+13	-13	-15	+15	+14	-14	-13	+13	+15
V_4^S	$B_\psi \setminus B_v$	+1	-10	-10	+12	+12	-11	-11	+10	+10	-12	-12	+11	+11
		-1	+12	+11	-11	-10	+10	+12	-12	-11	+11	+10	-10	-12
V_5^S	$B_\psi \setminus B_v$	+1	+16	+16	-18	-18	+17	+17	-16	-16	+18	+18	-17	-17
		-1	-18	-17	+17	+16	-16	-18	+18	+17	-17	-16	+16	+18
V_6^S	$B_\psi \setminus B_v$	+1	-13	-13	+15	+15	-14	-14	+13	+13	-15	-15	+14	+14
		-1	+15	+14	-14	-13	+13	+15	-15	-14	+14	+13	-13	-15

Total Block Diagram of DTC for DTMC



SIMULATION PARAMETERS

DTC - DTMC

HYSTERESIS CONTROLLER PARAMETERS

$\Delta\Psi = \pm 0.5\% \text{ of } \Psi_{\text{ref}}$

$\Delta T = \pm 10\% \text{ of } T \text{ full load}$

$\Delta V = \pm 0.5\% \text{ of } V \text{ rated line - line}$

$\Delta \sin \Psi = \pm 2\%$

$\Psi_{\text{ref}} = 80\% \text{ of } \Psi \text{ no load (0.7)} = 0.58 \text{ Wb}$

Average Switching frequency = 2.5 KHz

MACHINE PARAMETERS

3 Phase , V (Line-Line) = 400 V , 4 KW , 1430 rpm

$R_s = 1.405 \Omega$, $R_r = 1.395 \Omega$, $L_s = 5.82 \text{ mH}$, $L_r = 5.82 \text{ mH}$, $M = 172 \text{ mH}$

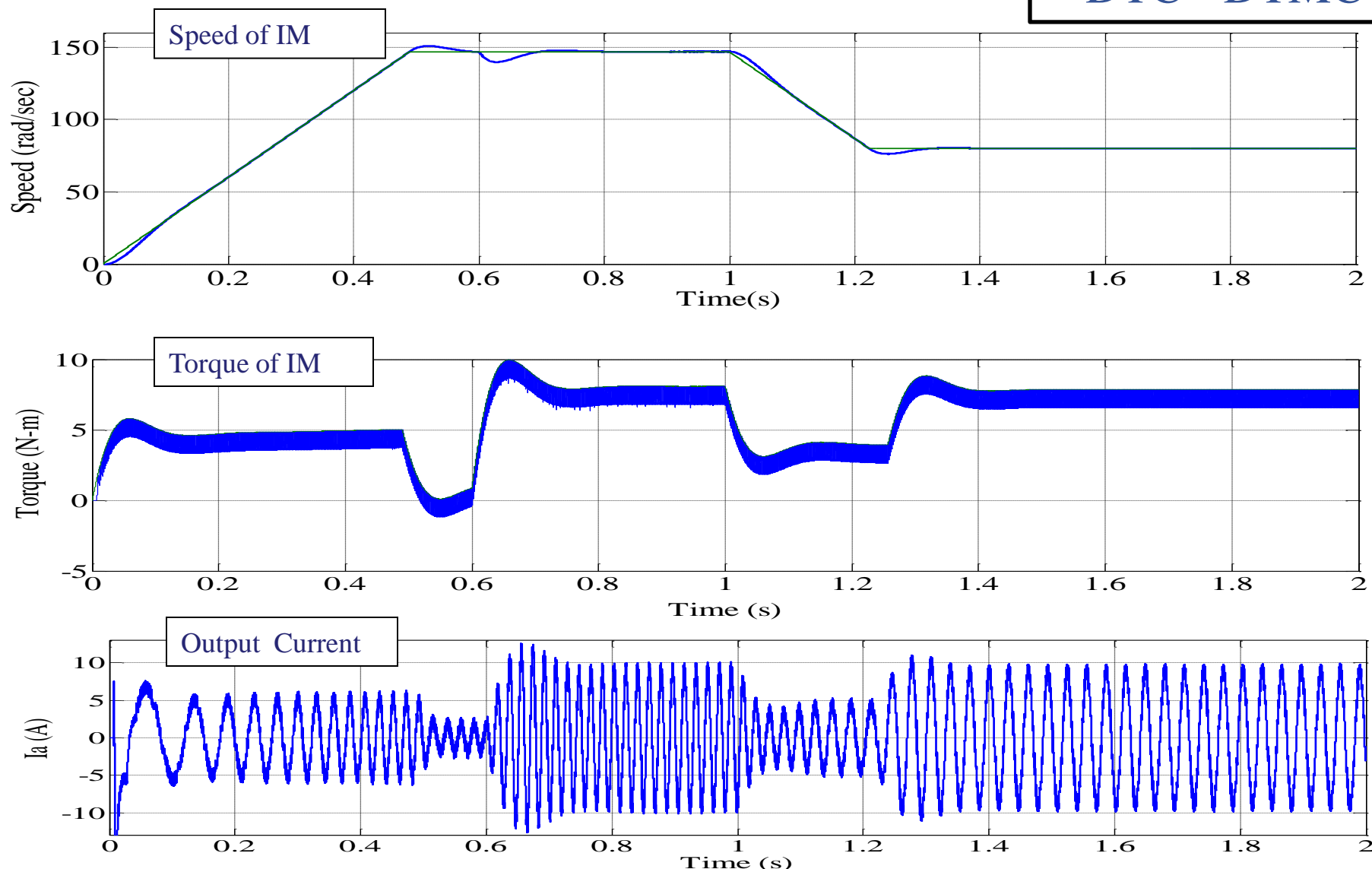
TIME OF SET POINT AND LOAD VARIATIONS

Set point - Speed is increased from 0 rpm to 1430 rpm slowly at 0 sec
is decreased from 1430 rpm to 770 rpm slowly at 1 sec
(i.e) 54% of rated speed

Load - is increased from 0 N-m to 7 N-m suddenly at 0.6 sec

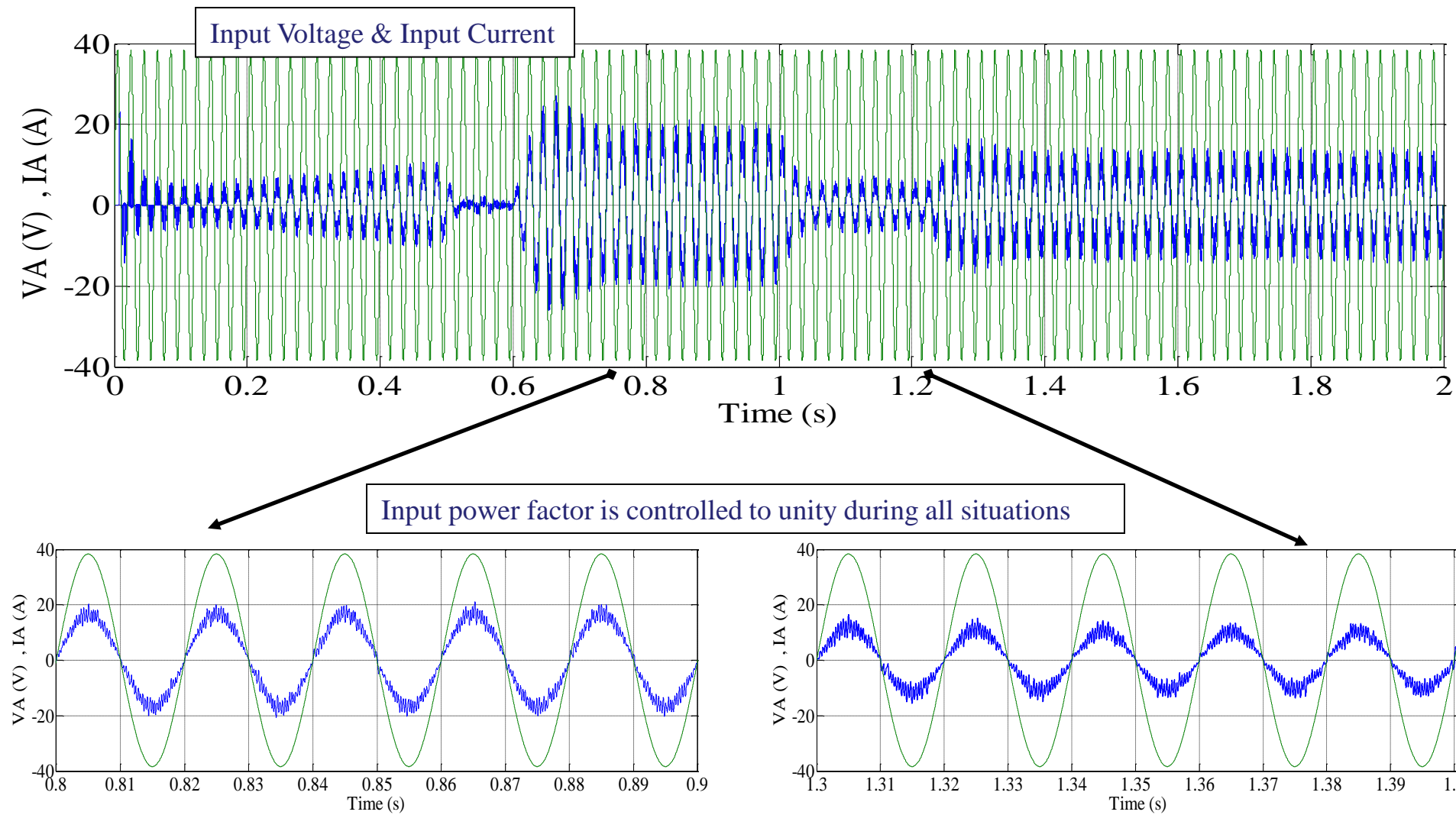
SIMULATION RESULTS

DTC - DTMC



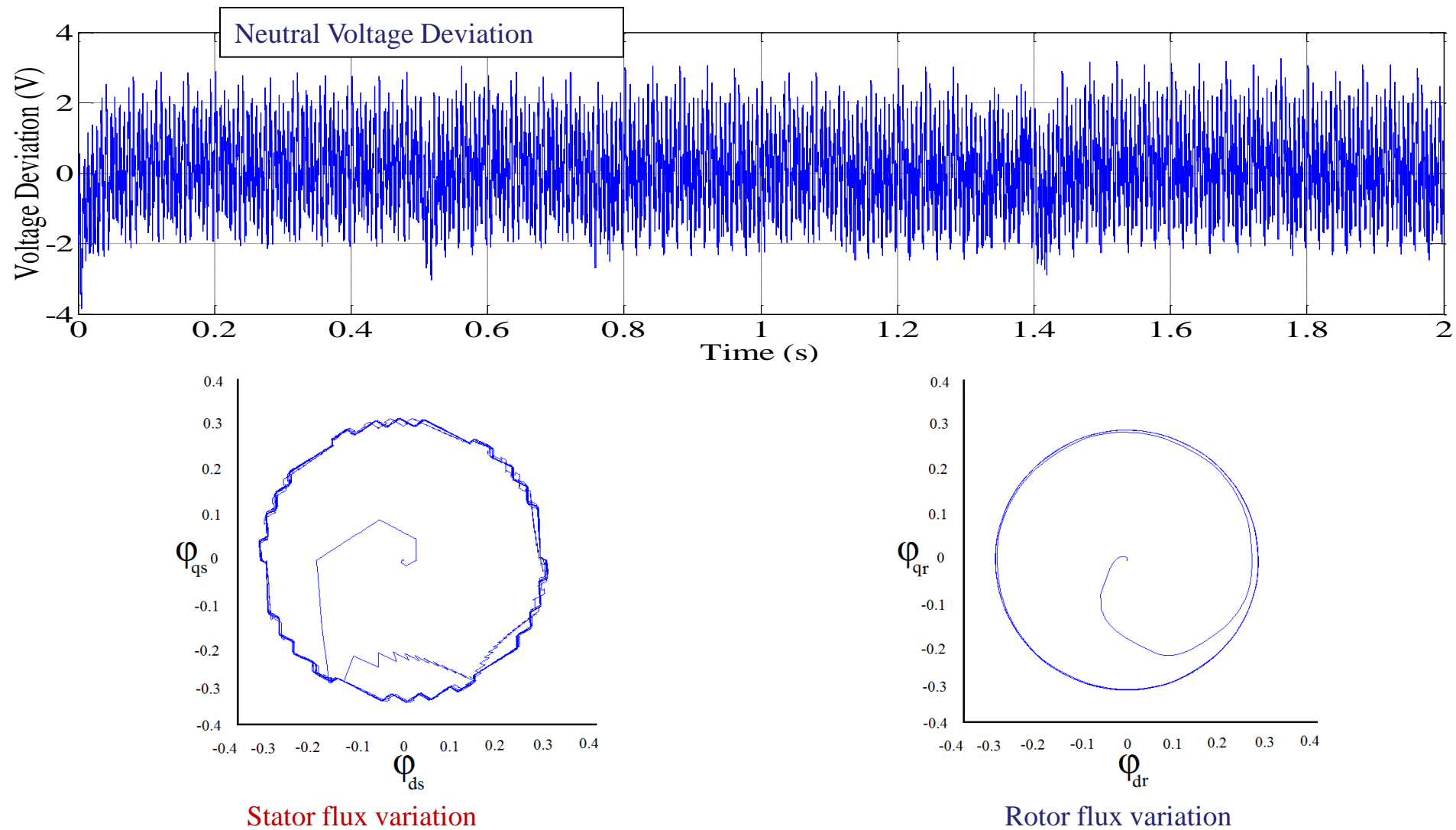
SIMULATION RESULTS

DTC - DTMC



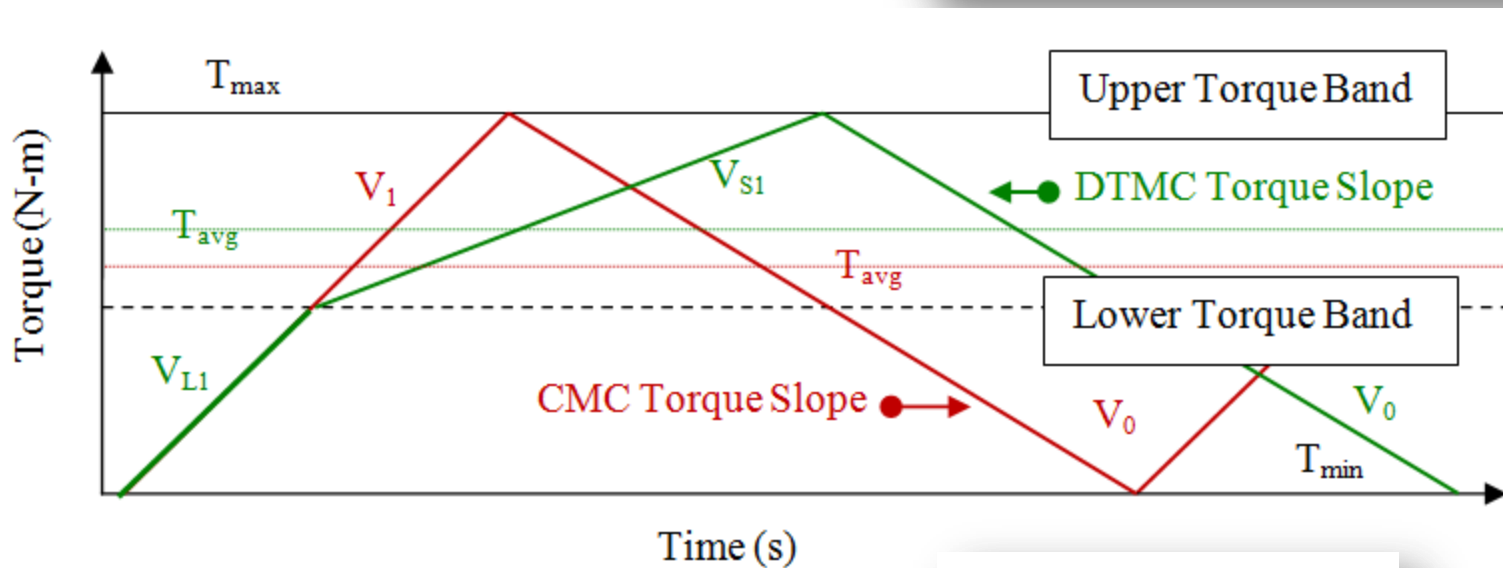
SIMULATION RESULTS

DTC - DTMC



TORQUE RIPPLE ANALYSIS

$$\text{Torque}_{\text{ripple}} = \frac{\text{Torque}_{\text{max}} - \text{Torque}_{\text{min}}}{\text{Torque}_{\text{Average}}}$$

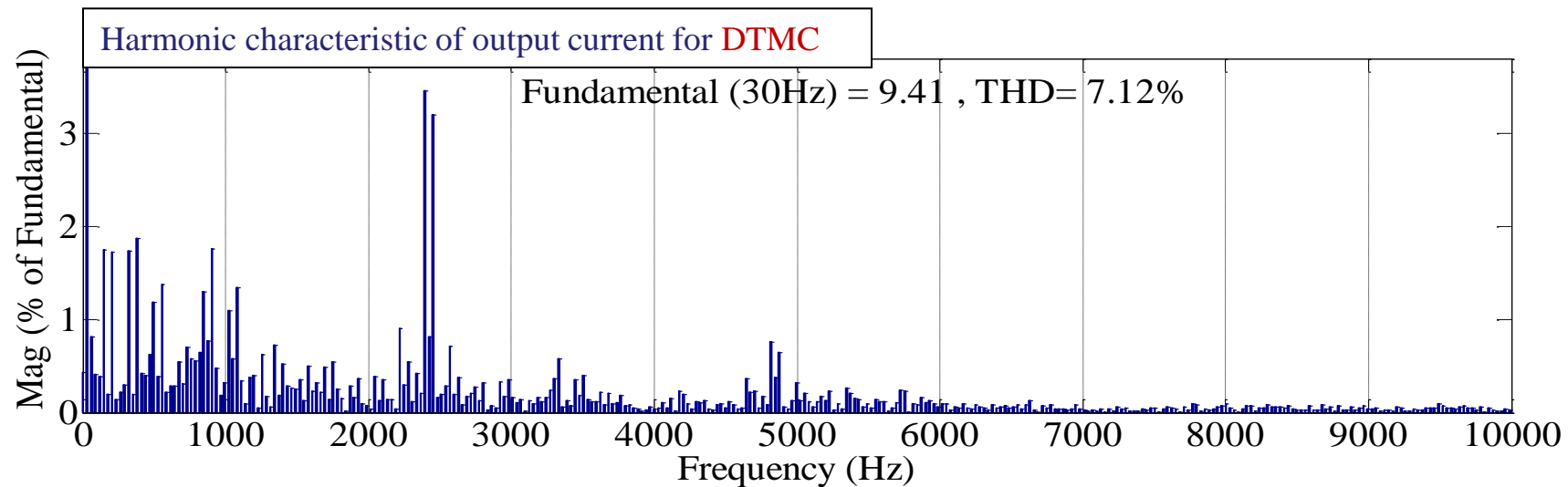
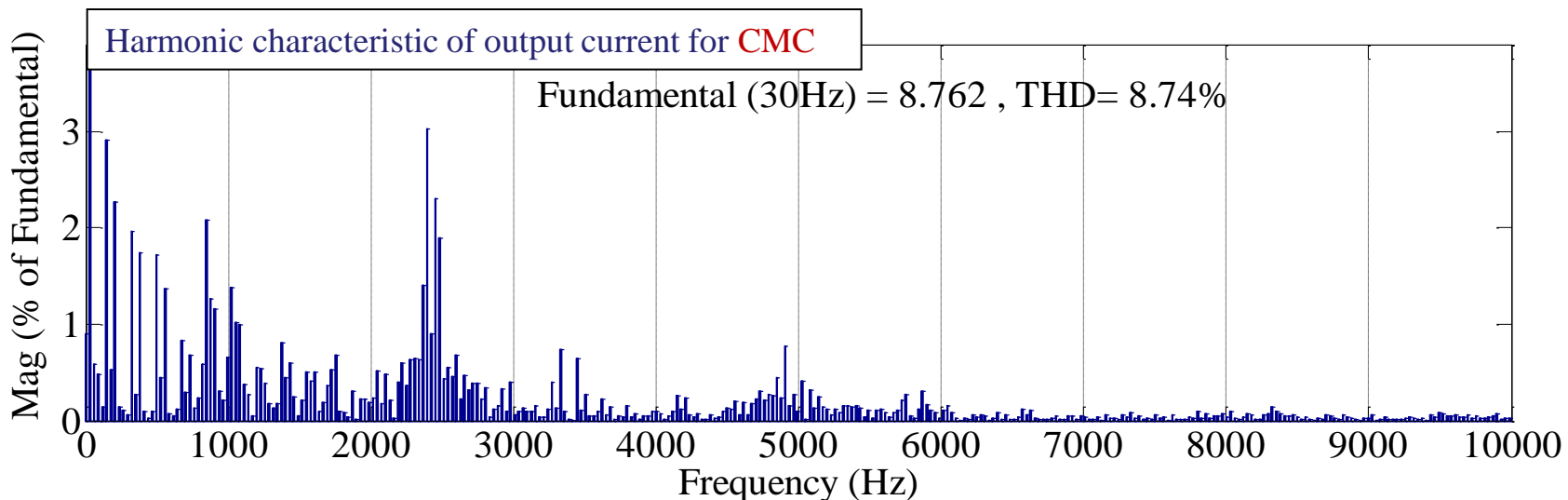


The method specified below was adopted as a measure of the torque ripple in the IM

The harmonic spectrum of the Machine input current is an indication of the ripple content of the machine torque.

TORQUE RIPPLE ANALYSIS

DTC-CMC / DTC-DTMC

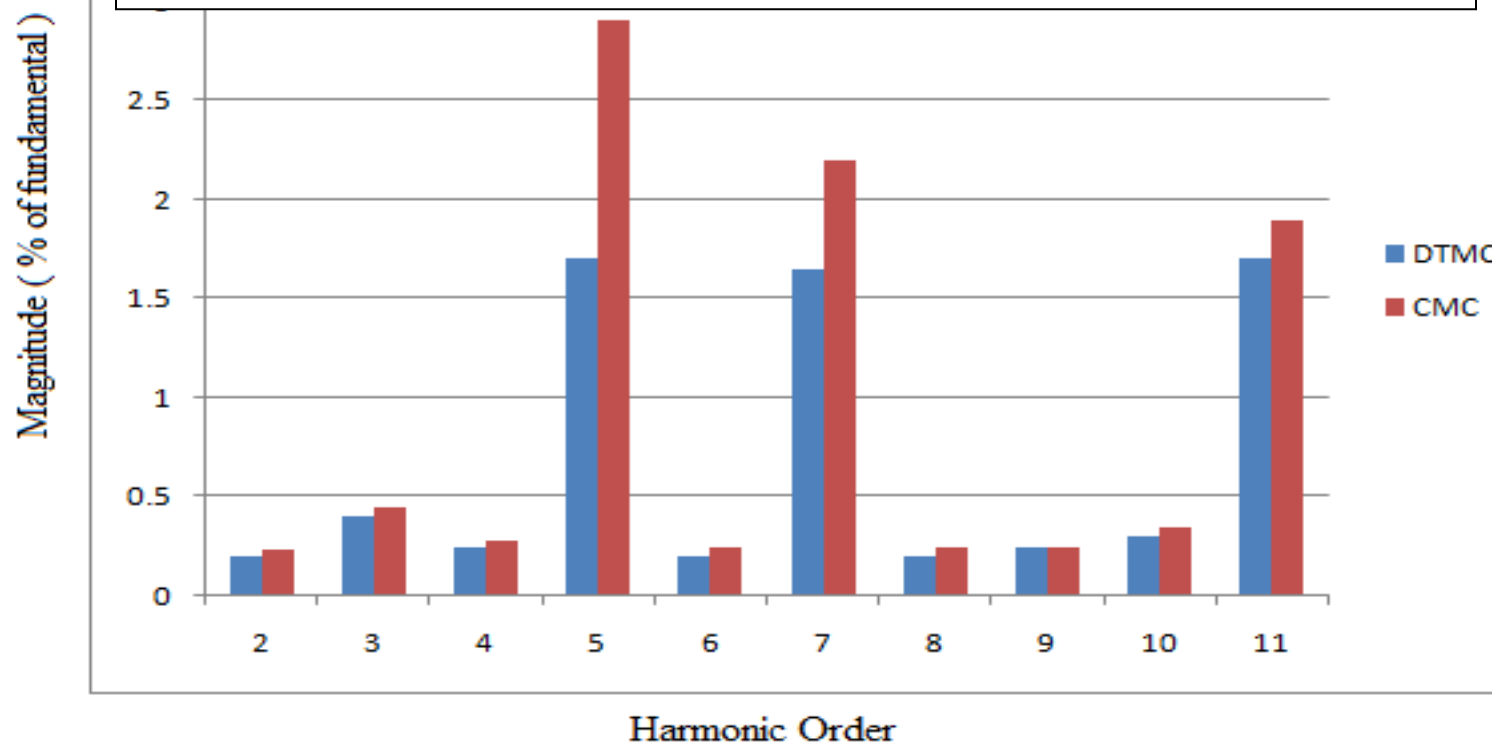


Reduction of output current % THD for DTC-DTMC compared to DTC-CMC is 12.5 %

TORQUE RIPPLE ANALYSIS

DTC-CMC / DTC-DTMC

2nd to 11th – Output current harmonic spectrum of DTC-CMC
&
DTC-DTMC Scheme



Considerable reduction of 5th 7th and 11th Harmonics for DTC-DTMC compared to DTC-CMC

SUMMARY

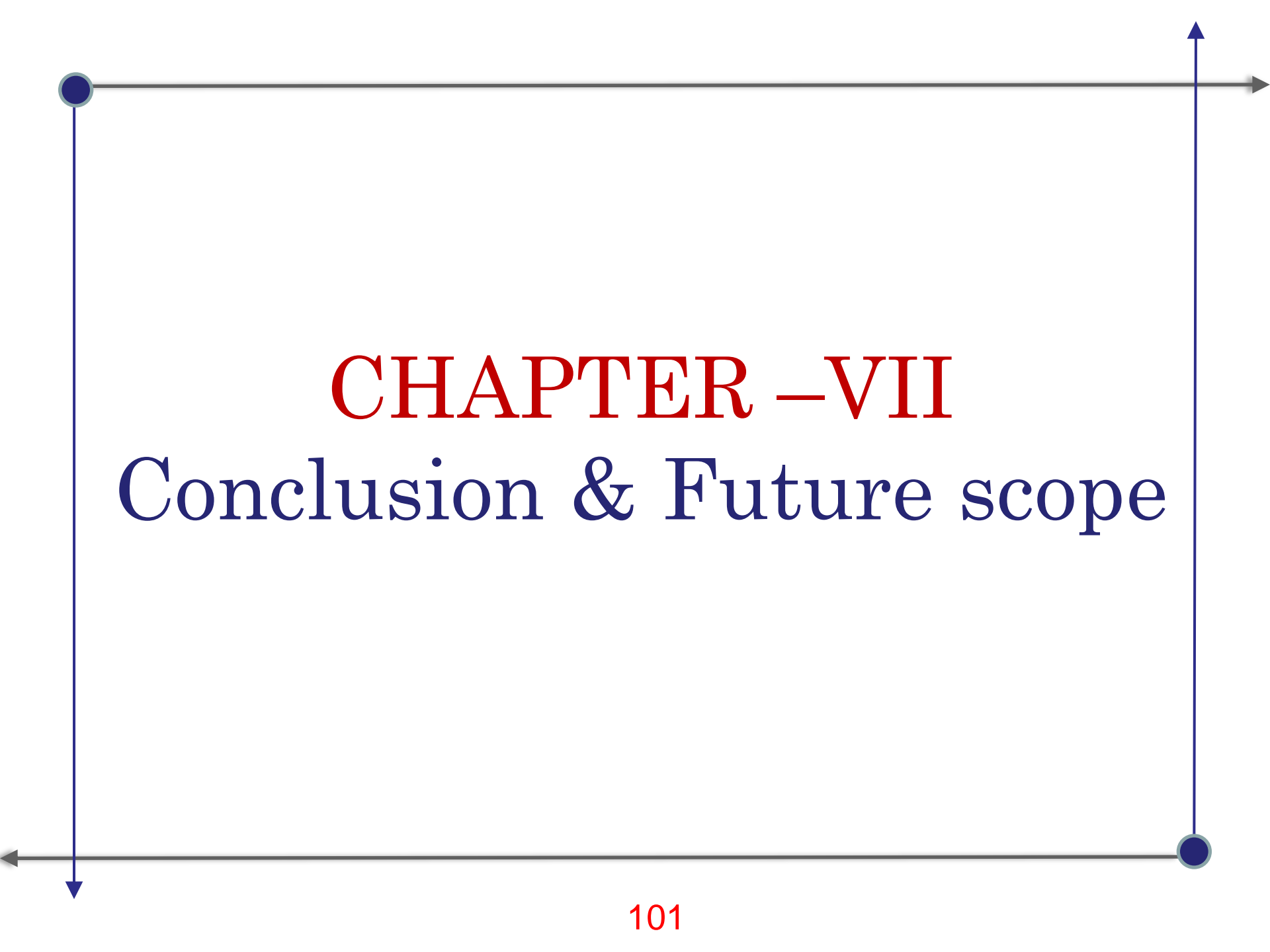
The Direct torque Procedures for VSI, MLI , CMC was discussed

The Direct torque Control Procedure of DTMC was developed.

The use of long voltage vectors during torque transition and short voltage vectors during steady state of DTMC was demonstrated for torque ripple reduction

The neutral current balancing and the input power factor control was performed using additional Hysteresis controllers [Sin and Voltage]

The Simulation Results of the DTC control of DTMC showed a considerable amount of %THD reduction up to 12.5% and hence Torque ripple reduction as compared to CMC – DTC under the same input, load and modulation conditions.



CHAPTER –VII

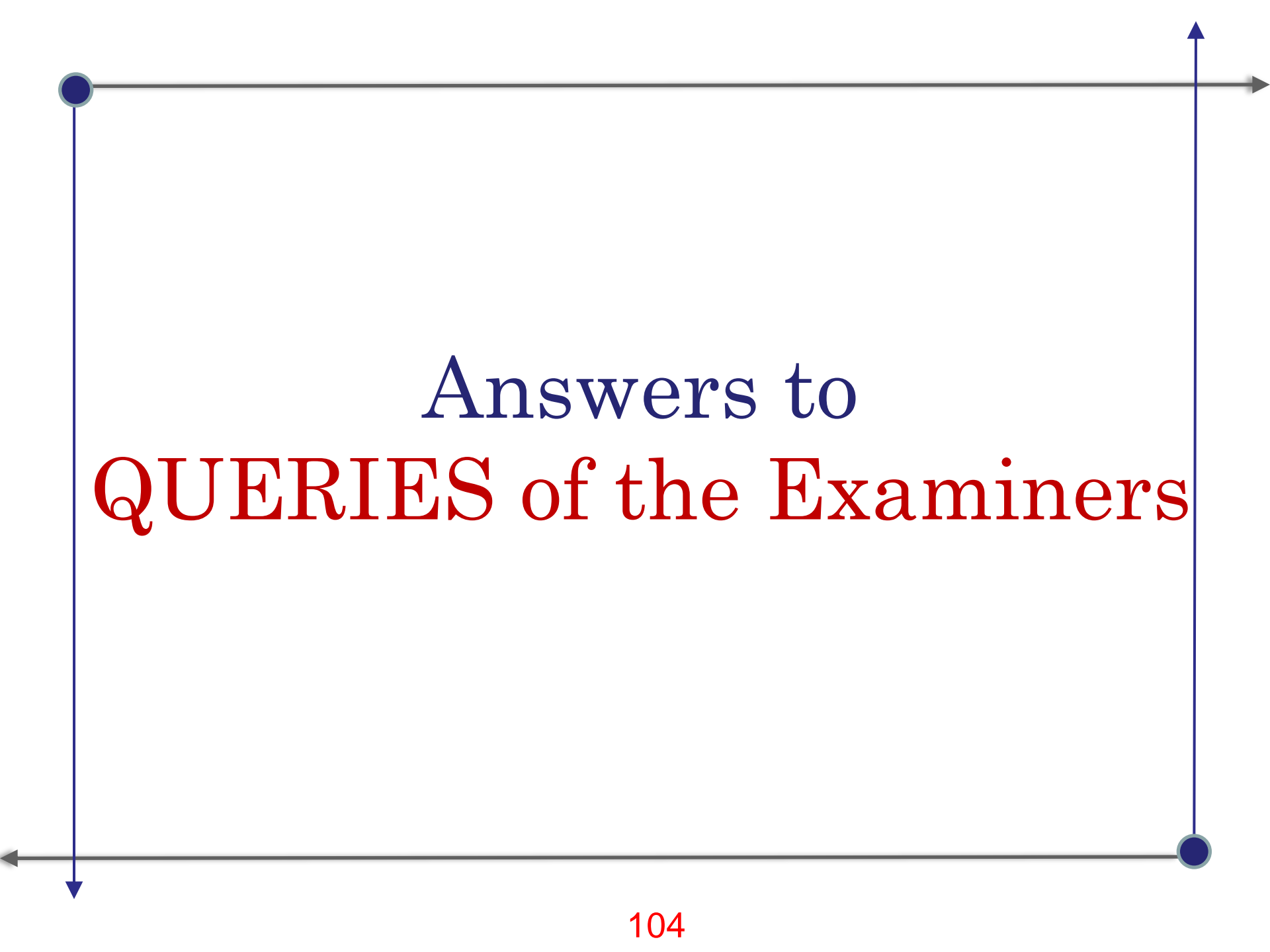
Conclusion & Future scope

CONCLUSION

- 1) A new Minimum error switching strategy (**MESS**) was proposed which has low switching losses , inherent quality to mitigate unbalance & suitable for high switching frequency
- 2) For a complete carrier based PWM technique for CMC **DIDC PWM** was proposed with carrier frequency adjustment technique to reduce the THD
- 3) With a Focus to eliminate common mode voltage in CMC **RSVM** technique was developed and a method to use **PDMC** to improve voltage transfer by 73% is proposed.
- 4) A **Simple Compensation** based on the Oscillations in the Fictitious DC bus was proposed for unbalance control at the output.
- 5) The **SVM** technique for **DTMC** was developed with **neutral current balancing** and **reduction of THD** using **virtual vectors & nearest three vectors**.
- 6) The **Direct torque Control** Procedure of DTMC was developed for torque ripple reduction.

SCOPE FOR FUTURE WORK

- 1) To study and implement the three-phase to single-phase matrix converters for **high frequency transformers**
- 2) To further investigate the proposed DTMC configuration for its common mode effects, over modulation operation and **study its control capability in closed-loop systems** for real-time applications.
- 3) To investigate the application of the **matrix converters** in the **wind energy conversion** systems using direct power control methods for the Doubly Fed Induction Generators (DFIG)
- 4) To investigate the hybrid **DTC-SVM** technique for DTMC for further improving the performance of torque ripple in the induction motor drives.
- 5) To investigate in details the **stability of matrix converters**
- 6) To investigate for the applications of **matrix converter** in **STATCOM, UPFC and IPFC**



Answers to
QUERIES of the Examiners

Answers to Queries of the Examiners

- 1) List of abbreviations are not in alphabetical order. Arrange it. Some of the symbols (eg: K_p etc....) are not listed in the list of symbols.**

Abbreviations were arranged in alphabetical order. Some symbols that were not included are included in the symbol list.

- 2) Most of the block diagrams are overlapping. Try to avoid this.**

The Figure 1.1 and 1.6 with overlapping blocks were redrawn without overlapping.

- 3) All the graphs(results) are better to draw in colour(eg. Fig.5.13 – 5.15)**

Figures 1.12, 1.16, 2.3, 2.5, 2.6, 2.8, 2.9, 2.10, 2.13(b), 5.8(b), 5.13(c), 5.14, 5.15, are printed in colour.

Continued.....

Answers to Queries of the Examiners

Simulation parameters and hardware parameters are not the same in many cases.

For DIDCPWM (Chapter 2)

For DTMC (Chapter 5)

It is not possible to compare. Change the simulation parameters according to the hardware parameters and then simulate.

The simulation parameters were set to the hardware parameters and the simulation was redone and the simulation results are presented in chapter-2 and chapter-5.

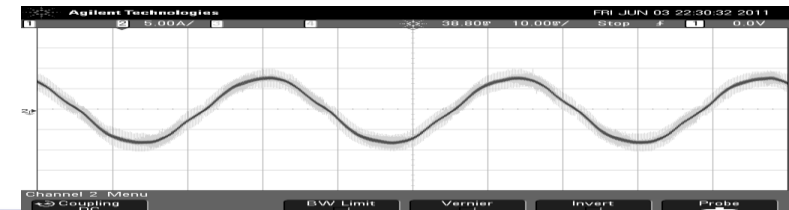
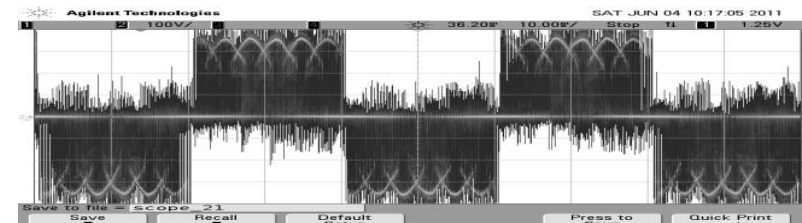
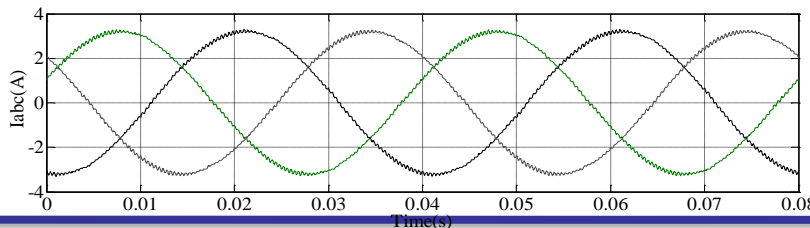
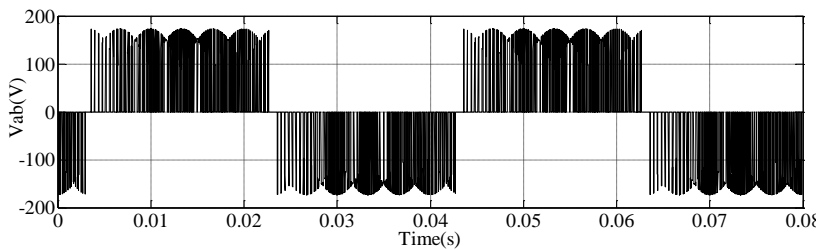
Explanation of Figure 2.17 is not clear. It is better to provide the actual circuit diagram for each module.

The actual circuit diagram of each module of the block diagram in figure 2.17 is provided in Appendix – 3

There is no comparison between simulation results and experimental results. There is no inference from the results (graphs). Discuss the results.

The deviation between the simulation and hardware results are discussed in detail in page 70 which is as follows:

In the practical implementation of the matrix converter, the four step commutation procedure is implemented, as discussed in chapter 1, to overcome the problem of commutation. This technique eliminates very narrow switching pulses, which leads to the open circuiting of the inductive load. In order to overcome this problem, the duty cycles are recalculated. Hence, the input and the output current waveforms for practical implementation deviate from those of the simulation as observed in Figures 2.16(a), 2.16(b), 2.18(a) and 2.18(b)

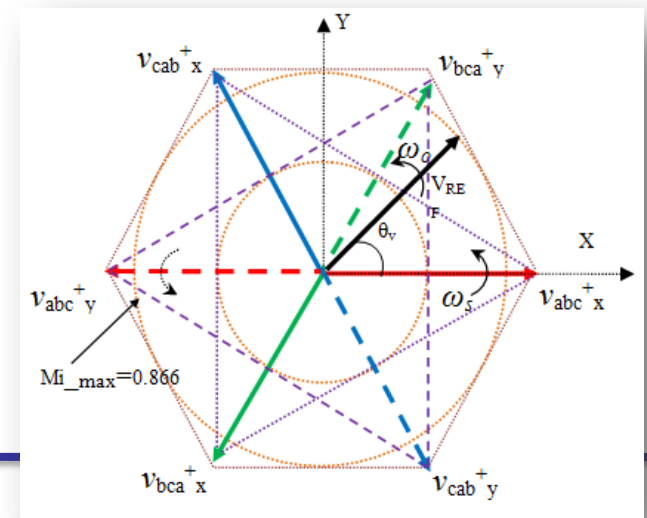
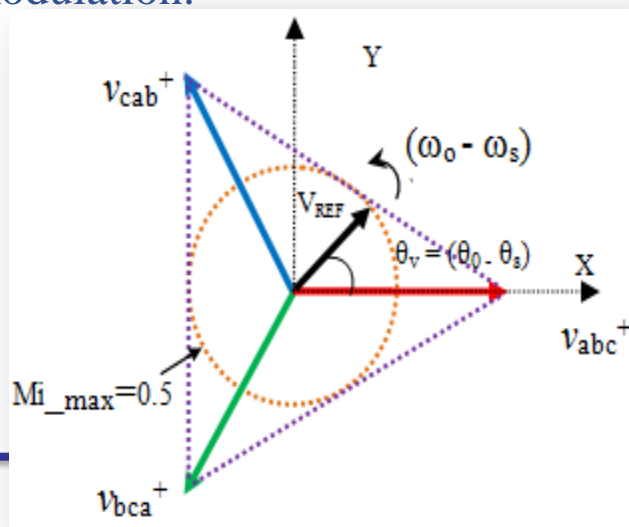


Answers to Queries of the Examiners

It is mentioned in page 90 “Figures 3.3 and 3.6 shows that the modulation index of the PSDSMC controlled by RSVM technique increases by 73.2% as compared to modulation index of the CMC controlled by RSVM technique.” How? Justify. But figures are not related to MI.

Figure 3.3 has an inscribed circle within the space vector distribution of CMC whose radius is 0.5 which indicates the maximum modulation range of CMC. Similarly Figure 3.6 has an inscribed circle within the space vector distribution of PSDSMC whose radius is 0.866 which indicates the maximum modulation index range of PSDSMC. Thus the factor by which the PSDSMC maximum modulation index increases with respect to CMC maximum modulation index range is 0.366 which corresponds to 73.2 % increase.

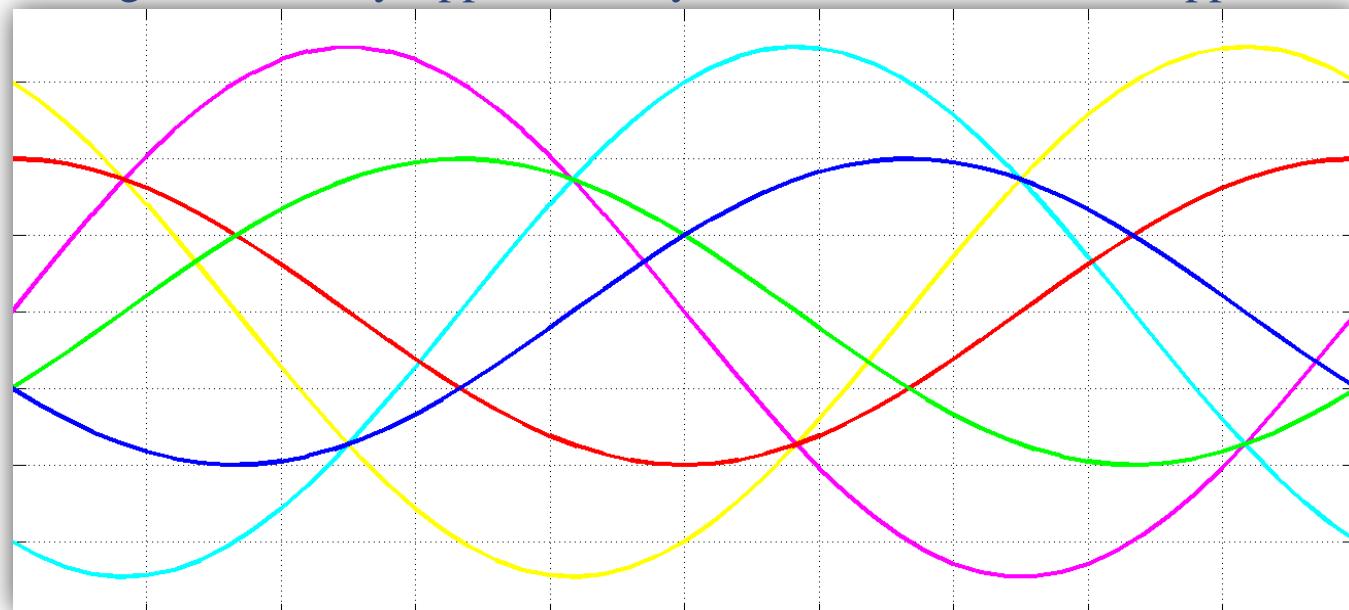
The Figures 3.3 and 3.6 are redrawn with a marking pointing out the value of maximum modulation.



Answers to Queries of the Examiners

It is mentioned in page 98 “ from Figures 3.13(b) happen”. Give the reason how voltage stress is reduced. How much voltage stress is reduced? Quantify it.

From Figures 3.3 and 3.6, it can be observed that for the CMC and the PSDSMC the space vectors are distributed by 120° and 60° respectively. Due to this, the maximum voltage stresses on the devices during the commutation for the CMC and the PSDSMC are ($\sqrt{3}V_m$) and V_m respectively. This factor can be quantified as $\sqrt{3}$. This factor indicates the ratio between the maximum voltage stresses during the instance of commutation in both the topologies. Hence the PSDSMC topology when operated with RSVM reduces the maximum commutation voltage stresses by approximately 57.7% than the CMC applied with RSVM technique.



Clearly bring out the inference from the results (Fig. 4.6 and 4.8)

The inference about the Figure 4.6 was already presented in page 115 and Figure 4.8 was already presented in page 117.

It is mentioned in page 147, “Fig. 5.14 (b) shows that the input power factor decreases, the output power factor of the converter also decreases. How? It is not clear.

It has been mentioned in the query that in page number 147, it was given “Fig. 5.14(b) shows that as the input power decreases the output power factor decreases”. However it is actually mentioned in the text that the output power (Not output power factor) decreases.

It is mentioned in page 147, “Fig 5.14(c) shows thatfor the CMC”. Is this inference from the result? It is obvious.

The mentioned statement, “switching losses vary with switching frequencies and conduction losses are constant with switching frequencies” is obvious and not an inference. So Fig. 5.14 (c) has been removed along with the statement supporting it

Continued.....

Answers to Queries of the Examiners

Discuss the results quantitatively from Fig. 5.13 – 5.15

The quantitative discussion of the Figures 5.13 to 5.15 has been included in page 146 and 147

Inference from chapter 6 needs to be explained.

The inference from chapter 6 has been explained in page 175 with Figure 6.14 in page 176.

To quote conference paper in the list of reference it should be added “Proceedings of” each conference paper.

The Quote “Proceedings of” has been added to all the conference papers in the reference list.

REFERENCE

- Alesina, A. and Venturini, M. “Analysis and Design of Optimum-Amplitude Nine-Switch Direct AC-AC Converters”, IEEE Transactions on Power Electronics, Vol. 4, No. 1, pp. 101-112, 1989.
- Burany, N. “Safe control of four-quadrant switches”, IEEE Industrial Applications Society Annual Meeting, pp. 1190–1194, 1989.
- Cardenas, R., Pena, R., Wheeler, P., Clare, J. and Asher, G. “Control of the reactive power supplied by a WECS based on an induction generator fed by a matrix converter”, IEEE Transactions on Industrial Electronics, Vol. 56, No. 2, pp. 429-438, 2009.
- Casadai, D., Serra, G. and Tani, A. “The use of Matrix Converters in Direct Torque Control of Induction Machines”, IEEE Transactions on Industrial Electronics, Vol. 48, No. 6, pp. 1057-1064, 2001.
- Gupta, R.K., Mohapatra, K.K., Somani, A. and Mohan, N., “Direct Matrix Converter based Drive for a Three-Phase Open-End Winding AC Machine with Advanced Features”, IEEE Transactions on Industrial Electronics, Vol. 57, No. 12, pp. 4032-4042, 2010..
- Hojabri, H., Mokhtari, H. and Chang, L. “Generalized Technique of Modeling, Analysis, and Control of a Matrix Converter Using SVD”, IEEE Transactions on Industrial Electronics, Vol. 58, No. 3, pp. 949-959, 2011.
- Huber, L. and Borojevic, D. “Space Vector Modulated Three-Phase to Three-Phase Matrix Converter with Input Power Factor Correction”, IEEE Transactions on Industry Applications, Vol. 31, No. 6, pp. 1234–1246, 1995.

- Lee, M.Y., Wheeler, P. and Klumpner, C. “Space-Vector Modulated Multilevel Matrix Converter”, IEEE Transactions on Industrial Electronics Vol. 57, No. 10, pp. 3385-3394, 2010.
- Luca, Z. “Control of Matrix Converters”, PhD dissertation, University of Bologna, Bologna, 2007.
- Neft, C.L. and Schauder, C.D. “Theory and design of a 30-HP matrix converter”, IEEE Transactions on Industrial Application, Vol. 28, pp. 546-551, 1992.
- Nguyen, T.D. and Hong-Hee Lee. “Modulation Strategies to Reduce Common-Mode Voltage for Indirect Matrix Converters”, IEEE Transactions on Industrial Electronics, Vol. 59, No. 1, pp. 129-140, 2012.
- Thuta, S. “Simplified Control of Matrix Converters and Investigations into its applications”, PhD dissertation, University of Minnesota, Minnesota, USA, 2007.
- Venturini, M. and Alesina, A. (1980), “The Generalized Transformer: A New Bidirectional Sinusoidal Waveform Frequency Converter with Continuously Adjustable Input Power Factor”, *Proceedings of the IEEE Power Electronics Specialist Conference, Atlanta*, IEEE, pp. 242-252.
- Wang, B.S. and Venkataramanan, G. “Analytical modeling of semiconductor losses in matrix converters”, Proceedings of the International Power Electronics and Motion Control Conference, Vol. 1, pp. 1-8, Aug. 2006.
- Zhou, K. and Wang, D. “Relationship between Space-Vector Modulation and Three-Phase Carrier-Based PWM: A Comprehensive Analysis”, IEEE Transactions on Industrial Electronics, Vol. 49, No. 1, pp. 186-196, 2002.

LIST OF PUBLICATIONS

International Journals

- Senthil Kumaran, M., Siddharth, R., Stalin, M., Divakhar, A. and Ranganath Muthu.“Constant Pulse Width Switching Strategy for Matrix Converter”, International Review on Modeling and Simulations (IREMOS), Vol. 4, No. 6, pp. 2954 - 2960, December 2011.
- Senthil Kumaran, M., Siddharth, R. and Ranganath Muthu. “Matrix Converter Switching Strategy for Abnormal Voltage Conditions using Selective Harmonic Tracking Algorithm”, International Journal of Modeling and Simulation,(ACTAPRESS) Vol. 32, No. 1, pp. 57 -64, 2012.
- Bhanuchandar, M., Adwaith, V., Senthil Kumaran, M., and Ranganath Muthu. “Twelve sector methodology for direct torque control of induction motor with fuzzy logic”, International Review of Automatic Control, (IREACO), Vol. 5, No. 4, pp. 516-522, July 2012.
- Senthil Kumaran, M., Siddharth, R. and Ranganath Muthu. “Minimum Error Switching Strategy for Matrix Converter with Input Current Control”, International Review of Electrical Engineering (IREE), Vol. 7, No. 4, pp. 4768 – 4775, July-August 2012.
- Senthil Kumaran, M., Siddharth, R. and Ranganath Muthu. “Elimination of Common Mode Voltage using Rotating Space Vectors and Phase Shifted Dual Source Matrix Converter,” accepted for publication in The International Journal for Computation and Mathematics in Electrical and Electronic Engineering (COMPEL).

International Conferences

- Senthil Kumaran, M., Siddharth, R. and Ranganath Muthu. “Simplified Control of Matrix Converter Represented as a Three-level Inverter”, Proceedings of the International Conference on Trends in Industrial Measurements and Automation (TIMA), pp. 110-113, 2009.
- Senthil Kumaran, M., Siddharth, R. and Ranganath Muthu. “Real-Time Controller Design for Matrix Converter for Load and Input Variations”, Proceedings of the Third International Conference on Emerging Trends in Engineering and Technology (ICTETET), pp. 396-400, 2010.
- Senthil Kumaran, M., and Ranganath Muthu. “FPGA Triggered Space Vector Modulated Voltage Source Inverter Using MATLAB/ System Generator®”, Proceedings of the Third International Conference on Trends in Information, Telecommunication and Computing, Lecture Notes in Electrical Engineering, Volume 150, pp. 505-514, 2013.

Questions

THANKS TO THE AUTHORS I OFTEN REFERRED

- 1) ALESINA & VENTURINI
- 2) LIPO & LIXIANG WEI
- 3) HANJU CHA & ERIKSON
- 4) WHEELER PATRICK & IMAYAVARAMBAN
- 5) NED MOHAN & MOHABATHRA
- 6) CASADAI , MARCO MATINI& GABERIAL GANDE
- 7) VENKATRAMAN GIRI & BINGSEN WANG

THANKS TO THE INSTITUTIONS – WHICH OFFERED HELP TOWARDS THIS WORK

- 1) SSNCE - KALAVAKKAM
- 2) DESIGN DESK - TNAGAR
- 3) CDAC – TRIVANDRAM
- 4) CWET – PALIKARANAI
- 5) POWER LABS - PERUNGUDI

MY SPECIAL THANKS

Guide:

Dr. Ranganath Muthu

UG Student:

R. Siddharth

Director Design Desk:

Mr. Shanmugam

CWET Scientist:

Mr. Rajesh Katyal

CDAC Scientist:

Mr. Saravana Kumar

HOD and All Staffs of EEE /SSNCE

All Students of SSNCE who extended their help in completion of this thesis work

All Audience present today for the public viva voce.

Specialization is an art of knowing more and more about less and less and finally knowing everything about nothing

- Zentill []

THANK YOU

Specialization is an art of knowing more and more about less and less and finally knowing everything about nothing

- Zentill []
